ANALYSIS OF THE CELLULAR AND MOLECULAR ORGANIZATION OF THE LACTATE SHUTTLE IN THE INNER RETINA

Tesis entregada a

LA UNIVERSIDAD DE VALPARAÍSO

en Cumplimiento Parcial de los requisitos para optar al grado de

Doctor en Ciencias con Mención en Neurociencia

Facultad De Ciencias

Por

Víctor Manuel Calbiague García

Enero, 2022

Dirigida por: Dr. Oliver Schmachtenberg

FACULTAD DE CIENCIAS

UNIVERSIDAD DE VALPARAÍSO

INFORME DE APROBACION

TESIS DE DOCTORADO

Se informa a la Facultad de Ciencias que la Tesis de Doctorado presentada por:

Víctor Manuel Calbiague García

Ha sido aprobada por la comisión de Evaluación de la tesis como requisito para optar al grado de Doctor en Ciencias con mención en Neurociencia, en el examen de Defensa de Tesis rendido el día 18 del Mes de enero de 2022

Director/a de Tesis:

Dr. Oliver Schmachtenberg .....

Comisión de Evaluación de la Tesis

Dr. François Paquet-Durand .....

Dr. Agustin Martinez .....

Dr. Andrés Chavez .....

Dedicado a mi mamá, hermano y papá y a mi perro tommy

Y a mi mami, que a pesar de que nos dejó hace años, su recuerdo y cariño siempre estará latente.

Agradecimientos

En primer lugar, me gustaría agradecer a mi familia: Mi mamá por ser la persona más dulce que puede existir y que me brinda todo el amor del mundo. A mi hermano, por ser esa voz sabia de mi vida, que siempre me da consejos con el amor que solo un hermano puede dar. Mi papá, por enseñarme lo que es el esfuerzo. Todo lo que soy hoy, es gracias a Uds. También agradecer al resto de mi familia, mi tía vero y mi tía chica y a todos mis primos por ser ese apoyo constante en mi vida, y sobre todo en los tiempos difíciles en pandemia que vivimos hace poco tiempo.

Agradecer a mi laboratorio, por las excelentes discusiones científicas, no científicas, las risas, y el apoyo diario. Específicamente agradecer a mi tutor principal, Dr. Oliver Schmachtenber, por ser más que un tutor, un consejero, y que me enseñó y me formó en mi vida científica. Gracias por estos 8 años en el laboratorio.

También agradecer al Dr. François Paquet-Durant por la gran colaboración que hemos realizado en mi tesis, y abrirme las puertas de su laboratorio para realizar una pasantía muy provechosa. Agradecer a mi comisión de tesis, por las gratificantes discusiones de mi tesis que me ayudaron a perfilar siempre de buena forma mi investigación.

Finalmente agradecer a mis amigos del colegio: Matias, Bayron, Bruno y Seba, mis hermanos del alma. A mis amigos de la universidad: Coni, Dani, Kelyna, Fran y David, sin su compañía diaria y amistad esto hubiera sido imposible. A mis amigas: Eyrllen y Mayito, su cariño es indispensable. A mi perro, tommy, ya que con el amor y cariño perruno la vida se hace más fácil. Y a Zash, por ser esa persona que hizo mi último año de doctorado un tiempo mucho más agradable y pacífico, entregándome mucho amor y cariño.

Finalmente, agradecer a las fuentes de financiamiento que hicieron posible esta tesis, la Beca Doctorado Nacional ANID, la Beca del Programa de Neurociencias UV y el proyecto FONDECYT Regular No. 1210790.

TABLE OF CONTENTS

LIST OF FIGURES AND TABLES

LIST OF ABBREVIATIONS

CNS	Central nervous system
ANLS	Astrocyte-to-neuron lactate shuttle
ATP	Adenosine Triphosphate
MCT	Monocarboxylate transporter
PRs	Photoreceptors
RPs	Rod photoreceptors
CPs	Cone photoreceptors
BCs	Bipolar cells
ACs	Amacrine cells
GCs	Ganglion cells
MCs	Müller cells
ONL	Outer nuclear layer
OPL	Outer plexiform layer
INL	Inner nuclear layer
IPL	Inner plexiform layer
GCL	Ganglion cell layer
RBCs	Rod bipolar cells
CBCs	Cone bipolar cells
cGMP	Cyclic guanosine monophosphate
OS	Outer segment
IS	Inner segment
RPE	Retinal pigment epithelium
TCA	tricarboxylic acid cycle
GLUT	Glucose transporter
PK	Pyruvate kinase
LDH	Lactate dehydrogenase
ERG	Electroretinogram
DR	Diabetic retinopathy
AR-C	AR-C155858
SR	SR-13800
Shik	Shikonin
AUC	Area under the curve
ROI	Region of interest
I_{out}	Outward current
I_{ca}	Calcium current
V_{memb}	Membrane potential
FRET	Förster resonance energy transfer
MCU	Mitochondrial calcium uniporter
NCLX	Na^{+}/Ca^{2+} exchanger

ABSTRACT

Metabolism is a fundamental issue for cell function. This becomes an important concern for the nervous system and, therefore, for neurons, since excitatory synapses consume almost 50% of ATP to restore the ion gradients challenged by depolarization. The retina shares several features with the brain, including its high energy demands. Nonetheless, it is known that the retina metabolizes glucose mainly by the energetic-inefficient aerobic glycolysis pathway, which is 18-fold less productive than oxidative phosphorylation and has as its final step the production of lactate. Many investigations have suggested the existence of a retinal lactate shuttle, but to date the possible cells that consume this extracellular lactate which is produced by aerobic glycolysis remain unclear. The aim of this study was to better understand the energy metabolism in the retina and especially propose a consumption of extracellular lactate as an alternative energy source for inner retinal cells.

Immunofluorescence experiments showed that the inner retina massively expressed a specific monocarboxylate transporter isoform (MCT2). Moreover, this transporter colocalizes with the rod bipolar cell (RBC) marker, PKCα, and the amacrine cell marker, calretinin. To test the functionality of this expression we cultured retinal explants, and we manipulated pharmacologically the lactate metabolism for 4 days. These different treatments altered the death cell rate and number of RBCs. Furthermore, calcium and sodium imaging experiments reveal that the inhibition of lactate transport disrupts the ion gradients, resulting in changes in intracellular levels of basal calcium and sodium, that alter the amplitude, and kinetics parameters of calcium and sodium responses, suggesting a disruption in ion pumps. Interestingly, single-cell experiments reveal that the exposure of retinal slices to an extracellular solution with lactate, maintains the outward current, calcium current, and membrane potential. But the addition of an MCT2 blocker decreases the

outward current, and calcium current and depolarizes RBCs. Finally, the study of intracellular lactate dynamics expressing the genetically-encoded FRET nanosensor Laconic, suggests that inner retinal neurons are capable of consuming extracellular lactate through MCT2 under culture basal conditions, which is exacerbated when the retina is subjected to general depolarization. Conversely, Müller cells display a producer profile under culture basal condition, which is reversed under a general depolarization.

In conclusion, our data support the notion that inner retinal neurons can import a portion of the extracellular lactate through MCT2 to meet their physiological demands, specifically cellular survival, ion homeostasis, and currents. In parallel, other observations suggest that Müller cells produce lactate under basal culture conditions, so they could be one of the cell types performing aerobic glycolysis in the retina. Likely, this extracellular lactate is used by retinal bipolar cells to produce ATP by classic oxidative phosphorylation.

INTRODUCTION

A correct metabolism is a fundamental issue for proper cell function. This becomes more critical when we focus on the brain and all the neurons that compose it, as this organ has a high energy demand, causing about 20% of the total energy consumption of our body (Harris et al., 2012). More than half of the energy is used by neurons to maintain the ionic gradients caused by excitatory neuronal activity (Attwell and Laughlin, 2001). Nevertheless, even though neurons have these high energy requirements, they are unique because they lack energy stores to meet unpredictable increases in energy demand. One of the fundamental questions in neuroscience is related to energy metabolism, specifically how neurons are capable to reach a perfect balance between energy consumption and a good performance.

Glucose metabolism in mammalian cells

Glucose is the principal fuel source for mammalian cells. The human brain consumes almost 25% of the total glucose supply and 20% of O_2 of our body, yet it accounts for only 2% of body mass (Harris et al., 2012; Deng and Yan, 2016). Once glucose is taken up by cells through glucose transporters (GLUT), it is metabolized to pyruvate or glycogen. The classic glycolytic pathway comprises 10 consecutive enzymatic reactions which mediate the conversion from 1 molecule of glucose to 2 molecules of pyruvates plus 2 molecules of ATP and NADH (Akram, 2013; Lenzen, 2014).

Some of the enzymes which are involved are hexokinase, aldolase, glyceraldehyde 3-phosphate dehydrogenase (GAPDH), enolase, and pyruvate kinase (PK), which correspond to the last steps of glycolysis. PK is responsible for producing 2 molecules of pyruvate plus 1 molecule of ATP from phosphoenolpyruvate (Xiong et al., 2011). Pyruvate produced in glycolysis can pass into the mitochondria, be converted to acetyl coenzyme A (acetyl Co-A) by pyruvate dehydrogenase (PDH) and undergo further metabolic processing in the Krebs cycle, also known as tricarboxylic acid cycle (TCA). This pathway is one of the most important metabolic pathways in mammalian cells and corresponds to a continuous series of reactions to degrade pyruvate until obtaining CO_2 (Sánchez-García et al., 2021). It is important to note, that this cycle does not have a direct production of chemical energy in form of adenosine triphosphate (ATP). For this, the TCA cycle is redox-coupled to oxidative phosphorylation (OXPHOS) in the mitochondrial inner membrane through two TCA products: NADH and $FADH_2$. These specific products feed the mitochondrial electron transport chain (*i.e.,* respiratory cycle), which is the main responsible to produce ATP in mammalian cells, in a process that depends on oxygen consumption (Cooper, 2000). Moreover, the product resulting from the NADH and $FADH_2$ reactions in OXPHOS (i.e., NAD^+ and FAD) are required for the TCA cycle (α-ketoglutarate dehydrogenase, succinate dehydrogenase, and malate dehydrogenase) to maintain it working (Cooper, 2000; Eales et al., 2016).

Thus, in anaerobic conditions, the respiratory cycle cannot function, disrupting the TCA cycle, and that is the reason why the TCA cycle is considered an aerobic metabolic pathway (Akram, 2013). The main characteristic of this process is its efficiency, since it generates 36 molecules of ATP for each molecule of glucose (Gatenby and Gillies, 2004).

But, as mentioned before, in anaerobic conditions (*e.g.,* hypoxic conditions), the production of ATP by OXPHOS becomes disrupted, since the cells cannot maintain the redox reactions involved in the respiratory cycle (Cooper, 2000; Eales et al., 2016). Also, this process involves an imbalance in cytoplasmatic and mitochondrial NAD^+ levels altering some reactions in both glycolysis (glyceraldehyde-3-phosphate dehydrogenase) and the TCA cycle (Eales et al., 2016). Hence, this

condition demands cells to produce energy by alternate metabolism. In this case, cells no longer convert pyruvate into Acetyl Co-A, but begin to convert it to lactate through Lactate dehydrogenase (LDH) (Overgaard et al., 2012; Adeva-Andany et al., 2014). This reaction is called anaerobic glycolysis and needs the oxidation of NADH to NAD^+ which restores the cytoplasmatic NADH:NAD^+ ratio, which is important for carrying out the preparatory phase of glycolysis (Adeva-Andany et al., 2014; Lenzen, 2014). Interestingly, this metabolic pathway can also occur under aerobic conditions and is known as aerobic glycolysis or the Warburg effect, which was discovered 100 years ago by Otto Warburg (Warburg, 1924).

This emergency metabolic pathway used by cells under hypoxia has two specific disadvantages: 1) The net ATP production is only 2 ATP per glucose molecule, making it an energetically inefficient process (Adeva-Andany et al., 2014; Lenzen, 2014). 2) Lactate produced during anaerobic conditions is a metabolic dead end, as it can only be metabolized in the liver (Manoj et al., 2022). Therefore, lactate is pumped out by monocarboxylate transporters (MCTs) and transported through the blood to the liver, and converted to pyruvate by LDH, in a process known as the Cory cycle (Passarella and Schurr, 2018).

Anaerobic glycolysis is common in muscles. Intense exercise causes muscles to deplete oxygen, requiring muscle cells to produce lactate to balance intracellular ATP levels (Stojan and Christopher-Stine, 2015). However, aerobic glycolysis is relevant in many cells that are not subjected to hypoxic conditions: cancer cells and some more specialized cells such as astrocytes and neurons (Luo and Semenza, 2012; Lerchundi et al., 2015; Mächler et al., 2016).

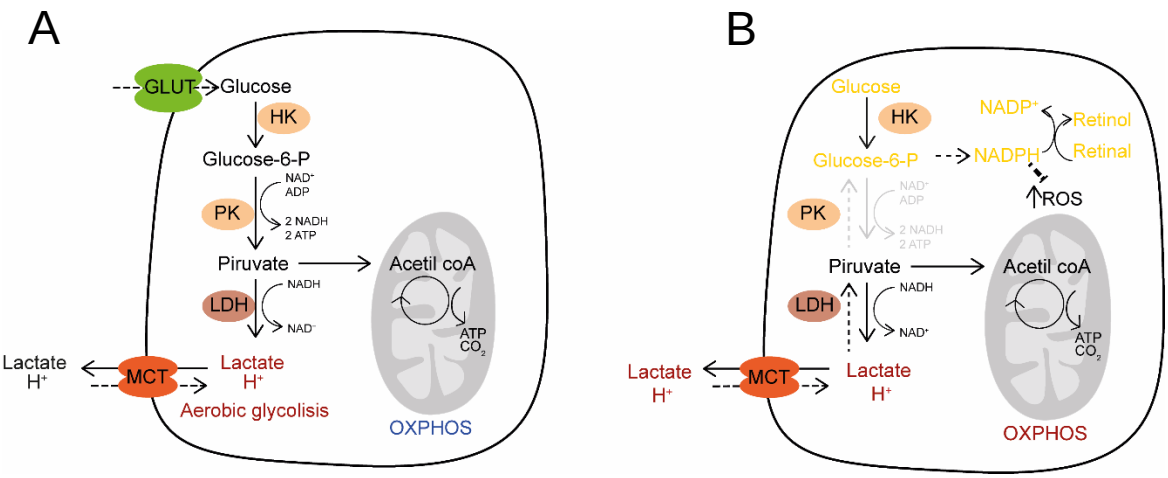

Figure 1.- Glucose metabolic pathways. (A) An overview summarizing glycolysis, aerobic glycolysis, and the enzymes related to these metabolic pathways. (B) Proposal scheme showing the change in glucose metabolism when cells begin to consume lactate. GLUT= glucose transporter; HK= Hexokinase; PK= Pyruvate kinase; LDH= Lactate dehydrogenase; MCT= Monocarboxylate transporter; OXPHOS= Oxidative phosphorylation.

Metabolic coupling in the central nervous system

As already mentioned, in general, cells have two main metabolic pathways to solve the energy problem they are undergoing: OXPHOS and aerobic glycolysis. The latter is an adaptation to metabolize glucose in a non-oxidative manner despite the presence of oxygen and is mainly used by proliferating cells (*e.g.* cancer cells) to satisfy their anabolic demands (Le et al., 2009; Miao et al., 2013). This metabolic pathway has as the final step the conversion of pyruvate to lactate, instead of the passage of pyruvate to the mitochondria for oxidation (Barros et al., 2020), allowing cells that use this pathway to obtain access to the metabolic intermediates of glycolysis (glucose 6-phosphate and glyceraldehyde 3-phosphate) and TCA cycle (citrate and Acetyl Co-A) to synthesize lipids and nucleic acids (pentose phosphate pathway (PPP)) for cell proliferation (Luo and Semenza, 2012; Baenke et al., 2013; Wong et al., 2013, 2015). Also, this process increases the levels of NADPH, an important reducing agent that is produced by the PPP pathway, and is important to control the oxidative stress that is a byproduct of mitochondrial metabolism (Wong et

al., 2013). Another characteristic is that it has a production rate 18-fold less efficient than the classical mitochondria pathway in producing ATP per mole of glucose.

It is important to note that two different metabolic regulations result in lactate production: The first is the Warburg effect and the second is the Crabtree effect (Barros et al., 2020). The main difference between the two is that the Crabtree effect produces lactate by inhibiting mitochondrial respiration due to increased glycolysis, whereas the Warburg effect only prevents oxidative phosphorylation in the presence of oxygen (Barros et al., 2020). Interestingly, the presence of these two metabolic pathways has been demonstrated in astrocytes, and they can be modulated by NH_4^+, nitric oxide, and, potassium (Bittner et al., 2011; Lerchundi et al., 2015; Sotelo-Hitschfeld et al., 2015; Fernández-Moncada et al., 2018). Neurons, in turn, apparently use mainly traditional OXPHOS to produce energy (Harris et al., 2012; Le Masson et al., 2014; Baeza-Lehnert et al., 2019).

Many studies have suggested that this metabolic configuration leads neurons to consume the lactate released by astrocytes prompted by neuronal activity (Chuquet et al., 2010; Suzuki et al., 2011; Barros and Weber, 2018; Jimenez-Blasco et al., 2020). This happens because during excitatory synaptic activity, neurons release K^+ and glutamate into the extracellular space, where K^+ concentration can reach 12 mM at maximal stimulation (Kofuji and Newman, 2004). Therefore, this extracellular increase in potassium leads to astrocytic depolarization, enhanced by a subsequent influx of Na^+ mediated by glutamate receptors that later activate Na^+/K^+ ATPase to restore ion gradients. This entire chain of events will increase astrocytic glycolysis to produce the ATP necessary to maintain Na^+/K^+ ATPase function. (Bittner et al., 2011). Interestingly, a regulation in glycolysis triggered by Na^+/K^+ ATPase activity has also been proposed. (Baeza-Lehnert et al., 2019). Thus, lactate released by astrocytes can potentially be taken up by neurons through MCTs and be reconverted to pyruvate by LDH. This shift to consuming lactate over glucose may help neurons to adapt more rapidly to changes in neuronal energy demand since lactate needs fewer metabolic steps to be converted into pyruvate (Barros, 2013).

This exchange of lactate between astrocytes and neurons is called astrocyte-to-neuron lactate shuttle (ANLS) and was proposed by Pellerin and Magistretti in the 1990s (Pellerin and Magistretti, 1994; Pellerin et al., 1998; Magistretti and Pellerin, 1999). But why, in the same scenario, do astrocytes and neurons have different metabolisms? Many ideas have been demonstrated over the years, and almost all of them are related to a difference in the phosphorylation and expression of key enzymes. First, the enzyme phosphofructokinase, a key glycolytic regulator that converts fructose 6-phosphate to fructose-1,6-bisphosphate, is poorly expressed in neurons (Herrero-Mendez et al., 2009). This results in an accumulation of glucose 6-phosphate that feeds the PPP pathway, which reduces the cytosol and protects cells against oxidative stress generated by mitochondrial metabolism (Herrero-Mendez et al., 2009; Barros, 2013). Secondly, in astrocytes, the PDH enzyme is highly phosphorylated causing less conversion of pyruvate to Acetyl Co-A, favoring the aerobic glycolytic profile. Whereas neurons have an active PDH that guides pyruvate into the Krebs cycle (Halim et al., 2010).

It should also be noted that, the researchers suggested the activation of aerobic glycolysis triggered by glutamate uptake in astrocytes, and that lactate could serve as an alternative fuel for neurons, emphasizing that direct glucose uptake by neurons could still occur (Pellerin and Magistretti, 1994). A similar mechanism has been described in non-mammalian animals such as drosophila, where astrocytes release alanine and lactate which are important for neuronal survival (Volkenhoff et al., 2015). This communication goes beyond lactate and the classic glutamate-glutamine cycle, in which astrocytes take up glutamate released by neurons and convert it into glutamine that is shuttled into neurons (Hertz and Rothman, 2017). Also, neuron-astrocyte communication with toxic fatty acids had been reported (Ioannou et al., 2019), and is apparently necessary for long-term memory formation. Here, the interruption of lactate release by blocking MCT leads to a disruption in long-term potentiation in behavioral experiments, and in electrophysiological recordings that are rescued with exogenous lactate (Suzuki et al., 2011).

Retinal structure and function

A special exacerbated example of a perfect energy balance is the retina, which is an ontological part of the central nervous system. Therefore, it shares several features with the brain, including high energy demands.

The retina is a neural tissue in which visual signals are transduced by photoreceptors and subsequently processed by inner retinal neurons. It is mainly composed of 5 layers that form the circuits responsible for receiving and processing visual information (Fig. 1). The outermost part of the retina corresponds to the outer nuclear layer (ONL), where two different types of photoreceptors (PRs) are densely grouped: rods (RPs) and cones (CPs) (Fig. 1). On average, RPs represent approximately 95% of the photoreceptors in the human and mice retina and are mainly involved in visual transduction under dim light (scotopic conditions), basically due to their remarkable sensitivity to light. On the other hand, CPs represent only 5% of the photoreceptors in the mammalian retina, are less sensitive than RPs, function mainly under daylight (photopic) conditions and allow color vision. The next retinal layer corresponds to the outer plexiform layer (OPL), and houses the synapses between photoreceptors, horizontal cells (HCs) and bipolar cells (BCs) (Fig. 1). Adjacent is the inner nuclear layer (INL) that groups the somas of the BCs, the amacrine cells (ACs) -the neuronal component-, and the Muller cells (MCs) -the glial component-. Then, the next layer is the inner plexiform layer (IPL), and here the projections of the BCs and ACs form synapses with the projections of the ganglion cells (GCs). The main filtering and processing of visual signals takes place in this cell layer. The somas of GCs are placed in the last layer: the ganglion cell layer (GCL). It is important to mention that in this layer the presence of displaced ACs is also observed. Projecting below the GCs are the MC endfeet (Euler et al., 2014) (Fig. 1). Finally, the axons of GCs conform the optic nerve, which transport the visual information to the brain to be further process.

To date, 22 types of GCs have been classified, 42 types of ACs, and more than 10 different BCs in mammals (Hartveit, 1997; Masland, 2012; Euler et al., 2014; Shekhar et al., 2016a; Vielma and

Schmachtenberg, 2016; Yan et al., 2020). This classification has been based on morphological characteristics, such as soma diameter, length of dendritic arborization, IPL stratification, electrophysiological patterns, and gene expression.

In the INL, BCs are the only neurons which provide the connection between PRs and GCs (Euler et al., 2014). In vertebrate retinas the number of BCs depends on the species. For example, in mammals about 15 different types have been described (Shekhar et al., 2016a), while in teleost fish more than 20 different types of BCs are known, which include BCs with bi and tri-stratification (Connaughton et al., 2004; Li et al., 2012). BCs can be classified according to their response to light as BCs ON or BCs OFF. ON BCs are those that depolarize upon an increase in light intensity, whereas OFF BCs show depolarization in response to a decrease in light intensity. The latter have also been electrophysiologically characterized according to their glutamate-evoked response, which makes the classification method more accurate (Vielma and Schmachtenberg, 2016).

This classification is possible since PRs release glutamate continuously in darkness, but this release is suppressed in light. OFF BCs express glutamatergic AMPA/kainate receptors which are ionotropic receptors causing depolarization in scotopic conditions. On the other hand, ON BCs are hyperpolarized in this condition due to the expression of metabotropic glutamate receptors (mGLUR6). This receptor triggers the enclosure of cationic channels as TRPM1, through intracellular signals (Koike et al., 2010).

All these BCs (ON and OFF) are known as cone BCs (CBCs) as they are connected to this type of PRs. Whereas there is only one type of BCs in contact with PRs, known as rod BCs (RBCs), which are the main type of BCs that can be found in mammalian retinas (Hartveit, 1997; Wassle et al., 2009). However, in some rodents it has been observed that certain CBCs can be in contact with RPs (Fyk-Kolodziej et al., 2003; Hack et al., 1999; Li et al., 2010; Maturaga et al., 2007), and RBCs can receive inputs from CPs, evidencing an interconnection between rod and cone pathway (Behrens et al., 2016).

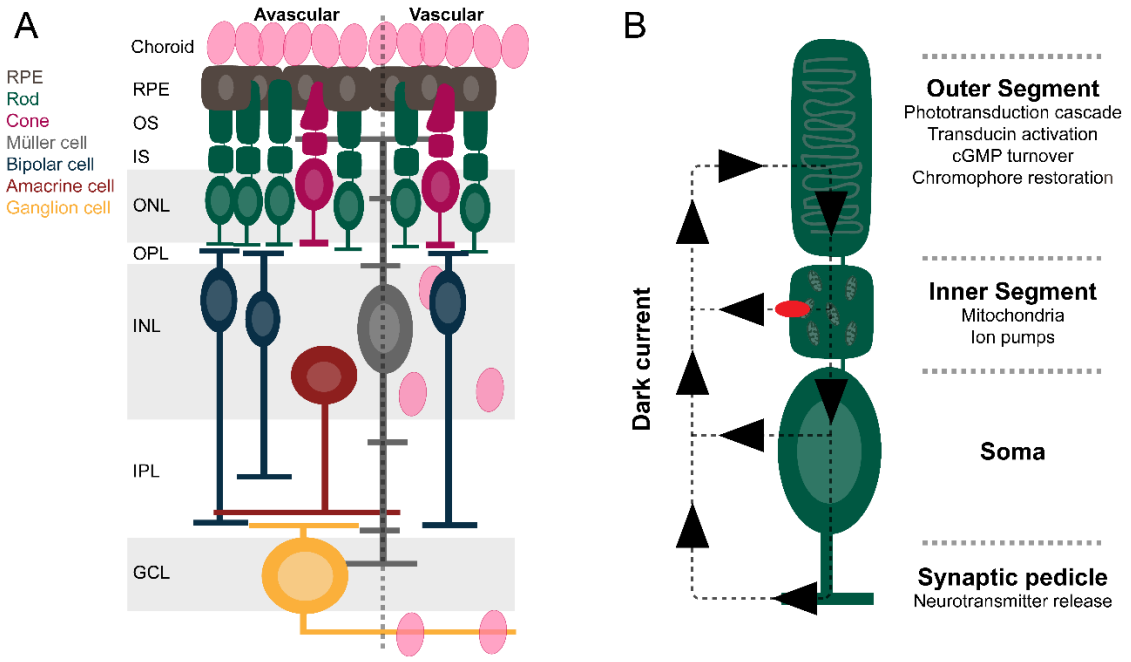

Figure 2.- Schematic layout of the retina. (A) Comparison between avascular and vascular retinas showing the presence of inner vascularity in vascular retinas. **(B)** A scheme of rod photoreceptors indicating its morphology, and the dark current flow.

The retina is the neuronal tissue with the highest energy demand

The retina is an interesting tissue because it functions differently from any other sensory tissue. Photoreceptors hyperpolarize when absorbing a photon, whereas in dark conditions they depolarize releasing glutamate. This occurs because photoreceptors express Na^+-permeable cyclic nucleotide-activated channels (CNGs) in their outer segments (OS). Therefore, when photopigments absorb light, G-protein-coupled opsins trigger a cascade that reduces the cytosolic concentration of cGMP. This reduction causes the closure of CNG channels. The influx of ions through the OS and their subsequent efflux through pumps in the inner segments (IS) produce the dark current, which has a high metabolic cost due to the constant activity of the Na^+/K^+ ATPase densely located in the IS. In addition, due to this high activity produced by the dark current and the constant renewal of the outer segments mediated by the retinal pigment epithelium (RPE), the

retina is considered the neural tissue with the highest energy demand (Ames et al., 1992a; Country, 2017).

Strikingly, metabolism plays such an important role in retinal function that it is crucial for understanding the evolution of eye design in different species (Baden et al., 2019). So much so that some animals that live in total darkness reverse their visual systems to save energy (Rétaux and Casane, 2013). This is a critical point because the presence of vascularization in the retina to carry out metabolites causes important physical problems. Due to blood vessels being opaque, they can disturb the light pathway to PRs (the light must pass through the entire retina; Fig. 2) (Yu and Cringle, 2001). So, the retina, which is a light-sensitive tissue, must solve this problem.

The main vascularization of the retina is the choroid, which is ubiquitous through all species and is located between the retina and the sclera, closer to the PRs (Nickla and Wallman, 2010). However, in some species not only is this the main vascularization but also the only, as in guinea pig and rabbits (Yu and Cringle, 2001). Other species have inner vascularity in the INL, IPL, and GCL (intraretinal capillaries and supraretinal capillaries; Fig. 2), that provides oxygen and metabolites to inner retinal cells as in the case of mice, rats, and primates (Yu and Cringle, 2001; Country, 2017). Therefore, the vertebrate retina must find a balance between these two physical constraints: highly vascularized retinas would alter light in the retina, whereas poorly vascularized retinas would limit the supply of metabolites, especially in the innermost layers of the retina, cause the metabolites and oxygen must diffuse for almost 200 µm (Yu and Cringle, 2001).

Some species have evolved special structures, such as birds and fish, to supply sufficient oxygen and blood to the retinal cells to ensure the metabolic substrate necessary to have the visual system they need to survive (Rétaux and Casane, 2013; Country, 2017; Krishnan and Rohner, 2017). For instance, teleost fish have a structure located before the choroid that is called the “rete system” (Wittenberg and Wittenberg, 1974; Eastman and Lannoo, 2007), which allows an increase in the partial pressure of O_2 in the eye (Wittenberg and Wittenberg, 1974; Country, 2017), while in birds

there is a structure called pecten oculi, which is an extension of the choroid, and is located on the vitreous side replacing the intraretinal vasculature (Braekevelt, 1991; Kiama et al., 2001).

Interestingly, Warburg's studies in 1924 pointed out an intriguing observation. He compared the rate of aerobic glycolysis between carcinoma cells and tissues where carcinomas and sarcomas arise such as resting epithelium, intestinal mucosa, liver, kidney, pancreas, submaxillary and thyroid, and other high energy consuming tissues such as brain and retina. He found that tumor cells and retina are mainly those that utilize aerobic glycolysis (Warburg, 1924). To date, many investigations have been done in the retina to support this observation, and some have reported that this tissue converts almost 70% of consumed glucose into lactate (Cohen and Noell, 1960; Winkler, 1981; Wang et al., 1997; Du et al., 2013), whereas the brain converts only 25% of glucose into lactate (Dienel and Hertz, 2001; Dienel, 2012).

These data are striking because the retina obtains glucose and oxygen more directly than the brain. Retinal cells consume glucose and oxygen that comes from the choroidal blood, only traversing the RPE -in some cases even more directly from some additional inner vascularity present in rodents and primates - while the glucose in the brain must cross four- plasma membranes to reach neurons and glia (Barros, 2013; Country, 2017; Hurley et al., 2015).

All this evidence leads to some obligatory questions: Why does such an energy-demanding tissue use mainly an inefficient metabolic pathway to obtain energy? Are there other benefits besides the energetic issue? What cells are producing this lactate? If there is a massive lactate production, exist cells that consume it? What cells are taking up this lactate? Over the years, some questions have been investigated deeper than others and have given us a better understanding. For example, the split of glycolysis and energy consumption could drive several advantages for tissues. For instance, it allows a faster adaptation to change in neuronal energy demand and can also reduce neuronal oxidative stress (Barros, 2013). Regarding why the retina produces lactate, the ANLS hypothesis could address the problem of this lactate overproduction (Fig. 3). In this context, it is interesting to mention the results reported by Tascopoulos et al. in the honeybee

drone and guinea pig retina were used by Pellerin and Magistretti to support their ANLS hypothesis (Tsacopoulos et al., 1988). Specifically, in honeybee drone neuronal slices, the researchers showed that in this nervous tissue preparation, upon activation of the photoreceptors by light, an increase in a glucose analog uptake can be observed predominantly in glial cells which surrounded the rosette composed by photoreceptors. But an increase in oxygen consumption was measured in PRs. Those results were interpreted as that glial cells take up glucose and then release a substrate that is oxidized by photoreceptors. Thereafter, these results gained further support by *in vitro* studies of the distribution of a glucose analog in guinea pig retinal slices where similar results were found in MCs. In this experiment these cells took up the glucose analog rather than neurons (Poitry-Yamate and Tsacopoulos, 1991). Another experiment performed by this research group studied the uptake of radioactive ^{14}C-glucose with retinal cell preparation of isolated MCs and PRs and revealed that MCs isolated metabolized glucose, while ^{14}C-lactate was largely found in the bath. On the other hand, the presence of PRs, decreased drastically the presence of ^{14}C-lactate (about 70%) suggesting that the lactate is released by MCs, and this is consumed by neurons (Poitry-Yamate et al., 1995). This decade of *in vitro* studies supports the idea of a retinal lactate shuttle, which may resemble the ANLS in brain (Poitry-Yamate et al., 1995; Poitry-Yamate & Tsacopoulos, 1991; Tsacopoulos et al., 1988, 1994; Tsacopoulos & Magistretti, 1996).

If the retina follows this mechanism, it may obtain other benefits beyond ATP production. As mentioned in the previous section, lactate consumed by the neuronal component of the retina, would be the main substrate for producing ATP by OXPHOS. Thus, most of the glucose consumed would feed the PPP pathway. This metabolic arrangement could be useful for photoreceptors, as the NADPH produced by the PPP pathway can reduce the oxidative stress generated by OXPHOS. This is critical for photoreceptors because the constant dark current has a high metabolic cost (Okawa et al., 2008; Ingram et al., 2020), because they need to produce the substrate (*i.e.,* ATP) for the ion pumps located in the IS. Therefore, this process will bring with it a high oxidative stress rate, that would be counterbalanced by NADPH. Moreover, this is not the

only benefit that photoreceptors can obtain from the PPP pathway, because this NADPH can also be used in the retinal-retinol cycle, an important reaction to maintain the operation of the rhodopsin. Here the retinol dehydrogenase needs the NADPH as a cofactor to reduce all-*trans*-retinal to all-*trans*-retinol, which is shuttled to RPE to be converted into 11-*cis*-retinal, the chromophore that is photoisomerized in rhodopsin (Tsacopoulos et al., 1998; Sahu and Maeda, 2016). Finally, this metabolic configuration also helps in lipid biosynthesis, which is crucial to sustaining the constant PRs OS renewal (Young, 1967; Chinchore et al., 2017).

Nevertheless, as in the CNS, in the retina, the ANLS hypothesis is not universally accepted and in practice, its relevance may depend on the specific properties of cells and tissues, as well as on the metabolic state (Hurley et al., 2015; Calbiague et al., 2022).

On the other hand, some recent studies have proposed that photoreceptors would be the site of aerobic glycolysis in the retina, releasing lactate which is used as fuel by both RPE and MCs (Fig. 3) (Lindsay et al., 2014; Du et al., 2016a; Chinchore et al., 2017; Kanow et al., 2017).

These conclusions come from results that show that MCs do not have the enzymatic machinery to support lactate production. These investigations demonstrated that MCs are lacking glucose transporters, pyruvate kinase, and the aspartate/glutamate carrier 1 (AGC1), a key component of the malate-aspartate shuttle, which is important to maintain a balance in the NADH:NAD^+ ratio (McKenna et al., 2006). This supports that photoreceptors, RPE, and MCs have differences in glucose metabolism, where photoreceptors consume glucose and release lactate (Du et al., 2016b; Kanow et al., 2017), while MCs are not able to produce pyruvate from glucose. The lack of AGC1 suggests that these cells cannot maintain a good NADH:NAD^+ ratio (important for converting lactate to pyruvate), indicating that MCs consume aspartate to oxidase NADH and hence support their lactate consumptions (Lindsay et al., 2014). This configuration would enhance the MC´s ability to synthesize glutamine and lead to the use of the intermediates of glycolysis for anabolic activities (Rajala et al., 2016; Rueda et al., 2016; Chinchore et al., 2017).

This metabolic model has become very popular in the last years, so much that mathematical models based on this hypothesis have been developed to try to understand the metabolism of cones, rods, RPE, their relationship, and the role of the viability of these cells in the onset of some disorders as retinitis pigmentosa (Camacho et al., 2016, 2019; Aparicio et al., 2022).

However, this hypothesis has some drawbacks: 1) It does not explain the high density of mitochondria in the inner segments of the photoreceptors. A recent study has proposed an extra-metabolic role for PR mitochondria, as they may act as microlenses to enhance photon delivery (Ball et al., 2022). 2) As Lindsay et al. 2014 state in their research: "...The disadvantage is that MCs become dependent on other cells to fuel their mitochondria", which is not required in the ANLS hypothesis.

Evidently, more evidence is required to understand the flow and consumption of lactate in the retina, especially, because the vast majority of the studies are performed in retinas without the presence of RPE, or in co-culture conditions, something that can lead to misreading the results since the neural retina has a high metabolic dependence on RPE (Chen et al., 2022).

Metabolism in the inner retina

For meeting the high energy requirements mentioned before, the retinal neurons can consume metabolites from different sources. For instance, PRs can consume glucose, oxygen, and other metabolites that come from the choroidal blood, which is the main retinal vascularization (Country, 2017), and from the RPE (Chen et al., 2022). Nonetheless, the inner retina will depend on whether the retina is avascular or vascular. In the avascular retina (*e.g.,* guinea pig, rabbit), BCs and ACs probably rely only on MCs, while in the vascular retinas (*e.g.,* rodents and primates), these cells can take up fuel from the inner vascularity, MCs, and astrocytes (Yu and Cringle, 2001).

Clearly, several studies support the idea of a "metabolic ecosystem" in the retina, where cells not only release lactate but also consume it. However, the dynamics and the extension of this shuttle in the inner retina are still a matter of discussion, especially in vascular retinas (Hurley et al., 2015).

Surprisingly, little is known -and even could be considered controversial- about the retinal expression patterns of enzyme systems relevant for neuronal energy metabolism.

If inner retinal cells consume glucose to produce ATP, they need to express any GLUT to uptake this metabolite. Nevertheless, to date, it is not clear which GLUT isoform is expressed in inner retinal neurons. As mentioned before, glucose reaches the retina from the blood vessels of the choroid and inner vascularity, in which endothelial cells express GLUT1 (Birnbaum et al., 1986). GLUT1 expression is also established in RPE cells (Mantych et al., 1993; Chen et al., 2022) but an expression of GLUT1 has also been proposed in MCs and both types of photoreceptors (Hsu and Molday, 1991; Aït-Ali et al., 2015; Kanow et al., 2017). Some past studies have described GLUT2 expression during the development of the rat retina, while in the adult retina it seems to be limited to Müller cell endfeet (Watanabe et al., 1994). However, a recent study has proposed the expression of GLUT2 in horizontal cells, which could support the transport of this metabolite to PRs synapses (Yang et al., 2022).

Finally, GLUT3 which is known as the neuronal glucose transporter, seems to be expressed in the basal part of PRs IS, OPL, some sublaminas in the IPL (seemly in the S1 and S3), and weakly in some somas of the INL, which seem to be neurons (Watanabe and Matsushima, 1996; Chen et al., 2022).

These investigations are noteworthy, because they only support a weak expression of GLUT3 in inner retinal cell projections in vascular retinas (*e.g.,* rat retinas). Furthermore, if these cells do not express glucose transporters, they should be able to process other metabolites, and/or have transporters for other metabolites, for instance, lactate. Then, if the inner retina produces or consumes lactate, it needs a specialized transporter.

The MCT is a proton-linked plasma membrane transporter that allows carrying lactate and pyruvate into/out of cells (Halestrap and Price, 1999; Halestrap, 2013b). These transporters catalyze the facilitated diffusion of lactate with a proton. There is no energy input other than that provided by the concentration gradients of lactate and protons, although the latter, in the form of

a pH gradient, can drive the accumulation or exclusion of the lactate anion (Poole and Halestrap, 1993; Juel, 1997). MCTs have been identified in all eukaryotic individuals of which genomes have been sequenced. There are four isoforms in the MCT family: MCT1, MCT2, MCT3, and MCT4, of which 3 are expressed in the brain. All these isoforms allow passing several monocarboxylate metabolites, such as pyruvate, L-lactate, and ketone bodies across the plasma membrane (Halestrap, 2013a; Pérez-Escuredo et al., 2016).

At the CNS level, the cellular distribution has been associated with the ANLS hypothesis. Of the 4 isoforms, MCT1 and MCT2 have been proposed as the neuronal transporters, while MCT4 as the astrocytic transporter (Pellerin et al., 1998; Pierre et al., 2002; Bergersen, 2007, 2015; Barros, 2013). In this sense, MCTs have different affinities for lactate: MCT1 and MCT2 have higher affinities (lactate intake), while MCT4 has a lower affinity (lactate release). The K_m for MCT1 has been calculated close to 4 mM, for MCT2 in 1 mM, while the MCT4 has about 30 mM. Nonetheless, a last study has proposed a Km of 1.3 mM for lactate uptake for MCT4 (Contreras-Baeza et al., 2019). Overall, the kinetics and expression of these transporters are in line with the idea of lactate release from astrocytes (Bergersen, 2007, 2015).

Some researchers have suggested that extracellular lactate levels increase about 2-fold during brain activity (Dienel, 2012), which would imply a lactate efflux from the producer cells. Consistent with this, MCT4 has a higher affinity for lactate than pyruvate, which allows saving pyruvate for the conversion to lactate, maintaining glycolysis, and then serve lactate efflux. At the extracellular levels, this lactate could be quickly taken up by cells that express MCT1 and MCT2.

It is important to note that specific expression of these transporters cannot be taken as indicative of a direction in the metabolic pathway, because the rate of transport in either direction depends on the prevailing gradients of substrate and pH. However, some studies have proposed that in certain conditions some transporters (*i.e.,* MCT2 and MCT4) can almost exclusively transport lactate in one direction (Contreras-Baeza et al., 2019).

The retina apparently expresses all 4 MCT isoforms. MCT1 has been observed in photoreceptor inner segments, Muller cells, retinal capillaries, RPE, and both plexiform layers (Gerhart et al., 1999; Chidlow et al., 2004). MCT2 expression has been reported in the OPL, while MCT3 has been observed in RPE (Chidlow et al., 2004). MCT4 immunolabeling was present only in the inner retina, particularly in Muller cells (Gerhart et al., 1999; Chidlow et al., 2004).

Role of metabolism in neuronal activity

Since the principal function of neurons is propagating electrical signals, it is intuitive to think that their functions depend on metabolism and how cells obtain the energy (Cohen and Noell, 1960). The first studies measuring the effect of metabolic substrates on retinal electrophysiological properties of mammals date back to the '70s (Winkler et al., 1971; Winkler, 1975). Here, the researchers isolated the neural retina (no RPE), kept it in a perfusion chamber with constant bath perfusion, and measured the a-wave and b-wave under different conditions. Specifically, the exposure to anoxia produced a reduction in both waves in rabbits (Winkler, 1975), but only a significant decrease in the b-wave amplitude in rats (Winkler et al., 1971; Winkler, 1975), revealing the importance of oxidative metabolism for the retina (Cohen and Noell, 1960), especially for ON BCs (*i.e.,* b-wave) in vascular retinas, as is the rat's case.

Later, *in vivo* ERG demonstrated similar and interesting observations, in rats, after a bilateral carotid artery occlusion. Curiously, transient occlusion of the carotids for 45 min reduced the b-wave, but not affected the a-wave. On the other hand, a prolonged occlusion (7 days), abolished the b-wave, and enhanced the a-wave (Barnett and Osborne, 1995), revealing the sensitivity of inner neurons (at least, ON BCs) to metabolites and oxygen deprivation. In cats, the reduction of arterial PO_2 affected the b-wave when is below than 40mmHg, while the a-wave is more sensitive since begins to change when PO_2 falls below 70-80 mmHg (Linsenmeier, 1990). These results raise the question as to how inner retinal activity can be maintained when the outer retinal function is disrupted, suggesting the option that inner neurons can rely on alternative energy fuels.

The observations in rats that inhibition of MCTs attenuates the ERG b-wave, and the oscillatory potentials (Bui et al., 2004), indicate the importance of lactate production for the depolarization of the inner retina. Moreover, this alteration could be partially ameliorated with exogenous lactate, revealing a potential lactate uptake by inner retinal neurons (Bui et al., 2004). This idea is supported by another study in live mice, where the genetic deletion of PKM2 (*i.e.,* aerobic glycolysis marker), which is expressed in PRs, decreased the b-wave in mice (Rajala et al., 2018), suggesting that the production of lactate is needed to maintain this wave.

Taking all this information into account, interestingly, there is some information on retinal metabolism that suggests a possible consumption of lactate by inner retinal neurons to maintain their physiological activity. But single-cell studies are lacking to determine and support what substrate each cell consumes under physiological conditions.

Thus, in the present study we tested the role of extracellular lactate as a possible alternative energy substrate for mouse retinal bipolar cells. To address this question, we expressed genetically encoded FRET nanosensors that allowed us to qualitatively or quantitatively determine the levels of some metabolites in real-time (San Martín et al., 2013, 2014b, 2014a; Barros et al., 2014). The study of the role of lactate as a substrate for maintaining the physiological activity of inner retinal neurons was determined by calcium imaging and electrophysiology experiments. These measurements were complemented by markers of specific enzymes involved in aerobic glycolysis, pharmacological blockade of lactate transporters and enzymes related to aerobic glycolysis, and markers of cell death

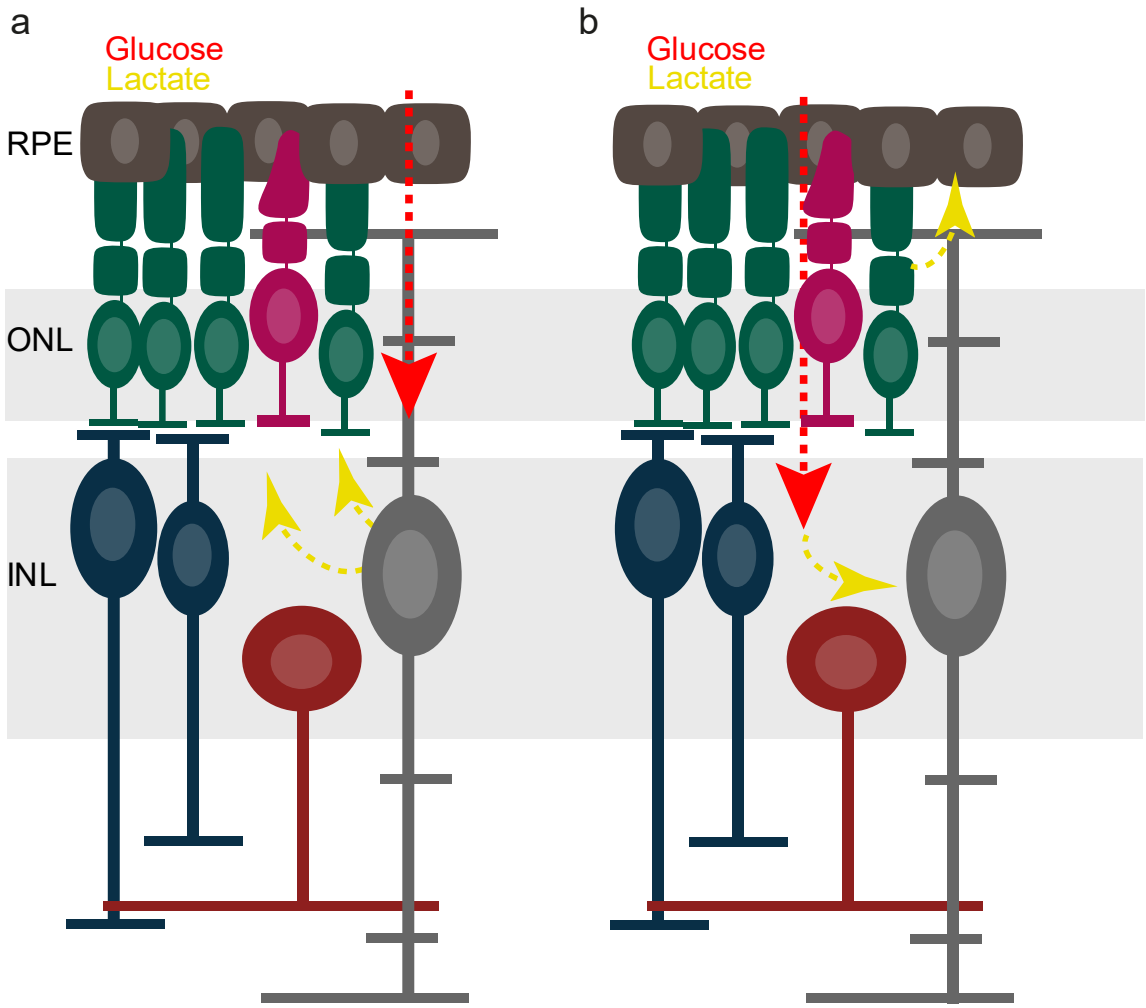

Figure 3.- Hypotheses on energy metabolism in the retina. (a) The astrocyte-neuron-lactate-shuttle (ANLS) hypothesis proposed by Pellerin and Magistretti in 1994 would mean for the retina that Müller glial cells perform glycolysis, whereas photoreceptors, would perform oxidative phosphorylation. **(b)** The hypothesis proposed by Kanow et al. 2017 states that retinal pigment epithelium (RPE) cells pass glucose to the photoreceptors, that photoreceptors are predominantly glycolytic, and that RPE cells and Müller cells then oxidatively recycle the lactate obtained from photoreceptors.

Hypothesis

It is increasingly being accepted that photoreceptors take up glucose and convert it partially into lactate by aerobic glycolysis, but the destiny of the produced lactate remain unclear. **Here I propose that this extracellular lactate can be taken up and used as fuel by bipolar cells to meet their physiological demands**.

Objectives

Main objective:

- To analyze the cellular and molecular organization of lactate shuttle in the inner retina.

Secondary objectives:

- To identify the expression pattern in the retina of key enzymes involved in aerobic glycolysis.
- To determine the role of lactate in the survival of retinal cells and the maintenance of their physiological activity.
- To determine the aerobic glycolysis rate in inner retinal cells.

DISCUSSION

Since the retina is an ontological part of the central nervous system, it shares several characteristics with the brain, including high energy demands. Therefore, the high production of lactate in the retina, which is energy inefficient, is so striking. Our work here adds important information regarding retinal lactate transport, combining different techniques for the purpose of demonstrating extracellular lactate consumption by INL cells (Fig. 4).

Effects of an alteration of lactate metabolism on INL cell survival.

The MCT2 expression in the inner retina is not surprising because this transporter is known as the neuronal MCT. Several authors have proposed in their models the neuronal consumption of lactate through this specific isoform over others (Pierre et al., 2002; Pérez-Escuredo et al., 2016; Magistretti and Allaman, 2018) and are in line with previous immunohistochemical studies in the retina (Gerhart et al., 1999; Chidlow et al., 2004). However, a functional demonstration of this expression and its role in the physiology of the inner retina was still needed, especially in vascular retinas, where the inner cells can obtain metabolites from a wider range of sources compared to photoreceptors (Yu and Cringle, 2001). Likely, this is the reason why we observed a low impact on the cell death rate in the TUNEL assay in the INL when we blocked MCT2 (only 1.67%). A previous work has demonstrated the ability of the neuroretina to be metabolically plastic to meet its energy demands (Chen et al., 2022). Although this study was focused on the outer retina, some

important enzymes involved in different metabolic pathways were expressed in the INL, therefore we cannot rule out the same capacity for the inner retina.

Moreover, here we found that under prolonged treatment with SR (MCT1 blocker), AR-C (MCT1 and MCT2 blockers) and shik (PKM2 inhibitor) that disrupt the lactate productions and transport, RBCs showed alterations in all conditions. This is interesting because it indicates a relevant dependence of RBCs on extracellular lactate. However, it is contradictory to the TUNEL results, as the number of RBCs decreased by almost 5%, compared to 1.6% in the TUNEL assay. One possible reason is a change in RBC identity. Previously, a couple of studies showed that a reduction in the number of RBCs is accompanied by a morphological change, especially in the dendrites, thus it may be indicative of reactive remodeling preceding the cell death process.(Jung et al., 2015; Yang et al., 2019). In addition, the TUNEL assay labels cells with substantial DNA damage. Therefore, in the process RBCs may have suffered alterations in important genes that regulate PKCα expression, producing a change in RBC markers that impairs immunolabeling, but these alterations may not be sufficient to become TUNEL-positive cells. (Jung et al., 2015).

An altered lactate metabolism has effects on intracellular ion homeostasis

Many studies have suggested dysregulation of calcium and sodium homeostasis under metabolic alterations (Llorente-Folch et al., 2015; Gerkau et al., 2017), and one possible explanation is the role of ATP production in the maintenance of ionic gradients after depolarizations (Country, 2017). Since transport of ions across biological membranes against concentration gradients is ATP-dependent, a disruption in the metabolism will affect the restoration of ions gradients (Karus et al., 2015a). Indeed, a delayed return to baseline is what we observed in the sodium signaling, strengthening the previous idea. Thus, this sluggish return can produce an accumulation of these ions in the cytoplasm leading to a reduction (and slowing) in the influx of different ions: in this study, specifically in calcium signaling (Gerkau et al., 2017). This accumulation of intracellular calcium may produce the depolarization in AR-C and mannitol conditions in RBCs in the

electrophysiology experiments, and in a long-term point of view likely is the reason of death cells process observed in the TUNEL assay.

Our initial hypothesis was that the blocking/inhibition of the enzymes involved in lactate metabolism would increase basal intracellular levels of different ions such as calcium or sodium, because the lack of ATP would reduce the capacity of different ion pumps. But the results not only demonstrate that this is not true for all the cases, but also that this disruption affects calcium and sodium homeostasis differentially. Moreover, the effect will depend on which transporter/enzyme is disrupted.

Indeed, it is surprising that the only case where we can explain our results with the idea mentioned before is under MCT2 blocking. This condition increases the basal calcium levels, probably due to the disruption in ion pump function reflected in the slowed decay time observed in the sodium experiments. This accumulation produces a smaller response amplitude due to lower calcium influx into the cell which is in line with a more positive intracellular environment that reduces the driving force. These alterations are also reflected in the slowed time-to-peak, and the depolarization observed in RBCs.

Nonetheless, this does not happen with sodium, where the application of AR-C induces a reduction in basal sodium levels. How can this be possible? Although this result explains the increment in the amplitude after a depolarization since a reduction in basal levels increases the driving force, this reduction does not support our hypothesis about the disruption of ion pump function.

On the other hand, this result might be explained by the role of these ions in mitochondrial function. It is well established that mitochondria are not only an energetic organelle, but also a calcium hub, where this ion, as well as sodium, might activate many enzymes related to the TCA cycle, enhancing ATP production (Nicholls, 2005; Satrústegui et al., 2007; Gellerich et al., 2009; Nita et al., 2014; Assali and Sekler, 2021; Cabral-Costa et al., 2022). These studies showed that an increase in cytoplasmic calcium concentrations directly produces a rise in mitochondrial calcium

levels, and this regulates 4 different dehydrogenases (as FAD-glycerol phosphate dehydrogenase, pyruvate dehydrogenase phosphatase, NAD-isocitrate dehydrogenase, oxoglutarate dehydrogenase), and different carriers (Denton, 2009; Gellerich et al., 2009; Rossi et al., 2019). The influx of this ion is through the mitochondrial calcium uniporter (MCU) and is driven by the high electronegative mitochondrial membrane potential. Subsequently, to recycle calcium ions, Ca^{2+} efflux is mediated by the electrogenic Na^{+}/ Ca^{2+} exchanger, NCLX (Denton, 2009; Cabral-Costa and Kowaltowski, 2020; Delierneux et al., 2020; Assali and Sekler, 2021). The activation of this exchanger might reduce the cytoplasmatic sodium concentration.

Intracellular sodium levels are also maintained by a dynamic equilibrium of influx and efflux regulated by many channels and transporters. Most of these transporters require a ligand and are involved only in sodium influx, because of its large concentration in the extracellular space. Therefore, the main sodium efflux carrier is the Na^{+}/K^{+} pump (Coppini et al., 2013), and this is exacerbated after a depolarization (Attwell and Laughlin, 2001). Another study proposed a non-canonical modulation of ATP levels by the Na^{+}/K^{+} pump, where the Na^{+} flux is capable of controlling glycolysis and ATP production (Baeza-Lehnert et al., 2019). Hence, the regulation of calcium and activation of Na^{+} pumping might induce the reduction of sodium in the cytoplasm.

Thus, the model proposed here to understand the results is: The blocking of MCT2 produces a reduction in OXPHOS, due to the presence of less substrate, triggering a drop in ATP levels. This metabolic imbalance leads to an increase in basal calcium levels, due to an accumulation of this ion by an alteration in ion pumping. This increase in calcium levels triggers an influx into the mitochondria that will enhance mitochondrial metabolism to restore ATP levels. This mitochondrial calcium influx leads to an activation of NCLX, causing a mitochondrial sodium influx. All this leads to a reduction in cytoplasmatic sodium and is amplified by an increased pump performance (Na^{+} efflux), triggered by cell depolarization (*e.g.,* in the RBC).

Nevertheless, since our experiments cannot directly demonstrate this idea in its entirety as we still need to rectify the participation of NCLX, further experiments will be needed to test this model.

Also, this explanation is for only one of the conditions tested here, while many questions remain open under other conditions (*i.e.,* SR, Shik and FX-11). However, as these enzymes apparently are not expressed in retinal inner neurons, indirect effects are likely to be involved.

Extracellular lactate as an alternative energy fuel to meet INL cells activity

If ion gradients are affected, then we should expect alterations in the different electrical responses. Some research has shown that ERG waves are sensitive to glucose deprivation and different metabolic stressors.(Ames et al., 1992; Winkler, 1981). Specifically, inhibition of MCTs with 4-CIN attenuates the b-wave with delayed implicit time, but in the presence of extracellular lactate a partial recovery was obtained (Bui et al., 2004). These results suggest a possible consumption of extracellular lactate by BCs to maintain electrical responses. Our results support this notion because inhibition of MCT2 produces a reduction in outward currents, calcium currents and increases the membrane potential in RBCs, triggered by an imbalance in calcium and sodium signaling. Additionally, the attenuation induced in the currents and membrane potential by glucose deprivation (*e.g.,* mannitol condition) is countered in presence of extracellular lactate (Karus et al., 2015b). Nevertheless, here we show that glucose is preferred over lactate to maintain its physiological activity (Winkler et al., 2004).

Retinal Müller cells as a possible place of lactate production

In the present study, we expressed glucose and lactate nanosensors in MCs of organotypic retinal explants to study changes in intracellular lactate concentrations under different conditions. Our observations may provide new insights into retinal metabolism through a live-cell imaging approach. Here, pharmacological data support MCT1, MCT2, and MCT4 isoform expression by MCs, fulfilling possibly different roles in lactate dynamics.

As expected, after a moderate general depolarization of +20 mV approximately (assuming intracellular concentrations of Na^+ and K^+ of 18 mM and 132 mM, respectively (Fernández et al., 2013)), MCs displayed glucose consumption as revealed by a reduction of the glucose sensor

signal. This variation supports the notion of a preference of glucose consumption by MCs in culture (Winkler et al., 2004; Toft-Kehler et al., 2018), and might explain the return to baseline of the Δ6 sensor in the presence of 10 mM glucose. The saturation of Δ6 at basal levels indicates that MCs work under a high intracellular glucose concentration, probably because of the metabolic coupling between these cells and the retinal neurons (Toft-Kehler et al., 2018; Grimes et al., 2021), which rely on MCs for the provision of different metabolites for their metabolic needs. Due to their central role in retinal metabolism and intimate association with blood vessels, MCs likely have high glucose uptake, used in part for the storage of glycogen (Toft-Kehler et al., 2018). On the other hand, in parallel to glucose consumption, MCs displayed an increase in lactate levels after depolarization. One explanation could be lactate accumulation accompanied by glucose consumption, as supported by the experiments under basal conditions. Nonetheless, under MCT inhibition, this increment in lactate levels is prevented. These results suggest that lactate flux may change depending on the activity of MCs and/or their surrounding neurons.

Our data support the expression of different MCT isoforms in MCs. The idea of MCT2 expression by MCs is surprising, since this transporter is known as the neuronal MCT (Pierre et al., 2002), and is indicative of a possible consumption of lactate under certain conditions. In fact, the aforementioned data support MCT2 expression in MCs of mouse retina, in line with previous immunohistochemical data for rats (Gerhart et al., 1999). These results could hence be interpreted as evidence against the ANLS hypothesis in the retina (Lindsay et al., 2014; Kanow et al., 2017). However, the demonstration of MCT4 expression and its role in lactate efflux are indicative of lactate production by MCs (Pellerin and Magistretti, 1994), supporting a complex metabolism in which retinal cells can change between lactate production and consumption, depending on the metabolic demands or the physiological context.

The expression of MCT1 in MCs expression is still somewhat uncertain, even though it was previously detected in rat retinal MCs (Gerhart et al., 1999), as well as very recently through single-cell transcriptomics analysis (Bisbach et al., 2022). However, our immunofluorescence

experiments did not confirm MCT1 in MCs, which could be due to different reasons. MCT1 expression might be developmentally regulated during the first weeks of life. As mentioned in methods, the retinal explant cultures were prepared from p9 mice (eyes closed) and maintained in culture for two weeks, while the retinal slices for immunostaining were prepared from p30 mice. This age difference could potentially produce a significant variation in MCT1 expression, given that the peak expression is apparently reached at p21, followed by a reduction in mRNA levels (Clamp et al., 2004). Furthermore, there is the possibility that MCT1 is not expressed in MCs. As observed in the immunolabelling and previously reported by others, there is a clear expression in photoreceptor inner segments (Bergersen et al., 1999; Chidlow et al., 2004; Peachey et al., 2018). Therefore, we cannot exclude the possibility that intracellular lactate in MCs might be indirectly affected by photoreceptors metabolically coupled to MCs. It would be relevant to further investigate why MCs might express different types of MCTs, and how the lactate flux through these transporters varies under different visual conditions. On the other hand, the functional results displayed suggest that MCT1, MCT2, and MCT4 are indeed expressed by MCs.

Here, we propose that MCT2 might be in charge of lactate influx and MCT1 and MCT4 of lactate efflux, according to prior suggestions in a high lactate environment (Contreras-Baeza et al., 2019). This suggests that MCs should express the intracellular enzymatic machinery to convert lactate to pyruvate, or pyruvate to lactate. It has been shown that MCs express the enzyme LDH-B isoform (Chinchore et al., 2017). Thus, MCs can convert lactate into pyruvate through LDH-B to fuel mitochondria and produce ATP through oxidative phosphorylation. On the other hand, MCs lack certain enzymes required for lactate production, specifically, the enzymes PKM2 and LDH-A (Lindsay et al., 2014; Chinchore et al., 2017; Rajala et al., 2018; Chen et al., 2022). It is possible that the expression of PKM1 and LDH-B are sufficient to sustain lactate synthesis in MCs and release it through MCT1 and MCT4 when metabolically required. Certainly, more direct evidence is required to test this idea in the future.

Inner retinal cells as potential lactate consumers

Although photoreceptors are known to be the most energy-consuming cells in the retina (Okawa et al., 2008; Ingram et al., 2020), it is important to understand the metabolism in less energy-consuming cells, cause the metabolism of the entire retina it is crucial to fully comprehend the evolution of the eye design (Baden et al., 2019). Especially the inner retina, where the processing of visual signals basically begins (Euler et al., 2014), but where it remains unclear which metabolic pathways the cells use to meet their physiological demands (Toft-Kehler et al., 2018; Vohra and Kolko, 2020).

Here, we expressed the FRET lactate nanosensor Laconic in organotypic retinal explant cultures to study lactate dynamics in putative BCs and ACs in real time. These types of nanosensor have become popular in recent years for the analysis of metabolic flux and transport of different metabolites in neurons, either in culture or *in vivo* (Bittner et al., 2011; San Martín et al., 2013; Mächler et al., 2016; Fernández-Moncada et al., 2018), showing a consumption on this metabolite by these cells.

In the present investigation, we propose the expression of MCT2 in INL and reveal the role of extracellular lactate in maintaining neuronal activity in INL cells, supporting a functional expression of MCT2. This result is expected since, as mentioned above, this isoform is known as the neuronal MCT (Pierre et al., 2002).

It is relevant that our observations not only suggest a possible role of extracellular lactate consumption by BCs and ACs to meet their neuronal activity by immunofluorescence and physiological experiments, but also demonstrate this idea with intracellular lactate measurements in inner neurons. In addition, we were able to study lactate dynamics under two different conditions: basal condition and depolarization. Here, our results indicate lactate consumption under basal conditions in inner retinal neurons, which is exacerbated under depolarization. Altogether, the results showed in this study indicate that the ANLS hypothesis is completely feasible under our conditions, where MCs might export lactate and inner neurons may import

lactate in culture basal conditions. However, we cannot exclude the option that other cells, as PRs, may export lactate in certain situations.

Previously, many studies had already proposed a possible metabolic coupling between MCs and inner retinal cells, especially, GCs (Vecino et al., 2016; Toft-Kehler et al., 2018; Vohra and Kolko, 2020). Those studies support the notion about a lactate production by MCs (Winkler et al., 2004; Vohra et al., 2017). The GCs are then capable of taking up this lactate and using it for OXPHOS and ATP production (Vohra et al., 2017). Furthermore, the present study extends these results to putative BCs and ACs, showing a direct consumption of intracellular lactate, and production by MCs in retinal explant culture.

Interestingly, this observation is not extrapolable to all inner neurons, since as shown, not all neurons show lactate consumption after depolarization. Although this is likely due to the great heterogeneity of cell types that compose the INL (Euler and Wässle, 1995; Euler et al., 2014; Shekhar et al., 2016a), and because it has been proposed that inner neurons also may be capable to produce lactate in primary culture conditions (Winkler et al., 2004).

Since all our experiments were carried out under scotopic/mesopic conditions, it is appropriate to consider that this metabolic model is subject to this specific environment. This assumption makes the retina a complex but interesting tissue to study metabolism, as different cells may have different metabolisms under different light levels, and metabolites to meet their metabolic demand may move between the RPE, the MCs, PRs, and now the INL (Vecino et al., 2016; Chen et al., 2022). The observations reported here allow us to point out that the inner retina participates in the retinal lactate shuttle, where MCs release lactate under basal conditions, and where BCs and ACs potentially consume a percentage of this extracellular lactate to meet their neuronal activity.

Although it is still a mystery how far this idea extends to global retinal lactate transport, and what could be the role of the outer retina in INL metabolism, some of our results could propose a possible interaction between PRs and INL (Vecino et al., 2016). Examples include the effects of blocking retinal MCT1 on MCs, a transporter that is not clearly expressed in these cells by

immunofluorescence experiments; the effects on calcium homeostasis under inhibition of MCT1, PKM2, and LDH-A, which are enzymes that are not directly expressed in BCs and ACs (Chen et al., 2022); and the small reduction in cytoplasmic lactate in BCs after MCT1 inhibition, which may reflect an impairment in lactate release by PRs.

Finally, it is important to emphasize that our study has limitations. For instance, all measurements were obtained from cell bodies, whereas the long cellular projections of MCs, BCs and ACs might be metabolically isolated and display different dynamics. Furthermore, the experimental conditions used here might will not accurately reflect the physiological conditions of *in vivo* retina. While retinas were light-adapted, photoreceptors can show variations in their activity after prolonged time in culture depending on the status of the RPE (Alarautalahti et al., 2019; Tolone et al., 2021).

Conclusion

The data presented in this investigation support the idea of lactate consumption by inner retinal cells. Therefore, they extend the types of cells in the retina capable of taking up lactate produced in this tissue. Here, we also propose that MCs are net lactate producers in a resting state and under *in vitro* conditions. However, these dynamics change under depolarization, indicating that the metabolism of MCs and their dependent neurons may vary according to retinal activity status.

Functional experiments indicate that BCs consume the extracellular lactate through MCT2 to meet their neuronal activity. Here we show that calcium and sodium homeostasis, inward and outward currents, and the membrane potential are sensitive to an impaired lactate metabolism in the short-term in RBCs, and cellular survival in the long-term.

Moreover, the successful expression of glucose and lactate nanosensors and the functional data obtained here with these may contribute to further understanding the complex retinal metabolism with cellular resolution, which is highly relevant for its physiology and retinopathies such as diabetic retinopathy.

In conclusion, our data support the notion that BCs can consume a portion of the extracellular lactate presented in the retina to meet their physiological demands. This lactate can be used to produce energy through OXPHOS.

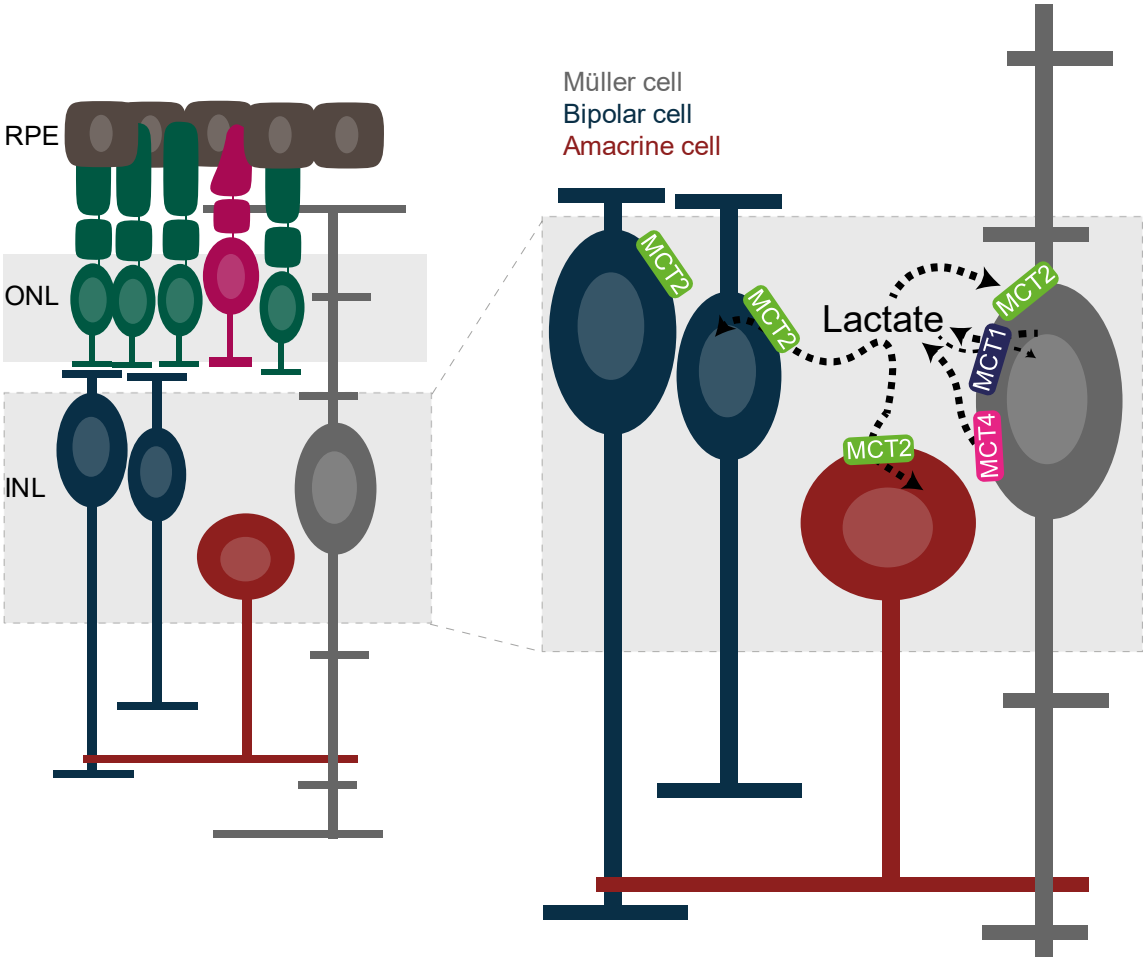

Figure 4.- Model for the lactate dynamics in the inner retinal cells. General model proposing a consumption of lactate by inner retinal cells. Our data demonstrate the functional expression of MCT1, MCT2 and MCT4 in MCs, where MCT2 regulates lactate influx (in a minor role also MCT1), and MCT4 of lactate efflux, contributing to the accumulation of extracellular lactate. This extracellular lactate produced by MCs and probably other retinal cell types is consumed by BCs and ACs through MCT2. MCT1= Monocarboxylate transporter 1; MCT2= Monocarboxylate transporter 2; MCT4= Monocarboxylate transporter 4.

REFERENCES

Adeva-Andany, M., López-Ojén, M., Funcasta-Calderón, R., Ameneiros-Rodríguez, E., Donapetry-García, C., Vila-Altesor, M., et al. (2014). Comprehensive review on lactate metabolism in human health. *Mitochondrion* 17, 76–100. doi:10.1016/j.mito.2014.05.007.

Aït-Ali, N., Fridlich, R., Millet-Puel, G., Clérin, E., Delalande, F., Jaillard, C., et al. (2015). Rod-derived cone viability factor promotes cone survival by stimulating aerobic glycolysis. *Cell* 161, 817–832. doi:10.1016/j.cell.2015.03.023.

Akram, M. (2013). Mini-review on glycolysis and cancer. *J. Cancer Educ.* 28, 454–457. doi:10.1007/s13187-013-0486-9.

Alarautalahti, V., Ragauskas, S., Hakkarainen, J. J., Uusitalo-Järvinen, H., Uusitalo, H., Hyttinen, J., et al. (2019). Viability of mouse retinal explant cultures assessed by preservation of functionality and morphology. *Investig. Ophthalmol. Vis. Sci.* 60, 1914–1927. doi:10.1167/iovs.18-25156.

Ames, A. I. I. I., Li, Y. Y., Heher, E. C., and Kimble, C. R. (1992a). Energy Metabolism of Rabbit Retina as Related to Function : High Cost of Na + Transport. *J. Neurosci.* 12, 840–853.

Ames, A., Li, Y.-Y., Heher, E. C., and Kimble, C. R. (1992b). Energy metabolism of rabbit retina as related to function: high cost of Na+ transport. *J. Neurosci.* 12, 840–853. doi:10.1523/JNEUROSCI.12-03-00840.1992.

Aparicio, A., Camacho, E. T., Philp, N. J., and Wirkus, S. A. (2022). A mathematical model of GLUT1 modulation in rods and RPE and its differential impact in cell metabolism. *Sci. Rep.* 12, 1–20. doi:10.1038/s41598-022-13950-3.

Assali, E. A., and Sekler, I. (2021). Sprinkling salt on mitochondria: The metabolic and

pathophysiological roles of mitochondrial Na+ signaling mediated by NCLX. *Cell Calcium* 97, 102416. doi:10.1016/j.ceca.2021.102416.

Attwell, D., and Laughlin, S. B. (2001). An energy budget for signaling in the grey matter of the brain. *J. Cereb. Blood Flow Metab.* 21, 1133–1145. doi:10.1097/00004647-200110000-00001.

Baden, T., Euler, T., and Berens, P. (2019). Understanding the retinal basis of vision across species. *Nat. Rev. Neurosci.* 21, 5–20. doi:10.1038/s41583-019-0242-1.

Baenke, F., Peck, B., Miess, H., and Schulze, A. (2013). Hooked on fat: The role of lipid synthesis in cancer metabolism and tumour development. *DMM Dis. Model. Mech.* 6, 1353–1363. doi:10.1242/dmm.011338.

Baeza-Lehnert, F., Saab, A. S., Gutiérrez, R., Larenas, V., Díaz, E., Horn, M., et al. (2019). Non-Canonical Control of Neuronal Energy Status by the Na + Pump. *Cell Metab.* 29, 668-680.e4. doi:10.1016/j.cmet.2018.11.005.

Ball, J. M., Chen, S., and Li, W. (2022). Mitochondria in cone photoreceptors act as microlenses to enhance photon delivery and confer directional sensitivity to light. *Sci. Adv.* 8. doi:10.1126/sciadv.abn2070.

Barnett, N., and Osborne, N. (1995). Prolonged Bilateral Carotid Artery Occlusion Induces Electrophysiological and Immunohistochemical Changes to the Rat Retina Without Causing Histological Damage. *Exp. Eye Res.* 61, 83–90.

Barros, L. F. (2013). Metabolic signaling by lactate in the brain. *Trends Neurosci.* 36, 396–404. doi:10.1016/j.tins.2013.04.002.

Barros, L. F., Baeza-Lehnert, F., Valdebenito, R., Ceballo, S., and Alegría, K. (2014). “Fluorescent Nanosensor Based Flux Analysis: Overview and the Example of Glucose.,” in *In Brain Energy* (New york: humana press), 145–159.

Barros, L. F., Ruminot, I., San Martín, A., Lerchundi, R., Fernández-Moncada, I., and Baeza-Lehnert, F. (2020). Aerobic Glycolysis in the Brain: Warburg and Crabtree Contra Pasteur. *Neurochem. Res.* doi:10.1007/s11064-020-02964-w.

Barros, L. F., and Weber, B. (2018). CrossTalk proposal: an important astrocyte-to-neuron lactate shuttle couples neuronal activity to glucose utilisation in the brain. *J. Physiol.* 596, 347–350. doi:10.1113/JP274944.

Behrens, C., Schubert, T., Haverkamp, S., Euler, T., and Berens, P. (2016). Connectivity map of bipolar cells and photoreceptors in the mouse retina. *Elife* 5, 1–20. doi:10.7554/eLife.20041.

Belhadj, S., Tolone, A., Christensen, G., Das, S., Chen, Y., and Paquet-Durand, F. (2020). Long-term, serum-free cultivation of organotypic mouse retina explants with intact retinal pigment epithelium. *J. Vis. Exp.* 2020, 1–13. doi:10.3791/61868.

Bergersen, L. H. (2007). REVIEW IS LACTATE FOOD FOR NEURONS ? COMPARISON OF MONOCARBOXYLATE TRANSPORTER SUBTYPES IN BRAIN AND MUSCLE. 145, 11–19. doi:10.1016/j.neuroscience.2006.11.062.

Bergersen, L. H. (2015). Lactate transport and signaling in the brain : potential therapeutic targets and roles in body – brain interaction. 176–185. doi:10.1038/jcbfm.2014.206.

Bergersen, L., Jo, E., Veruki, M. L., and Nagelhus, E. A. (1999). Cellular and subcellular expression of monocarboxylate transporters in the pigment epithelium and retina of the rat. *Neuroscience* 90, 319–331.

Birnbaum, M. J., Haspel, H. C., and Rosen, O. M. (1986). Cloning and characterization of a cDNA encoding the rat brain glucose-transporter protein. *Proc. Natl. Acad. Sci.* 83, 5784–5788.

Bisbach, C. M., Hass, D. T., Thomas, E. D., Cherry, T. J., Hurley, J. B., Ed, T., et al. (2022).

Monocarboxylate Transporter 1 (MCT1) mediates succinate export in the retina. *Invest. Ophthalmol. Vis. Sci.* 63, 1–1.

Bittner, C. X. (2010). High resolution measurement of the glycolytic rate. *Front. Neuroenergetics* 2, 1–11. doi:10.3389/fnene.2010.00026.

Bittner, C. X., Valdebenito, R., Ruminot, I., Loaiza, A., Larenas, V., Sotelo-Hitschfeld, T., et al. (2011). Fast and reversible stimulation of astrocytic glycolysis by K+ and a delayed and persistent effect of glutamate. *J. Neurosci.* 31, 4709–4713. doi:10.1523/JNEUROSCI.5311-10.2011.

Braekevelt, C. R. (1991). Fine structure of the pecten oculi of the emu Dromaius novaehollandiae]. *Tissue Cell* 30, 157–165. doi:10.1016/S0040-8166(98)80064-5.

Brini, M., Calì, T., Ottolini, D., and Carafoli, E. (2013). “Intracellular calcium homeostasis and signaling,” in *In Metallomics and the Cell*, 119–168. doi:10.1007/978-94-007-5561-1_5.

Bui, B. V, Kalloniatis, M., and Vingrys, A. J. (2004). Retinal Function Loss after Monocarboxylate Transport Inhibition. *Invest. Ophthalmol. Vis. Sci.* 45, 584–593. doi:10.1167/iovs.03-0695.

Cabral-Costa, J. V., and Kowaltowski, A. J. (2020). Neurological disorders and mitochondria. *Mol. Aspects Med.* 71, 100826. doi:10.1016/j.mam.2019.10.003.

Cabral-Costa, J. V., Vicente-Gutierrez, C., Agulla, J., Lapresa, R., Elrod, J. W., Almeida, A., et al. (2022). Mitochondrial sodium / calcium exchanger NCLX regulates glycolysis in astrocytes , impacting on cognitive performance. *bioRxiv*. doi:10.1101/2022.09.16.507284.

Calbiague, V., Chen, Y., Cádiz, B., and Paquet-durand, F. (2022). Imaging of lactate metabolism in retinal Müller cells with a FRET nanosensor. *bioRxiv*, 1–16. doi:10.1101/2022.10.05.510984.

Calbiague, V. M., Vielma, A. H., Cadiz, B., Paquet-Durand, F., and Schmachtenberg, O. (2020). Physiological assessment of high glucose neurotoxicity in mouse and rat retinal explants.

J. Comp. Neurol. 528, 989–1002. doi:10.1002/cne.24805.

Camacho, E. T., Brager, D., Elachouri, G., Korneyeva, T., Millet-Puel, G., Sahel, J. A., et al. (2019). A Mathematical Analysis of Aerobic Glycolysis Triggered by Glucose Uptake in Cones. *Sci. Rep.* 9, 1–18. doi:10.1038/s41598-019-39901-z.

Camacho, E. T., Punzo, C., and Wirkus, S. A. (2016). Quantifying the metabolic contribution to photoreceptor death in retinitis pigmentosa via a mathematical model. *J. Theor. Biol.* 408, 75–87. doi:10.1016/j.jtbi.2016.08.001.

Chávez, A. E., Singer, J. H., and Diamond, J. S. (2006). Fast neurotransmitter release triggered by Ca influx through AMPA-type glutamate receptors. *Nature* 443, 705–708. doi:10.1038/nature05123.

Chen, J., Xie, J., Jiang, Z., Wang, B., Wang, Y., and Hu, X. (2011). Shikonin and its analogs inhibit cancer cell glycolysis by targeting tumor pyruvate kinase-M2. *Oncogene* 30, 4297–4306. doi:10.1038/onc.2011.137.

Chen, Y., Zizmare, L., Calbiague, V., Yu, S., and Herberg, F. W. (2022). Retinal energy metabolism : Photoreceptors switch between Cori , Cahill , and mini-Krebs cycles to uncouple glycolysis from mitochondrial respiration. *bioRxiv*.

Chidlow, G., Wood, J. P. M., Graham, M., Osborne, N. N., Wood, J. P. M., and Graham, M. (2004). Expression of monocarboxylate transporters in rat ocular tissues. *Am. J. Physiol. Physiol.* 288, 416–428. doi:10.1152/ajpcell.00037.2004.

Chinchore, Y., Begaj, T., Wu, D., Drokhlyansky, E., and Cepko, C. L. (2017). Glycolytic reliance promotes anabolism in photoreceptors. *Elife* 6, 1–22. doi:10.7554/eLife.25946.

Christofk, H. R., Vander Heiden, M. G., Harris, M. H., Ramanathan, A., Gerszten, R. E., Wei, R., et al. (2008). The M2 splice isoform of pyruvate kinase is important for cancer metabolism and tumour growth. *Nature* 452, 230–233. doi:10.1038/nature06734.

Chuquet, J., Quilichini, P., Nimchinsky, E. A., and Buzsáki, G. (2010). Predominant enhancement of glucose uptake in astrocytes versus neurons during activation of the somatosensory cortex. *J. Neurosci.* 30, 15298–15303. doi:10.1523/JNEUROSCI.0762-10.2010.

Clamp, M. F., Ochrietor, J. D., Moroz, T. P., and Linser, P. J. (2004). Developmental analyses of 5A11/Basigin, 5A11/Basigin-2 and their putative binding partner MCT1 in the mouse eye. *Exp. Eye Res.* 78, 777–789. doi:10.1016/j.exer.2003.12.004.

Cohen, L. H., and Noell, W. K. (1960). Glucose Catabolism of Rabbit Retina Before and After Development of Visual Function. *J. Neurochem.* 5, 253–276. doi:10.1111/j.1471-4159.1960.tb13363.x.

Connaughton, V. P., Graham, D., and Nelson, R. (2004). Identification and morphological classification of horizontal, bipolar, and amacrine cells within the zebrafish retina. *J. Comp. Neurol.* 477, 371–385. doi:10.1002/cne.20261.

Contreras-Baeza, Y., Sandoval, P. Y., Alarcón, R., Galaz, A., Cortés-Molina, F., Alegriá, K., et al. (2019). Monocarboxylate transporter 4 (MCT4) is a high affinity transporter capable of exporting lactate in high-lactate microenvironments. *J. Biol. Chem.* 294, 20135–20147. doi:10.1074/jbc.RA119.009093.

Cooper, G. (2000). “The mechanism of oxidative phosporilation,” in *The cell: A molecular approach* (Sunderland (MA): Sinauer Associates).

Coppini, R., Ferrantini, C., Mazzoni, L., Sartiani, L., Olivotto, I., Poggesi, C., et al. (2013). Regulation of intracellular Na + in health and disease: pathophysiological mechanisms and implications for treatment . *Glob. Cardiol. Sci. Pract.* 2013, 30. doi:10.5339/gcsp.2013.30.

Country, M. W. (2017). Retinal metabolism : A comparative look at energetics in the retina. *Brain Res.* 1672, 50–57. doi:10.1016/j.brainres.2017.07.025.

Delierneux, C., Kouba, S., Shanmughapriya, S., Potier-Cartereau, M., Trebak, M., and Hempel, N. (2020). Mitochondrial Calcium Regulation of Redox Signaling in Cancer. *Cells* 9, 1–24. doi:10.3390/cells9020432.

Deng, D., and Yan, N. (2016). GLUT, SGLT, and SWEET: Structural and mechanistic investigations of the glucose transporters. *Protein Sci.* 25, 546–558. doi:10.1002/pro.2858.

Denton, R. M. (2009). Regulation of mitochondrial dehydrogenases by calcium ions. *Biochim. Biophys. Acta - Bioenerg.* 1787, 1309–1316. doi:10.1016/j.bbabio.2009.01.005.

Dienel, G. A. (2012). Brain lactate metabolism: The discoveries and the controversies. *J. Cereb. Blood Flow Metab.* 32, 1107–1138. doi:10.1038/jcbfm.2011.175.

Dienel, G., and Hertz, L. (2001). Glucose and lactate metabolism during brain activation. *J. Neurosci. Res.* 65, 824–838.

Du, J., Cleghorn, W., Contreras, L., Linton, J. D., Chan, G. C. K., Chertov, A. O., et al. (2013). Cytosolic reducing power preserves glutamate in retina. *Proc. Natl. Acad. Sci. U. S. A.* 110, 18501–18506. doi:10.1073/pnas.1311193110.

Du, J., Rountree, A., Cleghorn, W. M., Contreras, L., Lindsay, K. J., Sadilek, M., et al. (2016a). Phototransduction influences metabolic flux and nucleotide metabolism in mouse retina. *J. Biol. Chem.* 291, 4698–4710. doi:10.1074/jbc.M115.698985.

Du, J., Yanagida, A., Knight, K., Engel, A. L., Vo, A. H., Jankowski, C., et al. (2016b). Reductive carboxylation is a major metabolic pathway in the retinal pigment epithelium. *Proc. Natl. Acad. Sci. U. S. A.* 113, 14710–14715. doi:10.1073/pnas.1604572113.

Eales, K. L., Hollinshead, K. E. R., and Tennant, D. A. (2016). Hypoxia and metabolic adaptation of cancer cells. *Oncogenesis* 5. doi:10.1038/ONCSIS.2015.50.

Eastman, J., and Lannoo, M. (2007). Brain and sense organ Anatomy and Histology of two Species of Phyletically basal Non-antartic Thornfishes of the Antastic Suborder

Notothenioidei (Perciformes: Bovichtidae). *J. Morphol.* 503, 1042–1154. doi:10.1002/jmor.

Euler, T., Haverkamp, S., Schubert, T., and Baden, T. (2014). Retinal bipolar cells: Elementary building blocks of vision. *Nat. Rev. Neurosci.* 15, 507–519. doi:10.1038/nrn3783.

Euler, T., and Wässle, H. (1995). Immunocytochemical identification of cone bipolar cells in the rat retina. *J. Comp. Neurol.* 361, 461–478. doi:10.1002/cne.903610310.

Fernández-Moncada, I., Ruminot, I., Robles-Maldonado, D., Alegría, K., Deitmer, J. W., and Barros, L. F. (2018). Neuronal control of astrocytic respiration through a variant of the Crabtree effect. *Proc. Natl. Acad. Sci. U. S. A.* 115, 1623–1628. doi:10.1073/pnas.1716469115.

Fernández, J. M., Di Giusto, G., Kalstein, M., Melamud, L., Rivarola, V., Ford, P., et al. (2013). Cell Volume Regulation in Cultured Human Retinal Müller Cells Is Associated with Changes in Transmembrane Potential. *PLoS One* 8. doi:10.1371/journal.pone.0057268.

Fyk-Kolodziej, B., Qin, P., and Pourcho, R. G. (2003). Identification of a cone bipolar cell in cat retina which has input from both rod and cone photoreceptors. *J. Comp. Neurol.* 464, 104–113. doi:10.1002/cne.10784.

Gatenby, R. A., and Gillies, R. J. (2004). Why do cancers have high aerobic glycolysis? *Nat. Rev. Cancer* 4, 891–899. doi:10.1038/nrc1478.

Gellerich, F. N., Gizatullina, Z., Arandarcikaite, O., Jerzembek, D., Vielhaber, S., Seppet, E., et al. (2009). Extramitochondrial Ca2+ in the nanomolar range regulates glutamate-dependent oxidative phosphorylation on demand. *PLoS One* 4, 4–8. doi:10.1371/journal.pone.0008181.

Gerhart, D. Z., Leino, R. L., and Drewes, L. R. (1999). Distribution of monocarboxylate transporters MCT1 and MCT2 in rat retina. *Neuroscience* 92, 367–375.

Gerkau, N. J., Rakers, C., Petzold, G. C., and Rose, C. R. (2017). Differential effects of energy

deprivation on intracellular sodium homeostasis in neurons and astrocytes. *J. Neurosci. Res.* 95, 2275–2285. doi:10.1002/jnr.23995.

Grimes, W. N., Aytürk, D. G., Hoon, M., Yoshimatsu, T., Gamlin, C., Carrera, D., et al. (2021). A high-density narrow-field inhibitory retinal interneuron with direct coupling to Müller glia. *J. Neurosci.* 41, 6018–6037. doi:10.1523/JNEUROSCI.0199-20.2021.

Hack, I., Peichl, L., and Brandstätter, J. H. (1999). An alternative pathway for rod signals in the rodent retina: Rod photoreceptors, cone bipolar cells, and the localization of glutamate receptors. *Proc. Natl. Acad. Sci. U. S. A.* 96, 14130–14135. doi:10.1073/pnas.96.24.14130.

Halestrap, A. P. (2013a). Monocarboxylic Acid Transport. *Compr. Physiol.* 3, 1611–1643. doi:10.1002/cphy.c130008.

Halestrap, A. P. (2013b). The SLC16 gene family-Structure, role and regulation in health and disease. *Mol. Aspects Med.* 34, 337–349. doi:10.1016/j.mam.2012.05.003.

Halestrap, A. P., and Price, N. T. (1999). The proton-linked monocarboxylate transporter (MCT) family: structure, function and regulation. *Biochem. J.* 299, 281–299.

Halim, N. D., Mcfate, T., Mohyeldin, A., Okagaki, P., Korotchkina, L. G., Patel, M. S., et al. (2010). Phosphorylation status of pyruvate dehydrogenase distinguishes metabolic phenotypes of cultured rat brain astrocytes and neurons. *Glia* 58, 1168–1176. doi:10.1002/glia.20996.

Harris, J. J., Jolivet, R., and Attwell, D. (2012). Synaptic Energy Use and Supply. *Neuron* 75, 762–777. doi:10.1016/j.neuron.2012.08.019.

Hartveit, E. (1997). Functional organization of cone bipolar cells in the rat retina. *J. Neurophysiol.* 77, 1716–1730. doi:10.1152/jn.1997.77.4.1716.

Herrero-Mendez, A., Almeida, A., Fernández, E., Maestre, C., Moncada, S., and Bolaños, J. P. (2009). The bioenergetic and antioxidant status of neurons is controlled by continuous

degradation of a key glycolytic enzyme by APC/C-Cdh1. *Nat. Cell Biol.* 11, 747–752. doi:10.1038/ncb1881.

Hertz, L., and Rothman, D. L. (2017). Glutamine-glutamate cycle flux is similar in cultured astrocytes and brain and both glutamate production and oxidation are mainly catalyzed by aspartate aminotransferase. *Biology (Basel).* 6, 1–21. doi:10.3390/biology6010017.

Hsu, S., and Molday, R. S. (1991). Glycolytic Enzymes and a GLUT-1 Glucose Transporter in the Outer Segments of Rod and Cone Photoreceptor Cells. *J. Biol. Chem.* 266, 21745–21752.

Hurley, J. B., Lindsay, K. J., and Du, J. (2015a). Mini-Review Glucose , Lactate , and Shuttling of Metabolites in Vertebrate Retinas. 1092, 1079–1092. doi:10.1002/jnr.23583.

Hurley, J. B., Lindsay, K. J., and Du, J. (2015b). Mini-Review Glucose , Lactate , and Shuttling of Metabolites in Vertebrate Retinas. 1092, 1079–1092. doi:10.1002/jnr.23583.

Ingram, N. T., Fain, G. L., and Sampath, A. P. (2020). Elevated energy requirement of cone photoreceptors. *Proc. Natl. Acad. Sci. U. S. A.* 117, 19599–19603. doi:10.1073/pnas.2001776117.

Ioannou, M. S., Jackson, J., Sheu, S. H., Chang, C. L., Weigel, A. V., Liu, H., et al. (2019). Neuron-Astrocyte Metabolic Coupling Protects against Activity-Induced Fatty Acid Toxicity. *Cell* 177, 1522-1535.e14. doi:10.1016/j.cell.2019.04.001.

Jimenez-Blasco, D., Busquets-Garcia, A., Hebert-Chatelain, E., Serrat, R., Vicente-Gutierrez, C., Ioannidou, C., et al. (2020). Glucose metabolism links astroglial mitochondria to cannabinoid effects. *Nature*. doi:10.1038/s41586-020-2470-y.

Juel, C. (1997). Lactate-proton cotransport in skeletal muscle. *Physiol. Rev.* 77, 321–358. doi:10.1152/physrev.1997.77.2.321.

Jung, C. C., Atan, D., Ng, D., Ploder, L., Ross, S. E., Klein, M., et al. (2015). Transcription factor

PRDM8 is required for rod bipolar and type 2 OFF-cone bipolar cell survival and amacrine subtype identity. *Proc. Natl. Acad. Sci. U. S. A.* 112, E3010–E3019. doi:10.1073/pnas.1505870112.

Kanow, M. A., Giarmarco, M. M., Jankowski, C. S. R., Tsantilas, K., Engel, A. L., Du, J., et al. (2017). Biochemical adaptations of the retina and retinal pigment epithelium support a metabolic ecosystem in the vertebrate eye. *Elife* 6, 1–25. doi:10.7554/eLife.28899.

Karus, C., Mondragão, M. A., Ziemens, D., and Rose, C. R. (2015a). Astrocytes restrict discharge duration and neuronal sodium loads during recurrent network activity. *Glia* 63, 936–957. doi:10.1002/glia.22793.

Karus, C., Ziemens, D., and Rose, C. R. (2015b). Lactate rescues neuronal sodium homeostasis during impaired energy metabolism. *Channels (Austin).* 9, 200–208. doi:10.1080/19336950.2015.1050163.

Kiama, S. G., Maina, J. N., Bhattacharjee, J., and Weyrauch, K. D. (2001). Functional morphology of the pecten oculi in the nocturnal spotted eagle owl (Bubo bubo africanus), and the diurnal black kite (Milvus migrans) and domestic fowl (Gallus gallus var . domesticus): a comparative study. *J. Zool.* 254, 521–528.

Kofuji, P., and Newman, E. (2004). Potassium buffering in the central nervous system. *Neuroscience* 129, 1045–1056.

Koike, C., Numata, T., Ueda, H., Mori, Y., and Furukawa, T. (2010). TRPM1: A vertebrate TRP channel responsible for retinal ON bipolar function. *Cell Calcium* 48, 95–101. doi:10.1016/j.ceca.2010.08.004.

Kolko, M., Vosborg, F., Henriksen, U. L., Hasan-Olive, M. M., Diget, E. H., Vohra, R., et al. (2016). Lactate Transport and Receptor Actions in Retina: Potential Roles in Retinal Function and Disease. *Neurochem. Res.* 41, 1229–1236. doi:10.1007/s11064-015-1792-x.

Krishnan, J., and Rohner, N. (2017). Cavefish and the basis for eye loss. *Philos. Trans. R. Soc. B Biol. Sci.* 372. doi:10.1098/rstb.2015.0487.

Le, A., Cooper, C. R., Gouw, A. M., Dinavahi, R., Maitra, A., Deck, L. M., et al. (2009). Inhibition of lactate dehydrogenase A induces oxidative stress and inhibits tumor progression. *Proc. Natl. Acad. Sci.* 107, 2037–2042. doi:10.1073/pnas.0914433107.

Le Masson, G., Przedborski, S., and Abbott, L. F. (2014). A Computational Model of Motor Neuron Degeneration. *Neuron* 83, 975–988. doi:10.1016/j.neuron.2014.07.001.

Lenzen, S. (2014). A fresh view of glycolysis and glucokinase regulation: History and current status. *J. Biol. Chem.* 289, 12189–12194. doi:10.1074/jbc.R114.557314.

Lerchundi, R., Fernández-Moncada, I., Contreras-Baeza, Y., Sotelo-Hitschfeld, T., Mächler, P., Wyss, M. T., et al. (2015). NH4+ triggers the release of astrocytic lactate via mitochondrial pyruvate shunting. *Proc. Natl. Acad. Sci. U. S. A.* 112, 11090–11095. doi:10.1073/pnas.1508259112.

Li, W., Chen, S., and Devries, S. (2010). A fast rod photoreceptor signaling pathway in the mammalian retina. *Nat. Neurosci.* 13, 414–416. doi:10.1038/nn.2507.

Li, Y. N., Tsujimura, T., Kawamura, S., and Dowling, J. E. (2012). Bipolar cell-photoreceptor connectivity in the zebrafish (Danio rerio) retina. *J. Comp. Neurol.* 520, 3786–3802. doi:10.1002/cne.23168.

Lindsay, K. J., Du, J., Sloat, S. R., Contreras, L., Linton, J. D., Turner, S. J., et al. (2014). distributions reveal key metabolic links between neurons and glia in retina. *Proc. Natl. Acad. Sci.* 111, 15579–15584. doi:10.1073/pnas.1412441111.

Linsenmeier, R. A. (1990). Ophthalmology Electrophysiological consequences of retinal hypoxia. *Graefe's Arch. Clin. Exp. Ophthalmol.* 228, 143–150.

Llorente-Folch, I., Rueda, C. B., Pardo, B., Szabadkai, G., Duchen, M. R., and Satrustegui, J.

(2015). The regulation of neuronal mitochondrial metabolism by calcium. *J. Physiol.* 593, 3447–3462.

Luo, W., and Semenza, G. L. (2012). Emerging roles of PKM2 in cell metabolism and cancer progression. *Trends Endocrinol. Metab.* 23, 560–566. doi:10.1016/j.tem.2012.06.010.

Mächler, P., Wyss, M. T., Elsayed, M., Stobart, J., Gutierrez, R., Von Faber-Castell, A., et al. (2016). In Vivo Evidence for a Lactate Gradient from Astrocytes to Neurons. *Cell Metab.* 23, 94–102. doi:10.1016/j.cmet.2015.10.010.

Magistretti, P. J., and Allaman, I. (2018). Lactate in the brain: From metabolic end-product to signalling molecule. *Nat. Rev. Neurosci.* 19, 235–249. doi:10.1038/nrn.2018.19.

Magistretti, P. J., and Pellerin, L. (1999). Cellular mechanisms of brain energy metabolism and their relevance to functional brain imaging. *Philos. Trans. R. Soc. B Biol. Sci.* 354, 1155–1163. doi:10.1098/rstb.1999.0471.

Manoj, K. M., Nirusimhan, V., Parashar, A., Edward, J., and Gideon, D. A. (2022). Murburn precepts for lactic-acidosis, Cori cycle, and Warburg effect: Interactive dynamics of dehydrogenases, protons, and oxygen. *J. Cell. Physiol.* 237, 1902–1922. doi:10.1002/jcp.30661.

Mantych, G. J., Hageman, G. S., and Devaskar, S. U. (1993). Characterization of glucose transporter isoforms in the adult and developing human eye. *Endocrinology* 133, 600–607.

Masland, R. H. (2012). The Neuronal Organization of the Retina. *Neuron* 76, 266–280. doi:10.1016/j.neuron.2012.10.002.

Maturaga, A., Kremmer, E., and Müller, F. (2007). Type 3a and Type 3b OFF Cone Bipolar Cells Provide for the Alternative Rod Pathway in the Mouse Retina. *J. Comp. Neurol.* 502, 1123–1137. doi:10.1002/cne.21367.

McKenna, M. C., Waagepetersen, H. S., Schousboe, A., and Sonnewald, U. (2006). Neuronal

and astrocytic shuttle mechanisms for cytosolic-mitochondrial transfer of reducing equivalents: Current evidence and pharmacological tools. *Biochem. Pharmacol.* 71, 399–407. doi:10.1016/j.bcp.2005.10.011.

Miao, P., Sheng, S., Sun, X., Liu, J., and Huang, G. (2013). Lactate dehydrogenase A in cancer: a promising target for diagnosis and therapy. *IUBMB Life* 65, 904–910. doi:10.1002/iub.1216.

Nicholls, D. G. (2005). Mitochondria and calcium signaling. *Cell Calcium* 38, 311–317. doi:10.1016/j.ceca.2005.06.011.

Nickla, D., and Wallman, J. (2010). The multifunctional choroid. *Prog. Retin. Eye Res.* 29, 144–168.

Nita, I. I., Hershfinkel, M., Kantor, C., Rutter, G. A., Lewis, E. C., and Sekler, I. (2014). Pancreatic β-cell Na+ channels control global Ca 2+ signaling and oxidative metabolism by inducing Na+and Ca2+ responses that are propagated into mitochondria. *FASEB J.* 28, 3301–3312. doi:10.1096/fj.13-248161.

Okawa, H., Sampath, A. P., Laughlin, S. B., and Fain, G. L. (2008). Report ATP Consumption by Mammalian Rod Photoreceptors in Darkness and in Light. *Curr. Biol.* 18, 1917–1921. doi:10.1016/j.cub.2008.10.029.

Overgaard, M., Rasmussen, P., Bohm, A., Seifer, T., Brassard, P., Zaar, M., et al. (2012). Hypoxia and exercise provoke both lactate release and lactate oxidation by the human brain. *FASEB J.* 26, 3012–3020. doi:10.1096/fj.11-191999.

Passarella, S., and Schurr, A. (2018). L-lactate transport and metabolism in mitochondria of Hep G2 cells-the cori cycle revisited. *Front. Oncol.* 8, 1–4. doi:10.3389/fonc.2018.00120.

Peachey, N. S., Yu, M., Han, J. Y. S., Lengacher, S., Magistretti, P. J., Pellerin, L., et al. (2018). Impact of MCT1 haploinsufficiency on the mouse retina. *Adv. Exp. Med. Biol.* 1074, 375–

380. doi:10.1007/978-3-319-75402-4_46.

Pellerin, L., and Magistretti, P. J. (1994). Glutamate uptake into astrocytes stimulates aerobic glycolysis : A mechanism coupling neuronal activity to glucose utilization. *Proc. Natl. Acad. Sci.* 91, 10625–10629.

Pellerin, L., Pellegri, G., Bittar, P. G., Charnay, Y., Bouras, C., Martin, J. L., et al. (1998). Evidence supporting the existence of an activity-dependent astrocyte-neuron lactate shuttle. *Dev. Neurosci.* 20, 291–299. doi:10.1159/000017324.

Pérez-Escuredo, J., Van Hée, V. F., Sboarina, M., Falces, J., Payen, V. L., Pellerin, L., et al. (2016). Monocarboxylate transporters in the brain and in cancer. *Biochim. Biophys. Acta - Mol. Cell Res.* 1863, 2481–2497. doi:10.1016/j.bbamcr.2016.03.013.

Pierre, K., Magistretti, P. J., and Pellerin, L. (2002). MCT2 is a major neuronal monocarboxylate transporter in the adult mouse brain. *J. Cereb. Blood Flow Metab.* 22, 586–595. doi:10.1097/00004647-200205000-00010.

Poitry-Yamate, C. L., Poitry, S., and Tsacopoulos, M. (1995). Lactate Released by Miiller Glial Cells Is Metabolized Photoreceptors from Mammalian Retina. *J. Neurosci.* 15, 5179–5191.

Poitry-Yamate, C., and Tsacopoulos, M. (1991). Glial (Müller) cells take up and phosphorylate [3H]2-deoxy-d-glucose in a mammalian retina. *Neurosci. Lett.* 122, 241–244. doi:10.1016/0304-3940(91)90868-T.

Poole, R. C., and Halestrap, A. P. (1993). Transport of lactate and other monocarboxylates across mammalian plasma membranes. *Am. J. Physiol. - Cell Physiol.* 264, 761–782. doi:10.1152/ajpcell.1993.264.4.c761.

Rajala, A., Wang, Y., Brush, R. S., Tsantilas, K., Jankowski, C. S. R., Lindsay, K. J., et al. (2018). Pyruvate kinase M2 regulates photoreceptor structure, function, and viability article. *Cell Death Dis.* 9. doi:10.1038/s41419-018-0296-4.

Rajala, R. V. S., Rajala, A., Kooker, C., Wang, Y., and Anderson, R. E. (2016). The Warburg Effect Mediator Pyruvate Kinase M2 Expression and Regulation in the Retina. *Sci. Rep.* 6, 1–13. doi:10.1038/srep37727.

Rétaux, S., and Casane, D. (2013). Evolution of eye development in the darkness of caves: Adaptation, drift, or both? *Evodevo* 4, 1–12. doi:10.1186/2041-9139-4-26.

Rossi, A., Pizzo, P., and Filadi, R. (2019). Calcium, mitochondria and cell metabolism: A functional triangle in bioenergetics. *Biochim. Biophys. Acta - Mol. Cell Res.* 1866, 1068–1078. doi:10.1016/j.bbamcr.2018.10.016.

Rueda, E. M., Johnson, J. E., Giddabasappa, A., Swaroop, A., Brooks, M. J., Sigel, I., et al. (2016). The cellular and compartmental profile of mouse retinal glycolysis, tricarboxylic acid cycle, oxidative phosphorylation, and ~p transferring kinases. *Mol. Vis.* 22, 847–885.

Ruminot, I., Schmälzle, J., Leyton, B., Barros, L. F., and Deitmer, J. W. (2019). Tight coupling of astrocyte energy metabolism to synaptic activity revealed by genetically encoded FRET nanosensors in hippocampal tissue. *J. Cereb. Blood Flow Metab.* 39, 513–523. doi:10.1177/0271678X17737012.

Sahu, B., and Maeda, A. (2016). Retinol dehydrogenases regulate vitamin A metabolism for visual function. *Nutrients* 8, 1–16. doi:10.3390/nu8110746.

San Martín, A., Ceballo, S., Baeza-Lehnert, F., Lerchundi, R., Valdebenito, R., Contreras-Baeza, Y., et al. (2014a). Imaging mitochondrial flux in single cells with a FRET sensor for pyruvate. *PLoS One* 9. doi:10.1371/journal.pone.0085780.

San Martín, A., Ceballo, S., Ruminot, I., Lerchundi, R., Frommer, W. B., and Barros, L. F. (2013). A Genetically Encoded FRET Lactate Sensor and Its Use To Detect the Warburg Effect in Single Cancer Cells. *PLoS One* 8. doi:10.1371/journal.pone.0057712.

San Martín, A., Sotelo-Hitschfeld, T., Lerchundi, R., Fernández-Moncada, I., Ceballo, S.,

Valdebenito, R., and & Romero-Gómez, I. (2014b). Single-cell imaging tools for brain energy metabolism: a review. *neurophotonics* 1, 011004.

Sánchez-García, F. J., Pérez-Hernández, C. A., Rodríguez-Murillo, M., and Moreno-Altamirano, M. M. B. (2021). The Role of Tricarboxylic Acid Cycle Metabolites in Viral Infections. *Front. Cell. Infect. Microbiol.* 11, 1–9. doi:10.3389/fcimb.2021.725043.

Satrústegui, J., Pardo, B., and Del Arco, A. (2007). Mitochondrial transporters as novel targets for intracellular calcium signaling. *Physiol. Rev.* 87, 29–67. doi:10.1152/physrev.00005.2006.

Shekhar, K., Lapan, S. W., Whitney, I. E., Tran, N. M., Macosko, E. Z., Kowalczyk, M., et al. (2016a). Comprehensive Classification of Retinal Bipolar Neurons by Single-Cell Transcriptomics. *Cell* 166, 1308-1323.e30. doi:10.1016/j.cell.2016.07.054.

Shekhar, K., Lapan, S. W., Whitney, I. E., Tran, N. M., Macosko, E. Z., Kowalczyk, M., et al. (2016b). Comprehensive Classification of Retinal Bipolar Neurons by Single-Cell Transcriptomics. *Cell* 166, 1308-1323.e30. doi:10.1016/j.cell.2016.07.054.

Sotelo-Hitschfeld, T., Niemeyer, M. I., Mächler, P., Ruminot, I., Lerchundi, R., Wyss, M. T., et al. (2015). Channel-mediated lactate release by K+ -stimulated astrocytes. *J. Neurosci.* 35, 4168–4178. doi:10.1523/JNEUROSCI.5036-14.2015.

Stojan, G., and Christopher-Stine, L. (2015). Metabolic, drug-induced, and other noninflammatory myopathies. *Rheumatol. Sixth Ed.* 2–2, 1255–1263. doi:10.1016/B978-0-323-09138-1.00151-0.

Suzuki, A., Stern, S. A., Bozdagi, O., Huntley, G. W., Walker, R. H., Magistretti, P. J., et al. (2011). Astrocyte-neuron lactate transport is required for long-term memory formation. *Cell* 144, 810–823. doi:10.1016/j.cell.2011.02.018.

Toft-Kehler, A. K., Skytt, D. M., and Kolko, M. (2018). A Perspective on the Müller Cell-Neuron

Metabolic Partnership in the Inner Retina. *Mol. Neurobiol.* 55, 5353–5361. doi:10.1007/s12035-017-0760-7.

Tolone, A., Haq, W., Fachinger, A., Rentsch, A., Herberg, F. W., Schwede, F., et al. (2021). Retinal degeneration: Multilevel protection of photoreceptor and ganglion cell viability and function with the novel PKG inhibitor CN238. *bioRxiv*. Available at: https://doi.org/10.1101/2021.08.05.455191.

Tsacopoulos, M., Evêquoz-Mercier, V., Perrottet, P., and Buchner, E. (1988). Honeybee retinal glial cells transform glucose and supply the neurons with metabolic substrate. *Proc. Natl. Acad. Sci. U. S. A.* 85, 8727–8731. doi:10.1073/pnas.85.22.8727.

Tsacopoulos, M., and Magistretti, P. J. (1996). Metabolic coupling between glia and neurons. *J. Neurosci.* 16, 877–885. doi:10.1523/jneurosci.16-03-00877.1996.

Tsacopoulos, M., Poitry-Yamate, C. L., MacLeish, P. R., and Poitry, S. (1998). Trafficking of molecules and metabolic signals in the retina. *Prog. Retin. Eye Res.* 17, 429–442. doi:10.1016/S1350-9462(98)00010-X.

Tsacopoulos, M., Veuthey, A. L., Saravelos, S. G., Perrottet, P., and Tsoupras, G. (1994). Glial cells transform glucose to alanine, which fuels the neurons in the honeybee retina. *J. Neurosci.* 14, 1339–1351. doi:10.1523/jneurosci.14-03-01339.1994.

Valdés, J., Trachsel-Moncho, L., Sahaboglu, A., Trifunović, D., Miranda, M., Ueffing, M., et al. (2016). Organotypic retinal explant cultures as in vitro alternative for diabetic retinopathy studies. *ALTEX* 33, 459–464. doi:10.14573/altex.1603111.

Vecino, E., Rodriguez, F. D., Ruzafa, N., Pereiro, X., and Sharma, S. C. (2016). Glia-neuron interactions in the mammalian retina. *Prog. Retin. Eye Res.* 51, 1–40. doi:10.1016/j.preteyeres.2015.06.003.

Vielma, A. H., and Schmachtenberg, O. (2016). Electrophysiological fingerprints of OFF bipolar

cells in rat retina. *Sci. Rep.* 6, 1–15. doi:10.1038/srep30259.

Vohra, R., Gurubaran, I. S., Henriksen, U., Bergersen, L. H., Rasmussen, L. J., Desler, C., et al. (2017). Disturbed mitochondrial function restricts glutamate uptake in the human Müller glia cell line, MIO-M1. *Mitochondrion* 36, 52–59. doi:10.1016/j.mito.2017.02.003.

Vohra, R., and Kolko, M. (2020). Lactate: More Than Merely a Metabolic Waste Product in the Inner Retina. *Mol. Neurobiol.* 57, 2021–2037. doi:10.1007/s12035-019-01863-8.

Volkenhoff, A., Weiler, A., Letzel, M., Stehling, M., Klämbt, C., and Schirmeier, S. (2015). Glial glycolysis is essential for neuronal survival in drosophila. *Cell Metab.* 22, 437–447. doi:10.1016/j.cmet.2015.07.006.

Wang, L., Tornquist, P., and Billl, A. (1997). Glucose metabolism in pig outer retina in light and darkness. *Acta Physiol. Scand.* 160, 75–81.

Warburg, O. (1924). The metabolism of carcinoma cells. *J. Cancer Res.* 9, 148–163.

Wassle, H., Puller, C., Muller, F., and Haverkamp, S. (2009). Cone Contacts, Mosaics, and Territories of Bipolar Cells in the Mouse Retina. *J. Neurosci.* 29, 106–117. doi:10.1523/JNEUROSCI.4442-08.2009.

Watanabe, T., and Matsushima, S. (1996). Localization and ontogeny of GLUT3 expression in the rat retina. *Dev. Brain Res.* 94, 60–66.

Watanabe, T., Mio, Y., Hoshino, F. B., Nagamatsu, S., Hirosawa, K., and Nakahara, K. (1994). GLUT2 expression in the rat retina: localization at the apical ends of Müller cells. *Brain Res.* 655, 128–134.

Winkler, B. (1981). Glycolytic and Oxidative Metabolism in Relation to Retinal Function. *J. Gen. Physiol.* 77, 667–692.

Winkler, B. S. (1975). Dependence of Rat and Rabbit Photoreceptor Potentials upon Anaerobic and Aerobic Metabolism in vitro. *Exp. Eye Res.* 21, 545–548.

Winkler, B. S., Starnes, C. A., Sauer, M. W., Firouzgan, Z., and Chen, S. (2004). Cultured retinal neuronal cells and Müller cells both show net production of lactate. 45, 311–320. doi:10.1016/j.neuint.2003.08.017.

Winkler, B. S., York, N., and York, N. (1971). The electroretinogram of the isolated rat retina. *Vision Res.* 1, 1183–1198.

Wittenberg, J., and Wittenberg, B. (1974). The choroid rete mirabile of the fish eye. I. Oxygen secretion and structure: comparison with the swimbladder rete mirabile. *Biol. Bull.* 146, 116–136.

Wong-riley, M. (2010). Energy metabolism of the visual system. *Eye Brain* 2, 99.

Wong, N., De Melo, J., and Tang, D. (2013). PKM2, a central point of regulation in cancer metabolism. *Int. J. Cell Biol.* 2013. doi:10.1155/2013/242513.

Wong, N., Ojo, D., Yan, J., and Tang, D. (2015). PKM2 contributes to cancer metabolism. *Cancer Lett.* 356, 184–191. doi:10.1016/j.canlet.2014.01.031.

Xiong, Y., Lei, Q. Y., Zhao, S., and Guan, K. L. (2011). Regulation of glycolysis and gluconeogenesis by acetylation of PKM and PEPCK. *Cold Spring Harb. Symp. Quant. Biol.* 76, 285–289. doi:10.1101/sqb.2011.76.010942.

Yan, W., Peng, Y. R., van Zyl, T., Regev, A., Shekhar, K., Juric, D., et al. (2020). Cell Atlas of The Human Fovea and Peripheral Retina. *Sci. Rep.* 10, 1–17. doi:10.1038/s41598-020-66092-9.

Yang, M., Chen, Y., Vagionitis, S., Körtvely, E., Ueffing, M., Schmachtenberg, O., et al. (2022). Expression of glucose transporter-2 in murine retina: Evidence for glucose transport from horizontal cells to photoreceptor synapses. *J. Neurochem.* 160, 283–296. doi:10.1111/jnc.15533.

Yang, Y., Liu, W., Sun, K., Jiang, L., and Zhu, X. (2019). Tmem30a deficiency leads to retinal

rod bipolar cell degeneration. *J. Neurochem.* 148, 400–412. doi:10.1111/jnc.14643.

Young, R. W. (1967). The renewal of photoreceptor cell outer segments. *J. Cell Biol.* 33, 61–72. doi:10.1083/jcb.33.1.61.

Yu, D., and Cringle, S. (2001). Oxygen distribution and consumption within the retina in vascularised and avascular retinas and in animal models of retinal disease. *Prog. Retin. Eye Res.* 20, 175–208. Available at: http://www.embase.com/search/results?subaction=viewrecord&from=export&id=L32153715%0Ahttp://dx.doi.org/10.1016/S1350-9462(00)00027-6.

Zhao, X., Zhu, Y., Hu, J., Jiang, L., Li, L., Jia, S., et al. (2018). Shikonin Inhibits Tumor Growth in Mice by Suppressing Pyruvate Kinase M2-mediated Aerobic Glycolysis. *Sci. Rep.* 8, 1–8. doi:10.1038/s41598-018-31615-y.

SUPPLEMENTARY INFORMATION I

Imaging of lactate metabolism in retinal Müller cells with a FRET nanosensor

Víctor Calbiague García[1,2], Yiyi Chen[3], Bárbara Cádiz[2], Lan Wang[3], François Paquet-Durand[3], and Oliver Schmachtenberg[2]*

[1] PhD Program in Neuroscience, Universidad de Valparaíso, Valparaíso, Chile

[2] CINV, Instituto de Biología, Universidad de Valparaíso, Chile

[3] Institute for Ophthalmic Research, University of Tübingen, Germany

*Corresponding Author:

Dr. Oliver Schmachtenberg

CINV, Instituto de Biología, Facultad de Ciencias, Universidad de Valparaíso

Avda. Gran Bretaña 1111, 2360102 Valparaíso, Chile

E-mail: oliver.schmachtenberg@uv.cl

Tel.: +56-32-2508034

Running title:

Lactate metabolism in Müller cells

Keywords: Retina, metabolism, lactate, Müller cells, monocarboxylate transporters, diabetic retinopathy

Number of words main text = 3154

Number of figures = 2

Abstract

Müller cells, the glial cells of the retina, provide metabolic support for photoreceptors and inner retinal neurons, and have been proposed as source of the significant lactate production of this tissue. To better understand the role of lactate in retinal metabolism, we expressed a lactate and a glucose nanosensor in organotypic mouse retinal explants cultured for 14 days, and used FRET imaging in acute vibratome sections of the explants to study metabolite flux in real time. Pharmacological manipulation with specific monocarboxylate transporter (MCT) inhibitors and immunohistochemistry revealed the functional expression of MCT1, MCT2 and MCT4 in Müller cells of retinal explants. The introduction of FRET nanosensors to measure key metabolites at the cellular level may contribute to a better understanding of heretofore poorly understood issues in retinal metabolism.

Introduction

Adequate metabolism is a prerequisite for optimal cell function. This issue is critical in tissues with high energy demands, for which the retina is a prime example (Ames et al., 1992; Country, 2017). Interestingly, Warburg´s studies from 1924 pointed out that tumor cells and the retina share the use of aerobic glycolysis for energy production, converting almost 70% of consumed glucose into lactate, despite the presence of all elements necessary for the much more efficient oxidative phosphorylation (Wang et al., 1997; Warburg, 1924). However, the reasons for this peculiar metabolism, the specific cell types performing aerobic glycolysis in the retina, and the conditions under which it may occur remain unknown to date. Several studies concluded that Müller cells (MC), the glial cells of the retina, are the source of retinal lactate which is supplied to neurons, especially photoreceptors (Poitry-Yamate et al., 1995; Tsacopoulos et al., 1988). However, a direct measurement of retinal lactate flux in real-time and with cellular resolution has not been reported to date.

Here, we expressed the FRET lactate nanosensor Laconic in organotypic retinal explant cultures to study the lactate dynamics in MCs and compared these with glucose levels assessed with the glucose nanosensor FLII12Pglu-700Δ6, hereafter named Δ6. These types of nanosensors have become popular in recent years for the analysis of metabolic flux and transport of different metabolites in neurons and astrocytes, either in culture or in vivo (Mächler et al., 2016; San Martín et al., 2013). In the present study, we applied a functional approach to characterize the expression of different monocarboxylate transporters (MCTs) in MCs. The successful expression of nanosensors in the retina and the results of our analysis may help to further understand the complex, yet enigmatic retinal metabolism at a single cell level, with ramifications for pathological conditions such as diabetic retinopathy.

Methods

In this study, healthy 9-day old C57BL/6 mice were used irrespective of sex or weight. Animals were born and raised in the animal facility of the University of Valparaiso, held at 20 – 25°C under a 12h photoperiod with water and food ad libitum. The experimental protocols were approved by the bioethics committee of the University of Valparaiso and in accordance with the Chilean animal protection law. To isolate the retinas, mice were deeply anesthetized with isoflurane (Sigma Aldrich) before being sacrificed by decapitation.

Retinal explants obtained from post-natal (p) day 9 wild-type mice were cultured as previously described (Belhadj et al., 2020; Calbiague et al., 2020; Valdés et al., 2016). Briefly, the eyes were treated for 15 min with 0.12% Proteinase K (Cat. No. P2308, Sigma-Aldrich) at 37°C for isolation of the retina together with its retinal pigment epithelium (RPE). Then, the eyes were placed for 5 min in DMEM medium with 10% fetal bovine serum (FBS) to deactivate Proteinase K. The retinas were separated from the choroid and placed with the RPE facing down on cell culture inserts (Millicell, Cat. No. PICM0RG50, Merck Millipore) with DMEM culture medium (Cat. No. 31600034, Thermo Fisher Scientific), containing 10% FBS (Sigma-Aldrich) with 15 mM glucose, which was replaced every two days. The cultures were incubated at 37°C in 5% CO2, and 95% humidity for

14 days in a water-jacketed incubator (Thermo Scientific). At p11 and p12 the explants were transduced by overnight incubation with 5x106 plaque-forming units (PFU) of Ad Laconic, AAV-Laconic or Δ6, and imaged after two weeks in cultures. Adenoviral serotype vectors encoding FRET nanosensor Ad FLII12Pglu-700Δ6 (Takanaga et al., 2008)) and Ad Laconic (San Martín et al., 2013) were a gift from Dr. Ivan Ruminot from the Centro de Estudios Científicos (CECs) in Valdivia, Chile. AAV-GFAP-Laconic was constructed by the viral vector facility of ETH Zurich (Laconic: Addgene #44238; hGFAP promoter fragment: DOI: 10.1002/glia.20622).

For retinal slice preparation, the explants were separated from the culture inserts and placed in a chamber with extracellular solution, containing (in mM): 119 NaCl, 23 NaHCO3, 1.25 NaH2PO4, 2.5 KCl, 2.5 CaCl2, 1.5 MgSO4, 20 glucose and 2 Na+ pyruvate, aerated with 95% O2 and 5% CO2, pH 7.4. The tissue was embedded in type VII agarose (Cat. No. 39346-81-1 Sigma Aldrich) and cut with a vibratome (Leica VT1000S) to 200 µm thickness. The slices were transferred to the microscope recording chamber, sustained by a U-shaped platinum wire and superfused with oxygenated extracellular solution at room temperature (20°C) under photopic conditions. For live cell imaging, retinal slices were maintained in extracellular solution containing (in mM): 119 NaCl, 23 NaHCO3, 1.25 NaH2PO4, 2.5 KCl, 2.5 CaCl2, 1.5 MgSO4, 5 glucose and 1 lactate and, aerated with 95% O2 and 5% CO2, pH 7.4. The lactate concentration was chosen not to saturate the lactate sensor. Since there is only a limited number of commercial MCT inhibitors available, based on prior reports (Murray et al., 2005; Ovens et al., 2010; Vélez et al., 2021), we used three potent and specific inhibitors to isolate MCT isoforms: SR-13800 for MCT1 (Cat. No. 5431, Tocris), AR-C155858 (Cat. No. 4960, Tocris) for MCT1 and MCT2, and Syrosingopine (Cat. No. SML1908, Sigma Aldrich) to inhibit MCT1 and MCT4.

Since the lactate and glucose sensors used here have similar excitation/emission spectra (Laconic: 460/492 nm for mTFP and 515/526 for Venus; Δ6: 440/480 nm for CFP and 513/530 nm for YFP), retinal slices were excited at 430 nm and visualized at 480 nm and 530 nm peak wavelength, as previously reported (Fig. 1A) (Barros et al., 2014; San Martín et al., 2013). All

experiments were performed at room temperature (22–25°C) with an upright fluorescence microscope (Olympus BX51) equipped with a 40x water-immersion objective, an Optosplit II emission image splitter (Cairn, UK), and a Sensicam QE digital camera (Cooke Corp.). Data acquisition was performed by custom software written in Python 4.0.1. At the end of the experiments, data were exported for off-line analysis of fluorescence intensities from each emission channel. To obtain the FRET ratio for Laconic (mTFP/Venus) and Δ6 (YFP/CFP), fluorescence intensity values from each ROI and background were measured in ImageJ, version 1.52p (NIH, RRID: SCR_003070). In this study, all ROIs were chosen from the somas of MCs for all experiments (Fig. 1B and D). The FRET data are displayed as the relative FRET ratio, in percentage of change over time of single experiments.

Retinas from p30 mice were fixed in 4% paraformaldehyde for 45 minutes, washed in PBS, cryopreserved with PBS containing 10, 20, and 30% sucrose successively, before embedding in tissue-freezing medium, and stored frozen at -20°C. Transverse sections of 14 µm diameter were obtained with a cryostat (Leica CM-1900) and deposited on poly-L-lysine-coated slides, which were dried at 37°C for 30 min and rehydrated for 10 min in PBS at room temperature (RT). For immunofluorescent labelling, the tissue was incubated in blocking solution (10% normal goat serum, 1% bovine serum albumin in 0.3% PBS-Triton X 100) for 1 h at RT. The primary antibodies: Anti-MCT1 (SLC16A1) (Cat. No. AMT-011, Alomone labs, RRID: AB_2756669), Anti-MCT2 (SLC16A7) (Cat. No. AMT-012, Alomone labs, RRID: AB_2340997), Anti-MCT4 (SLC16A4) (Cat. No. AB180699, Abcam), Anti-Glutamine synthetase (Cat. No. AB73593, Abcam, RRID: AB_2247588) and Anti-glutamate-aspartate transporter (Cat. No. AGC-021, Alomone labs, RRID: AB_2039885) were diluted 1:100 in blocking solution and incubated at 4°C overnight. The slides were washed 3 times for 10 min each with PBS. Subsequently, the secondary antibody, diluted 1:350 in PBS, was applied for 1h at RT. Finally, the slides were washed with PBS and covered in Vectashield mounting medium with DAPI (Vector Laboratories).

To calculate the delta ratio between the depletion and the saturation for both sensors, the minimum response (depletion) was obtained during the application of 10 mM pyruvate, and the maximum response (saturation) during the 10 mM lactate stimulation, their difference yielding the delta ratio. To evaluate the effect of different MCT blockers on lactate influx, the positive amplitude peak was measured before and after drug application. The decay time of these responses was calculated as the time required to return to the baseline from the response peak. In both cases, the lactate response and the decay time were first normalized per cell based on the control response and then averaged throughout the experiments. Statistical analysis was performed using GraphPad Prism software (RRID:SCR_002798). The data were first analyzed for normality using the Shapiro–Wilk test. In all cases, the test determined that the data did not conform to a normal distribution, therefore significant differences were established with the Wilcoxon Matched-Pairs Signed Ranks Test. The α value was set to 0.05. Unless otherwise stated, data values are given as mean ± SD. Significance levels as indicated by asterisks were: * $p < 0.05$; **$p < 0.01$, *** $p < 0.001$.

Results and discussion

Here, we took advantage of the advantages of the defined and controlled ex vivo conditions of organotypic retinal explants to express the FRET nanosensors Laconic (San Martín et al., 2013) and Δ6 (Takanaga et al., 2008). Previously, we had shown that our protocol allowed the culture of mouse retinal explants for up to two weeks without morphological disorganization or major physiological changes (Calbiague et al., 2020). The retinas were cultured at p9, and at p11 and again at p12, the explants were transfected by overnight incubation with one of the nanosensors. Imaging took place after two weeks in culture (Fig. 1A). It is important to note that these sensors have been widely used in different tissues and have been shown to be stable at physiological pH and at room temperature (Mächler et al., 2016; San Martín et al., 2013).

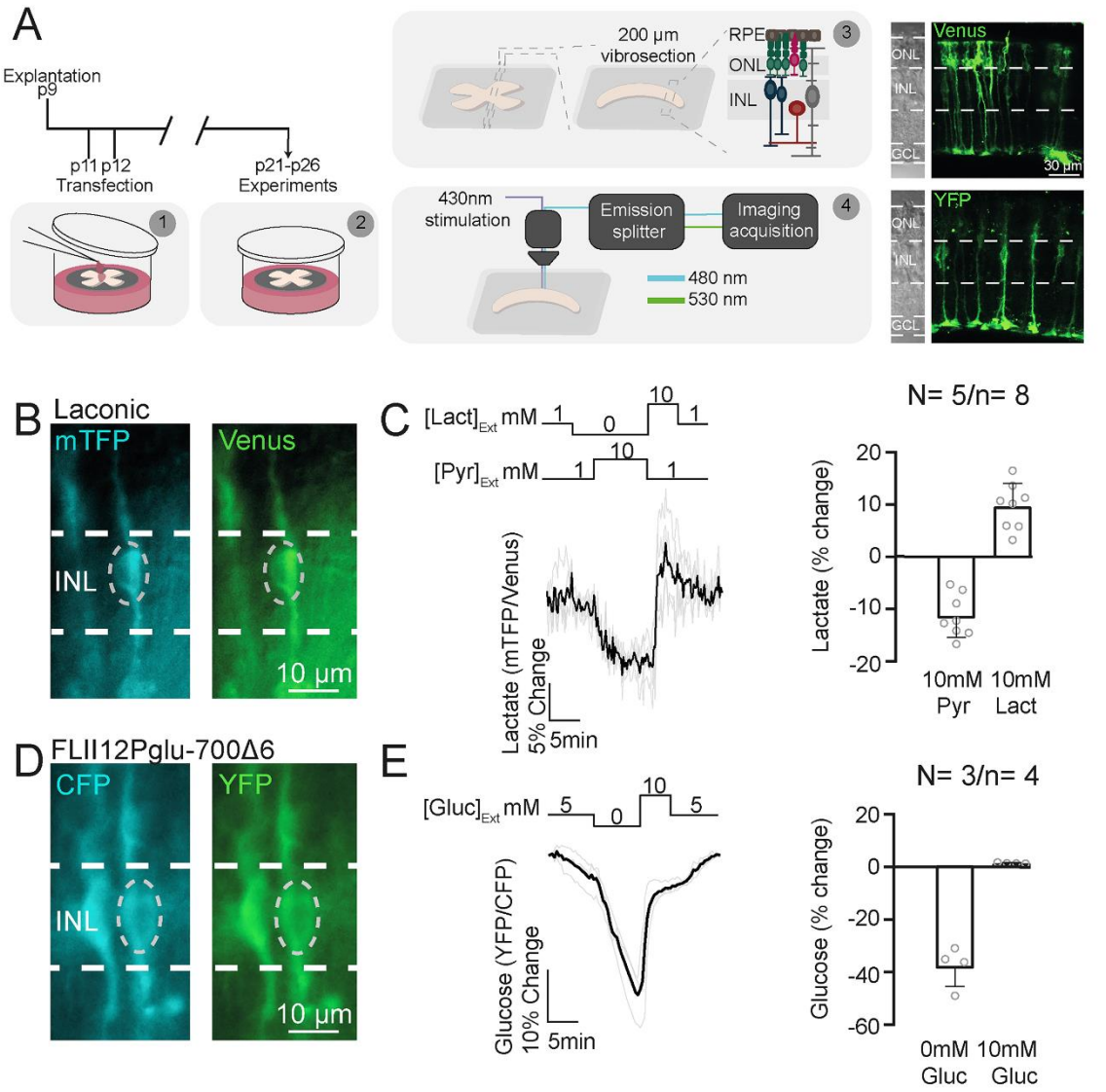

Fig 1.- The Laconic nanosensor can be functionally expressed in retinal MCs. (A, left) Scheme of the transfection protocol and the experimental setup. (A, right) Confocal image of Laconic (Venus) and glucose (YFP) sensors expression in retinal explants after two weeks in culture. (B and D) Representative images of the expression of the lactate sensor (Laconic) and glucose sensors (FLII12Pglu-700Δ6). Dash circles show the area recorded. (C and E) Dynamic range of the lactate and glucose sensor in MCs. The light grey traces represent responses of single cells, and the black trace represents their average. The number of experiments is represented as: N= number of explants; n= number of cells recorded. ONL= outer nuclear layer; INL= inner nuclear layer; GCL= ganglion cell layer; MC(s)= Müller cell(s).

To demonstrate functional nanosensor expression, we measured the ratio between the emissions obtained from monomeric teal fluorescent protein (mTFP)/Venus for Laconic and yellow fluorescent protein/cyan fluorescent protein (YFP/CFP) for Δ6 in the soma (Fig. 1B, D). Then, we saturated the lactate and glucose nanosensors with 10 mM lactate or 10 mM glucose respectively (Fig. 1C, E). To deplete intracellular levels of these metabolites, we took advantage of a property of monocarboxylate transporters (MCTs) called trans-acceleration (Poole and Halestrap, 1993), where an extracellular exposure to a monocarboxylate triggers intracellular substrate efflux. Here, 10 mM pyruvate were applied to deplete intracellular lactate (Fig. 1C). We observed a decrease of the intracellular lactate levels when we changed the solution to 0 mM lactate, indicating that this metabolite flowed in a gradient-dependent way (Fig. 1C). Then, we saturated the lactate and glucose nanosensors with 10 mM lactate or 10 mM glucose respectively (Fig. 1C, E) (Ruminot et al., 2019). Interestingly, when we applied 10 mM glucose, fluorescence levels returned to baseline, suggesting that MCs are working under a saturated intracellular glucose concentration in basal conditions (Fig. 1E). The delta ratio between the depletion and the saturation for Laconic was 17.8 ± 7.2% (Fig. 1C), and for the glucose nanosensor Δ6 38.7 ± 7.6% (Fig. 1E), which is similar to responses reported in other cells and tissues (Ruminot et al., 2019; San Martín et al., 2013). Together, these results demonstrate that different FRET nanosensors can be functionally expressed in retinal explant cultures to study metabolic dynamics on a single-cell level.

The retinal expression patterns of the different MCTs are still unclear. MCTs are encoded by the SLC16A gene family, and act as bidirectional proton-linked carriers of monocarboxylates such as lactate, pyruvate, and ketoacids (Halestrap, 2013). Here, we used the expression of Laconic and complementary immunostaining experiments to determine the expression of MCTs in retinal MCs. Since these transporters work bidirectionally, we applied a pulse of 10 mM lactate to trigger its influx into MCs. The relative amplitude of this response was 13.9 ± 5.2% (Fig. 2A). In mammals, the lactate concentration in the retina fluctuates between 5 and 50 mM depending on the species (Kolko et al., 2016). For this study, we measured the lactate released by retinal explants after 4 days in culture and obtained a concentration of 16.7 ± 5.7 mM lactate in the culture medium (n =

4), therefore the concentration of lactate used for acute stimulation is unlikely have caused neurotoxic effects.

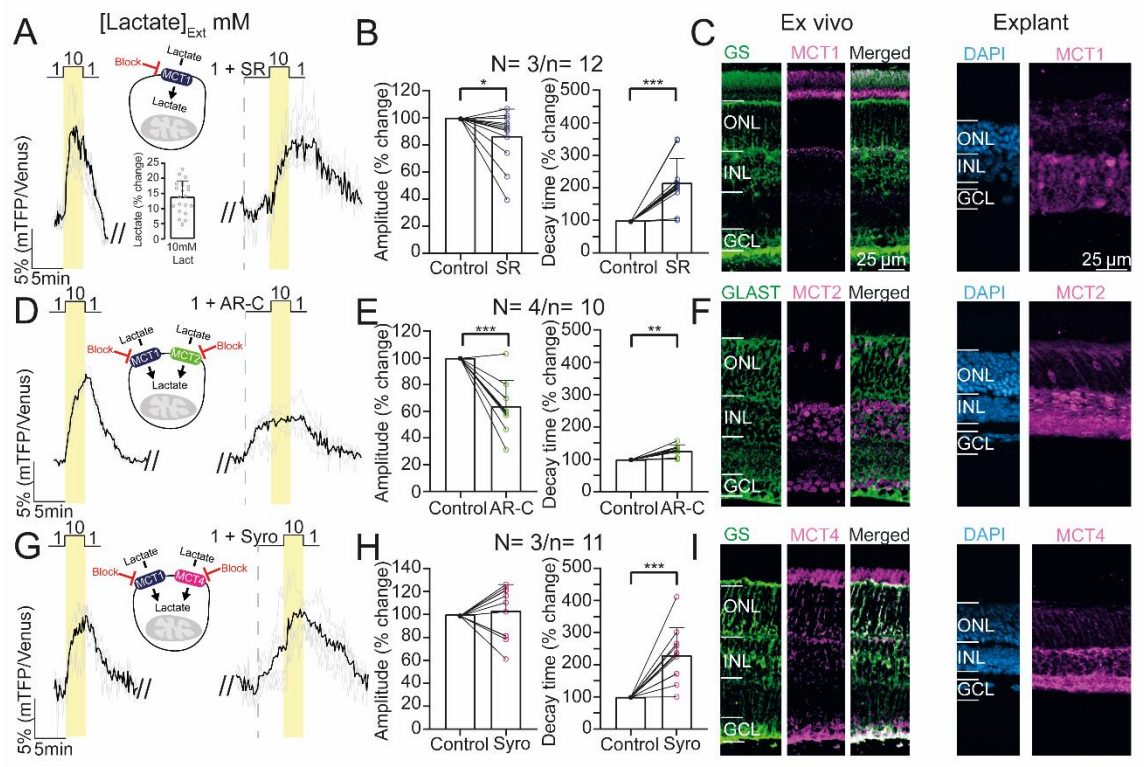

Fig 2.- Inhibition of lactate transport disrupts lactate influx in retinal MCs. (A, D, and G, left) Lactate influx evoked after a stimulation with 10 mM lactate. (A, D, and G, right) Lactate influx responses after an incubation with different drugs which target monocarboxylate transporters (MCTs). The light grey traces represent responses of single cells, and the black trace represents their average. (B, E, and H) Statistical analysis of the response amplitude and the decay time of the lactate influx. Paired Student´s t-test followed by Wilcoxon's post hoc. (C, F, and I) Immunofluorescence for different MCTs in the retina showing co-labelling with MC markers in ex vivo or explant condition. All the images display the same scale bar. Graphs display the mean ± SD. * Indicates $p < .05$; ** indicates $p < .01$. *** indicates $p < .001$. ONL= outer nuclear layer; INL= inner nuclear layer; GCL= ganglion cell layer; MC(s)= Müller cell(s); GLAST= glutamate-aspartate transporter; GS= glutamine synthetase. SR= MCT1 blocker; AR-C= MCT1 and MCT2 blocker; Syro= MCT1 and MCT4 blocker. The number of experiments is represented as: N= number of explants; n= number of cells recorded.

The presence of the specific MCT1 inhibitor SR-13800 (0,1 µM) (Murray et al., 2005), produced a decrease of 13.4 ± 19.8% in the peak response (Fig. 2B, left). The decay time was even more affected and was extended by 115.6 ± 75.1% (Fig. 2A, B, right). Curiously, the MCT1 immunofluorescence indicated an expression in photoreceptor inner segments and the outer plexiform layer but failed to show co-labelling with the MC marker glutamine synthetase in ex-vivo slices (GS; Fig. 2C, left), while immunostaining in p25 retinal explants revealed stronger labelling in INL cells (Fig. 2C, right).

When we did the same experiment in the presence of a potent inhibitor of both MCT1 and MCT2, AR-C155858 (2 µM; Fig. 2D) (Ovens et al., 2010), the response peak decreased by 36.0 ± 19.2% (Fig. 2D, left), suggesting that lactate influx was mainly mediated by MCT2. We also observed an increase in the decay time by 26.8 ± 18.3% (Fig. 2D, E, right). On the other hand, MCT2 immunostaining displayed strong labelling in the inner nuclear layer (INL), and in some cell bodies in the outer nuclear layer, likely corresponding to cones. Although co-labelling with the MC-marker glutamate-aspartate transporter (GLAST) did not show a clear colocalization in the INL, GLAST labelling surrounds MCT2 expression in this layer in ex vivo slices, while p25 explants showed additional labeling in the inner plexiform layer (Fig. 2F).

Finally, when MCT1 and MCT4 were inhibited simultaneously with syrosingopine (4 µM) (Vélez et al., 2021), we did not observe any change in the response amplitudes (Fig. 2G, left). Nonetheless, the decay time had a significant increase of 130.1 ± 85.0% (Fig. 2G, H, right), supporting the hypothesis that MCT1 and MCT4 mediate lactate efflux in MCs. Immunostaining of MCT4 revealed clear co-labelling of MCT4 and the MC marker glutamine synthase (GS), confirming expression of this transporter in MCs in ex vivo slices; a pattern similar to that of p25 explants, with additional labeling of the inner plexiform layer (Fig. 2I).

In the present study, we expressed glucose and lactate nanosensors in MCs of organotypic retinal explants to study changes in intracellular lactate concentrations under different conditions. Our observations may provide new insights into retinal metabolism through a live-cell imaging

approach. Here, pharmacological data support MCT1, MCT2, and MCT4 isoform expression by MCs, possibly fulfilling different roles in lactate dynamics.

The saturation of Δ6 at basal levels indicates that MCs work under a high intracellular glucose concentration, probably because of the metabolic coupling between these cells and the retinal neurons (Grimes et al., 2021; Toft-Kehler et al., 2018), which rely on MCs for the provision of different metabolites for their metabolic needs. Due to their central role in retinal metabolism and intimate association with blood vessels, MCs likely have high glucose uptake, used in part for the storage of glycogen (Toft-Kehler et al., 2018).

Our data support the expression of different MCT isoforms in MCs. The suggestion of MCT2 expression by MCs is puzzling, since this transporter is known as the neuronal MCT (Pierre et al., 2002), and is indicative of a possible consumption of lactate under certain conditions. In fact, the aforementioned data support MCT2 expression in MCs of mouse retina, in line with previous immunohistochemical data for rats (Gerhart et al., 1999). These results could hence be interpreted as evidence against the ANLS hypothesis in the retina (Kanow et al., 2017; Lindsay et al., 2014). However, the demonstration of MCT4 expression and its role in lactate efflux are indicative of lactate production by MCs (Pellerin and Magistretti, 1994), supporting a complex metabolism in which retinal cells can change between lactate production and consumption, depending on the metabolic demands or the physiological context.

The expression of MCT1 in mouse MCs remains to be confirmed, even though it was previously detected by immunohistochemistry in rat retinal MCs (Gerhart et al., 1999), as well as recently through single-cell transcriptomics analysis (Bisbach et al., 2022). However, our immunofluorescence experiments reveal a different expression pattern in p25 retinal explants, which could be due to different reasons. MCT1 expression might be developmentally regulated during the first weeks of life. As mentioned in above, the retinal explant cultures were prepared from p9 mice (eyes closed) and maintained in culture for two weeks, while the retinal slices for immunostaining were prepared from p30 mice. This age difference could potentially produce a

significant variation in MCT1 expression, given that the peak expression is apparently reached at p21, followed by a reduction in mRNA levels (Clamp et al., 2004). This may explain the labeling of putative MC cell bodies in p25 explants shown in Fig. 2C (right). Furthermore, as observed in the immunolabelling in Fig. 2C and previously reported by others, there is a clear MCT1 expression in photoreceptor inner segments (Bergersen et al., 1999; Chidlow et al., 2004; Peachey et al., 2018). Therefore, we cannot exclude the possibility that intracellular lactate in MCs might be indirectly affected by photoreceptors metabolically coupled to MCs. It would be interesting to further investigate why MCs might express different types of MCTs, if MCT expression is developmentally regulated, and if lactate flux through these transporters varies under different visual conditions.

Here, we propose that MCT2 might be in charge of lactate influx and MCT1 and MCT4 of lactate efflux, according to prior suggestions in a high lactate environment (Contreras-Baeza et al., 2019). This suggests that MCs should express the intracellular enzymatic machinery to convert lactate to pyruvate, or pyruvate to lactate. It has been shown that MCs express the lactate dehydrogenase B (LDH-B) isoform (Chinchore et al., 2017). Thus, MCs could convert lactate into pyruvate through LDH-B to fuel mitochondria and produce ATP through oxidative phosphorylation. However, MCs lack the enzymes pyruvate kinase M2 (PKM2) and lactate dehydrogenase A (LDH-A) required for lactate production (Chen et al., 2022; Chinchore et al., 2017; Lindsay et al., 2014; Rajala et al., 2018). It is possible that the expression of pyruvate kinase M1 (PKM1) and LDH-B are sufficient to sustain lactate synthesis in MCs and release it through MCT1 and MCT4 when metabolically required. Certainly, more direct evidence is required to test this idea in the future.

It is important to indicate the limitations of our study. All measurements were obtained from cell bodies, whereas the long cellular projections of MCs might be metabolically isolated and display different metabolite dynamics. Furthermore, the experimental conditions used here might will not accurately reflect the physiological conditions of in vivo retina. While retinas were light-adapted,

photoreceptors can show variations in their activity after prolonged time in culture depending on the status of the RPE (Alarautalahti et al., 2019; Tolone et al., 2021).

In summary, our physiological and immunohistochemical results support expression and function of MCT1, MCT2 and MCT4 in MCs of retinal explants, while immunohistochemisty confirms MCT2 and MCT4 expression also in ex vivo retina. The proof of concept of glucose and lactate nanosensor expression and function in organotypic retinal explants opens a wide range of experiments which will contribute to further understand the complex retinal metabolism under physiological and pathological conditions.

Funding

This study was supported by FONDECYT grant No. 1210790 and ANID PhD scholarship No. 21180443 to VCG.

Author Contributions

VCG and OS contributed to the conception and design of the study. VCG, YC and LW contributed to data acquisition, analysis, and figures preparation. VCG, YC, BC, FPD and OS contributed to article writing and approved the submitted version.

Acknowledgments

We wish to thank Dr. Ivan Ruminot, Dr. Felipe Baeza-Lehnert, and Dr. Felipe Barros from Centros de Estudios Científicos (CECs) in Valdivia (Chile) for sharing its expertise in FRET measurements, and to Felipe Tapia from Universidad de Valparaiso for helping in the data analysis.

Declaration of competing interest

The authors declare no competing interests

Ethics statements

The animal study was reviewed and approved by the Bioethics Committee of the Universidad de Valparaiso, in accordance with local legislation.

1 References

Alarautalahti, V., Ragauskas, S., Hakkarainen, J.J., Uusitalo-Järvinen, H., Uusitalo, H., Hyttinen, J., Kalesnykas, G., Nymark, S., 2019. Viability of mouse retinal explant cultures assessed by preservation of functionality and morphology. Investig. Ophthalmol. Vis. Sci. 60, 1914–1927. https://doi.org/10.1167/iovs.18-25156

Ames, A., Li, Y.Y., Heher, E.C., Kimble, C.R., 1992. Energy metabolism of rabbit retina as related to function: High cost of Na+ transport. J. Neurosci. 12, 840–853. https://doi.org/10.1523/jneurosci.12-03-00840.1992

Barros, L.F., Baeza-Lehnert, F., Valdebenito, R., Ceballo, S., Alegría, K., 2014. Fluorescent Nanosensor Based Flux Analysis: Overview and the Example of Glucose., in: In Brain Energy. humana press, New york, pp. 145–159.

Belhadj, S., Tolone, A., Christensen, G., Das, S., Chen, Y., Paquet-Durand, F., 2020. Long-term, serum-free cultivation of organotypic mouse retina explants with intact retinal pigment epithelium. J. Vis. Exp. 2020, 1–13. https://doi.org/10.3791/61868

Bergersen, L., Jo, E., Veruki, M.L., Nagelhus, E.A., 1999. Cellular and subcellular expression of monocarboxylate transporters in the pigment epithelium and retina of the rat. Neuroscience 90, 319–331.

Bisbach, C.M., Hass, D.T., Thomas, E.D., Cherry, T.J., Hurley, J.B., Ed, T., Tj, C., Jb, H., 2022. Monocarboxylate Transporter 1 (MCT1) mediates succinate export in the retina. Invest. Ophthalmol. Vis. Sci. 63, 1–1.

Calbiague, V.M., Vielma, A.H., Cadiz, B., Paquet-Durand, F., Schmachtenberg, O., 2020. Physiological assessment of high glucose neurotoxicity in mouse and rat retinal explants. J. Comp. Neurol. 528, 989–1002. https://doi.org/10.1002/cne.24805

Chen, Y., Zizmare, L., Calbiague, V., Yu, S., Herberg, F.W., 2022. Retinal energy metabolism : Photoreceptors switch between Cori , Cahill , and mini-Krebs cycles to uncouple glycolysis from mitochondrial respiration. bioRxiv.

Chidlow, G., Wood, J.P.M., Graham, M., Osborne, N.N., Wood, J.P.M., Graham, M., 2004. Expression of monocarboxylate transporters in rat ocular tissues. Am. J. Physiol. Physiol. 288, 416–428. https://doi.org/10.1152/ajpcell.00037.2004.

Chinchore, Y., Begaj, T., Wu, D., Drokhlyansky, E., Cepko, C.L., 2017. Glycolytic reliance promotes anabolism in photoreceptors. Elife 6, 1–22. https://doi.org/10.7554/eLife.25946

Clamp, M.F., Ochrietor, J.D., Moroz, T.P., Linser, P.J., 2004. Developmental analyses of 5A11/Basigin, 5A11/Basigin-2 and their putative binding partner MCT1 in the mouse eye. Exp. Eye Res. 78, 777–789. https://doi.org/10.1016/j.exer.2003.12.004

Contreras-Baeza, Y., Sandoval, P.Y., Alarcón, R., Galaz, A., Cortés-Molina, F., Alegriá, K., Baeza-Lehnert, F., Arce-Molina, R., Guequén, A., Flores, C.A., Martín, A.S., Barros, L.F., 2019. Monocarboxylate transporter 4 (MCT4) is a high affinity transporter capable of exporting lactate in high-lactate microenvironments. J. Biol. Chem. 294, 20135–20147. https://doi.org/10.1074/jbc.RA119.009093

Country, M.W., 2017. Retinal metabolism : A comparative look at energetics in the retina. Brain Res. 1672, 50–57. https://doi.org/10.1016/j.brainres.2017.07.025

Gerhart, D.Z., Leino, R.L., Drewes, L.R., 1999. Distribution of monocarboxylate transporters MCT1 and MCT2 in rat retina. Neuroscience 92, 367–375.

Grimes, W.N., Aytürk, D.G., Hoon, M., Yoshimatsu, T., Gamlin, C., Carrera, D., Nath, A., Nadal-Nicolás, F.M., Ahlquist, R.M., Sabnis, A., Berson, D.M., Diamond, J.S., Wong, R.O., Cepko, C., Rieke, F., 2021. A high-density narrow-field inhibitory retinal interneuron with direct coupling to Müller glia. J. Neurosci. 41, 6018–6037. https://doi.org/10.1523/JNEUROSCI.0199-20.2021

Halestrap, A.P., 2013. Monocarboxylic Acid Transport. Compr. Physiol. 3, 1611–1643. https://doi.org/10.1002/cphy.c130008

Kanow, M.A., Giarmarco, M.M., Jankowski, C.S.R., Tsantilas, K., Engel, A.L., Du, J., Linton, J.D., Farnsworth, C.C., Sloat, S.R., Rountree, A., Sweet, I.R., Lindsay, K.J., Parker, E.D., Brockerhoff, S.E., Sadilek, M., Chao, J.R., Hurley, J.B., 2017. Biochemical adaptations of the retina and retinal pigment epithelium support a metabolic ecosystem in the vertebrate eye. Elife 6, 1–25. https://doi.org/10.7554/eLife.28899

Kolko, M., Vosborg, F., Henriksen, U.L., Hasan-Olive, M.M., Diget, E.H., Vohra, R., Gurubaran, I.R.S., Gjedde, A., Mariga, S.T., Skytt, D.M., Utheim, T.P., Storm-Mathisen, J., Bergersen, L.H., 2016. Lactate Transport and Receptor Actions in Retina: Potential Roles in Retinal Function and Disease. Neurochem. Res. 41, 1229–1236. https://doi.org/10.1007/s11064-015-1792-x

Lindsay, K.J., Du, J., Sloat, S.R., Contreras, L., Linton, J.D., Turner, S.J., Sadilek, M., Satrústegui, J., Hurley, J.B., 2014. distributions reveal key metabolic links between neurons and glia in retina. Proc. Natl. Acad. Sci. 111, 15579–15584. https://doi.org/10.1073/pnas.1412441111

Mächler, P., Wyss, M.T., Elsayed, M., Stobart, J., Gutierrez, R., Von Faber-Castell, A., Kaelin, V., Zuend, M., San Martín, A., Romero-Gómez, I., Baeza-Lehnert, F., Lengacher, S., Schneider, B.L., Aebischer, P., Magistretti, P.J., Barros, L.F., Weber, B., 2016. In Vivo Evidence for a Lactate Gradient from Astrocytes to Neurons. Cell Metab. 23, 94–102. https://doi.org/10.1016/j.cmet.2015.10.010

Murray, C.M., Hutchinson, R., Bantick, J.R., Belfield, G.P., Benjamin, A.D., Brazma, D., Bundick, R. V., Cook, I.D., Craggs, R.I., Edwards, S., Evans, L.R., Harrison, R., Holness, E., Jackson, A.P.,

Jackson, C.G., Kingston, L.P., Perry, M.W.D., Ross, A.R.J., Rugman, P.A., Sidhu, S.S., Sullivan, M., Taylor-Fishwick, D.A., Walker, P.C., Whitehead, Y.M., Wilkinson, D.J., Wright, A., Donald, D.K., 2005. Monocarboxylate Transporter Mctl is a Target for Immunosuppression. Nat. Chem. Biol. 1, 371–376. https://doi.org/10.1038/nchembio744

Ovens, M.J., Davies, A.J., Wilson, M.C., Murray, C.M., Halestrap, A.P., 2010. AR-C155858 is a potent inhibitor of monocarboxylate transporters MCT1 and MCT2 that binds to an intracellular site involving transmembrane helices 7-10. Biochem. J. 425, 523–530. https://doi.org/10.1042/BJ20091515

Peachey, N.S., Yu, M., Han, J.Y.S., Lengacher, S., Magistretti, P.J., Pellerin, L., Philp, N.J., 2018. Impact of MCT1 haploinsufficiency on the mouse retina. Adv. Exp. Med. Biol. 1074, 375–380. https://doi.org/10.1007/978-3-319-75402-4_46

Pellerin, L., Magistretti, P.J., 1994. Glutamate uptake into astrocytes stimulates aerobic glycolysis: A mechanism coupling neuronal activity to glucose utilization. Proc. Natl. Acad. Sci. U. S. A. 91, 10625–10629. https://doi.org/10.1073/pnas.91.22.10625

Pierre, K., Magistretti, P.J., Pellerin, L., 2002. MCT2 is a major neuronal monocarboxylate transporter in the adult mouse brain. J. Cereb. Blood Flow Metab. 22, 586–595. https://doi.org/10.1097/00004647-200205000-00010

Poitry-Yamate, C.L., Poitry, S., Tsacopoulos, M., 1995. Lactate Released by Miiller Glial Cells Is Metabolized Photoreceptors from Mammalian Retina. J. Neurosci. 15, 5179–5191.

Poole, R.C., Halestrap, A.P., 1993. Transport of lactate and other monocarboxylates across mammalian plasma membranes. Am. J. Physiol. - Cell Physiol. 264, 761–782. https://doi.org/10.1152/ajpcell.1993.264.4.c761

Rajala, A., Wang, Y., Brush, R.S., Tsantilas, K., Jankowski, C.S.R., Lindsay, K.J., Linton, J.D., Hurley, J.B., Anderson, R.E., Rajala, R.V.S., 2018. Pyruvate kinase M2 regulates photoreceptor

structure, function, and viability article. Cell Death Dis. 9. https://doi.org/10.1038/s41419-018-0296-4

Ruminot, I., Schmälzle, J., Leyton, B., Barros, L.F., Deitmer, J.W., 2019. Tight coupling of astrocyte energy metabolism to synaptic activity revealed by genetically encoded FRET nanosensors in hippocampal tissue. J. Cereb. Blood Flow Metab. 39, 513–523. https://doi.org/10.1177/0271678X17737012

San Martín, A., Ceballo, S., Ruminot, I., Lerchundi, R., Frommer, W.B., Barros, L.F., 2013. A Genetically Encoded FRET Lactate Sensor and Its Use To Detect the Warburg Effect in Single Cancer Cells. PLoS One 8. https://doi.org/10.1371/journal.pone.0057712

Takanaga, H., Chaudhuri, B., Frommer, W.B., 2008. GLUT1 and GLUT9 as major contributors to glucose influx in HepG2 cells identified by a high sensitivity intramolecular FRET glucose sensor. Biochim. Biophys. Acta (BBA)-Biomembranes 1778, 1091–1099. https://doi.org/10.1201/b18990-115

Toft-Kehler, A.K., Skytt, D.M., Kolko, M., 2018. A Perspective on the Müller Cell-Neuron Metabolic Partnership in the Inner Retina. Mol. Neurobiol. 55, 5353–5361. https://doi.org/10.1007/s12035-017-0760-7

Tolone, A., Haq, W., Fachinger, A., Rentsch, A., Herberg, F.W., Schwede, F., Paquet-Durand, F., 2021. Retinal degeneration: Multilevel protection of photoreceptor and ganglion cell viability and function with the novel PKG inhibitor CN238. bioRxiv.

Tsacopoulos, M., Evêquoz-Mercier, V., Perrottet, P., Buchner, E., 1988. Honeybee retinal glial cells transform glucose and supply the neurons with metabolic substrate. Proc. Natl. Acad. Sci. U. S. A. 85, 8727–8731. https://doi.org/10.1073/pnas.85.22.8727

Valdés, J., Trachsel-Moncho, L., Sahaboglu, A., Trifunović, D., Miranda, M., Ueffing, M., Paquet-Durand, F., Schmachtenberg, O., 2016. Organotypic retinal explant cultures as in vitro alternative for diabetic retinopathy studies. ALTEX 33, 459–464. https://doi.org/10.14573/altex.1603111

Vélez, L., Velasquez, Z., Silva, L.M.R., Gärtner, U., Failing, K., Daugschies, A., Mazurek, S., Hermosilla, C., Taubert, A., 2021. Metabolic Signatures of Cryptosporidium parvum -Infected HCT-8 Cells and Impact of Selected Metabolic Inhibitors on. Biology (Basel). 10, 60.

Wang, L., Tornquist, P., Billl, A., 1997. Glucose metabolism in pig outer retina in light and darkness. Acta Physiol. Scand. 160, 75–81.

Warburg, O., 1924. The metabolism of carcinoma cells. J. Cancer Res. 9, 148–163.

SUPPLEMENTARY INFORMATION II

Extracellular lactate as an alternative energy source for retinal bipolar cells

Authors

Victor Calbiague Garcia[1,2], Yiyi Chen [3], Bárbara Cádiz[2], François Paquet-Durand[3], Oliver Schmachtenberg[2*]

[1] PhD Program in Neuroscience, Universidad de Valparaíso, Valparaíso, Chile

[2] CINV, Universidad de Valparaíso, Chile

[3] Institute for Ophthalmic Research, University of Tübingen, Germany

Corresponding author:

Dr. Oliver Schmachtenberg

CINV, Facultad de Ciencias, Universidad de Valparaíso

Avda. Gran Bretaña 1111, 2360102 Valparaíso, Chile

E-mail: oliver.schmachtenberg@uv.cl

Tel.: +56-32-2995505

Abstract

Retinal bipolar and amacrine cells regulate the first steps in retinal image processing, but to date the flux and consumption of metabolites such as lactate in this group of cells is still unclear. Over the years many studies have suggested the existence of a retinal lactate shuttle due to the high production of this metabolite under aerobic conditions. Here we demonstrate the ability of inner retinal neurons to consume extracellular lactate as an alternative fuel. In addition, this lactate is used to maintain homeostasis of different ions, and electrical responses in rod bipolar cells. Finally, we provide evidence for a functional expression of MCT2 in inner retinal cells, revealing the role of this transporter in the influx of extracellular lactate and the importance in the maintenance of different physiological responses.

Introduction

The retina is a neural tissue in which visual signals are transduced by photoreceptors (PRs) and subsequently processed by inner neurons. Interestingly, this phototransduction process underlies a high energy demand triggered by the dark current produced in the PRs under scotopic conditions. This high activity produced by the large ATP consumption by the ion pumps in the inner segment (IS) of the PRs to maintain the dark current and the constant turnover of the outer segments (OS) are probably the reasons that become the retina the most energy-demanding neural tissue (Ames et al., 1992b; Wong-riley, 2010; Country, 2017). To meet these high energy requirements, retinal neurons can consume metabolites from different sources. For example, RPs can consume glucose, oxygen, and other metabolites from the choroidal blood, which is the main vasculature of the retina (Country, 2017), and from the retinal pigment epithelium ((RPE; (Chen et al., 2022)). Nonetheless, the inner retina will depend on whether the retina is avascular or vascular. In the avascular retina (*e.g.* guinea pig, rabbit), bipolar cells (BCs) and amacrine cells (ACs) probably rely only on Müller cells (MCs), while in the vascular retinas (*e.g.* rodents and primates) the cells can take up the fuel from inner vascularity, MCs, and astrocytes (Hurley et al., 2015b; Country, 2017).

Interestingly, Warburg's results in 1924 pointed out that tumor cells and the retina are the cells that utilize aerobic glycolysis, converting almost 70% of the glucose consumed into lactate (Warburg, 1924; Wang et al., 1997), and many studies have supported the idea about a retinal lactate shuttle (Poitry-Yamate et al., 1995; Lindsay et al., 2014; Kanow et al., 2017). Although the specific site and metabolic condition at which this lactate is released are still unclear, these investigations support the notion of a "metabolic ecosystem" between MCss, RPE, and photoreceptors, in which cells not only produce lactate but also consume it. However, the dynamics and extent of the inner retina of this shuttle remain a matter of debate, especially in vascular retinas (Hurley et al., 2015).

To better understand the general retinal metabolism, we studied the effect of the inhibition of different glycolysis-related enzymes to determine the role of aerobic glycolysis in the maintenance of the activity in the inner retina. Here, we mix different techniques either in *ex vivo* or retinal explant culture performing immunostaining, cell death markers, general calcium imaging, and more specific techniques related to cellular resolution as electrophysiology and FRET sensors to test how extent can be used the extracellular lactate by inner retinal cells. We found the inhibition of lactate transport caused an increase in inner retinal cell death and also altered different physiological responses. These results led to suggest that inner retinal cells can use lactate to maintain physiological activity, therefore they can participate in the retinal lactate shuttle consuming this metabolite.

Results

Inner retina express monocarboxylate transporters

To elucidate the potential role of extracellular lactate in the inner retina, we examined the expression of monocarboxylate transporters (MCTs) in the retina of wild-type mice. The MCT is a proton-linked plasma membrane transporter that allows the carrying of lactate and pyruvate into/out of cells (Halestrap, 2013a). Specifically, we investigated the pattern expression of the MCT2 isoform because it has been suggested to be the neuronal importer of lactate (Pierre et al., 2002; Magistretti and Allaman, 2018), in high lactate environments (Contreras-Baeza et al., 2019). Immunofluorescence localization indicated that MCT2 was exclusively expressed in some somas in the outer nuclear layer (ONL; probably cones) and abundantly expressed in the cells of the inner nuclear layer (INL, Fig. 1a). Co-immunostaining in the INL with different markers indicate that MCT2 colocalize with rod bipolar cell (RBCs), and ACs (Fig. 1a), suggesting that extracellular lactate can be potentially consumed by inner retinal cells.

Inhibition of lactate transport increases cell death in the inner retina

The massive expression of MCT2 in the INL led us to hypothesize that extracellular lactate may be used by inner cells to meet their physiological activity. Then, to study the role of lactate in the inner retina in a functional approach, we cultured mouse retinal explants for 7 days that allowing us to perform experiments under controlled conditions (Calbiague et al., 2020). The effects of the different conditions were characterized by quantifying the cell death rate as the fraction of dying cells in the INL after 4 days of treatment using the TUNEL assay. Since there are no commercial drugs that block only MCT2, we treated retinal explants with MCT1 or MCT1/MCT2 blockers, so we were able to separate the possible effect of MCT1 on MCT2.

In the control condition, the cell death rate was 0.06% ± 0.07 (n=5), and a comparatively low rate (0.44% ± 0.61, n= 6) in the INL was found when we blocked MCT1 with the potent and selective drug SR-13800 0.1 µM (SR, Fig. 1b and 1c) (Murray et al., 2005). On another hand, when we used AR-155858 (2 µM, AR-C), a potent inhibitor of MCT1 and MCT2 (Ovens et al., 2010), a

significant increase (1.67% ± 0.94, n= 6) in TUNEL-positive cells was observed after 4 days of treatment (Fig. 1b and 1c), indicating that the specific blocking of MCT2 has effects in the INL survival rate.

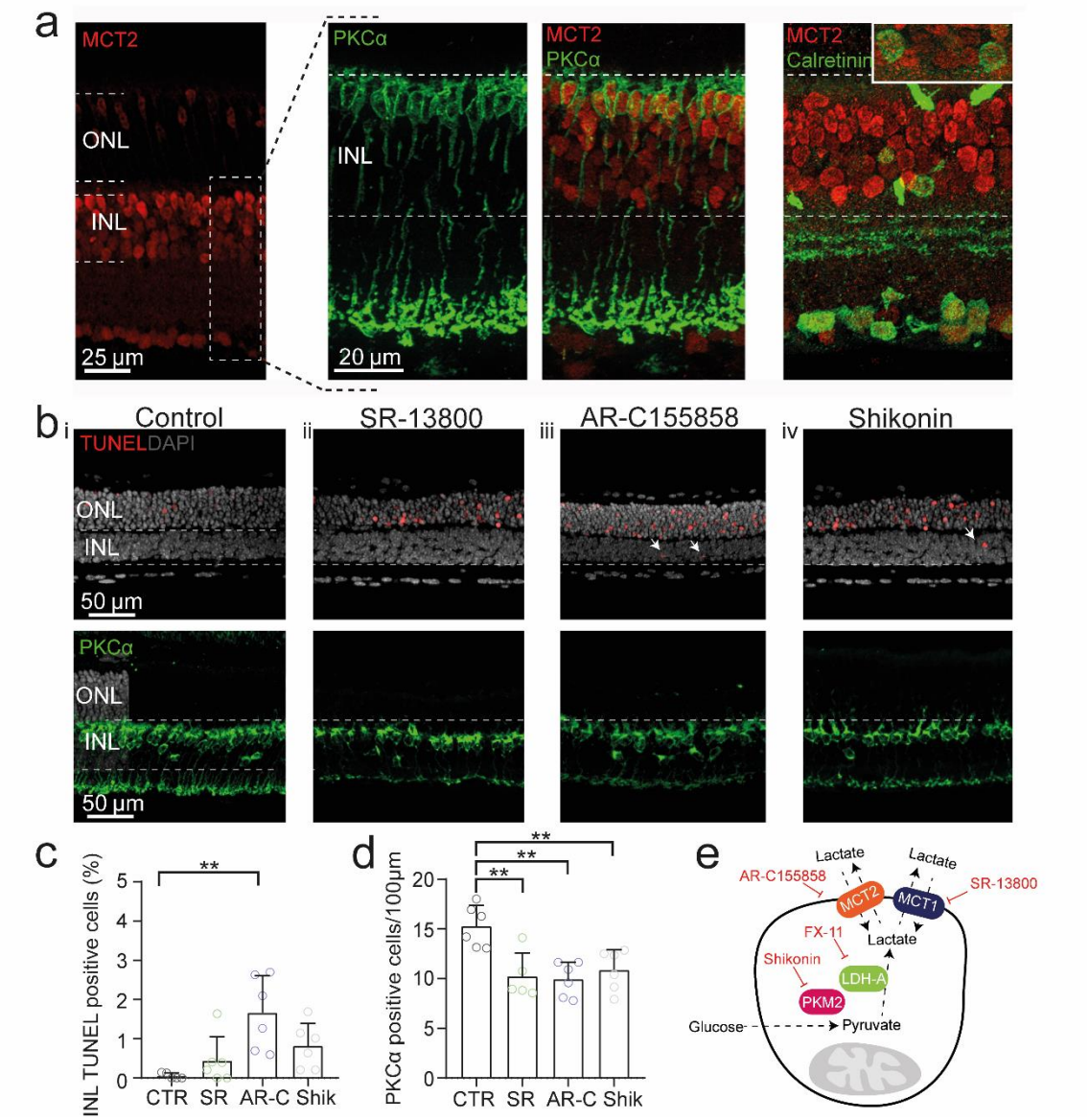

Fig. 1.- Lactate metabolism is required for inner neurons survival. **a**, Immunofluorescence showing MCT2 expression in the inner retina, and a specific co-labelling with PKCα and calretinin revealing that RBCs and ACs express this specific transporter. **bi-iv (top), c**, Statistical analysis, and quantification of the cell death assay (TUNEL), performed in organotypic retinal explants showed occasional reactive nuclei (arrowhead) in AR-C (p= 0.0014), and shik (p= 0.0502)

condition, but a low rate in the SR condition (p= 0.6347). The data were analysed using Kruskal-Wallis test, with Dunn's multiple comparison post hoc test. **bi-iv (bottom), d**, Quantification of the RBCs per 100 µm revealed a reduction of this cell type either in the SR (p= 0.0034), AR-C (p= 0.0012) or shik (p= 0.0070) indicating a specific effect of extracellular lactate on this cell. The data were analyzed by ordinary one-way ANOVA, with a subsequent Tukey's multiple comparison post hoc test. Each dot reflects a single retinal explant. **e**, Schematic summary showing the different drugs and its respective effects in the lactate metabolism. Shikonin and FX-11 inhibit the lactate production directly, while AR-C155858 and SR-13800 block the lactate transport through the membrane. It is important to note that AR-C155858 inhibit MCT1 and MCT2. Graphs display the mean ± SD; asterisks indicate * p < .05, **p < .01. ONL= Outer nuclear layer; INL= Inner nuclear layer; PKCα= Protein kinase C α; MCT1= Monocarboxylate transporter 1; MCT2= Monocarboxylate transporter 2; PKM2= Pyruvate kinase M2; LDH-A= Lactate dehydrigenase A. SR= MCT1 blocker; AR-C= MCT2 blocker; Shikonin= PKM2 inhibitor.

To further understand the possible effects in the reduction of lactate production, we inhibited the enzyme pyruvate kinase (PK) M2 with shikonin 4 µM (Shik) (Chen et al., 2011; Zhao et al., 2018). PK is a key glycolytic enzyme that control the final step of the glycolysis, converting phosphoenolpyruvate to pyruvate, and the M2 isoform in specific is associated with tumor cells and is known as a key regulator of aerobic glycolysis (Christofk et al., 2008; Luo and Semenza, 2012; Wong et al., 2015). The treatment with shik resulted in similar results as in the AR-C condition (0.82 ± 0.57, n= 6), nonetheless, it was not significant (Fig. 1b and 1c). As expected, in all the conditions the number of TUNEL-positive cells are much higher in the ONL, indicating the sensitivity of photoreceptor to metabolic disruptions (Chen et al., 2022).

Since we determine the expression of MCT2 in RBCs, we wanted to explore the effects in the inhibition of the lactate metabolism in the survival rate of this specific cell type. For this reason, the RBCs number per 100 µm was counted, reaching 15.3 ± 2.1 cells (n= 5, Fig. 1b and 1d) in the control condition. Interestingly, in all the treatments the RBCs number decreased (Fig.1b and 1d) compared to the control condition: SR (10.2 ± 2.3, n= 6), AR-C (9.9 ± 1.7, n= 6), and shik (10.8 ± 2.0, n= 6) revealing that lactate metabolism is important for maintaining RBCs alive in culture.

Taken together, these results indicate that the inner retinal cell survival is sensitive to an inhibition of the lactate metabolism, and specifically, RBCs need lactate for surviving in culture, but in a minor level compared to ONL.

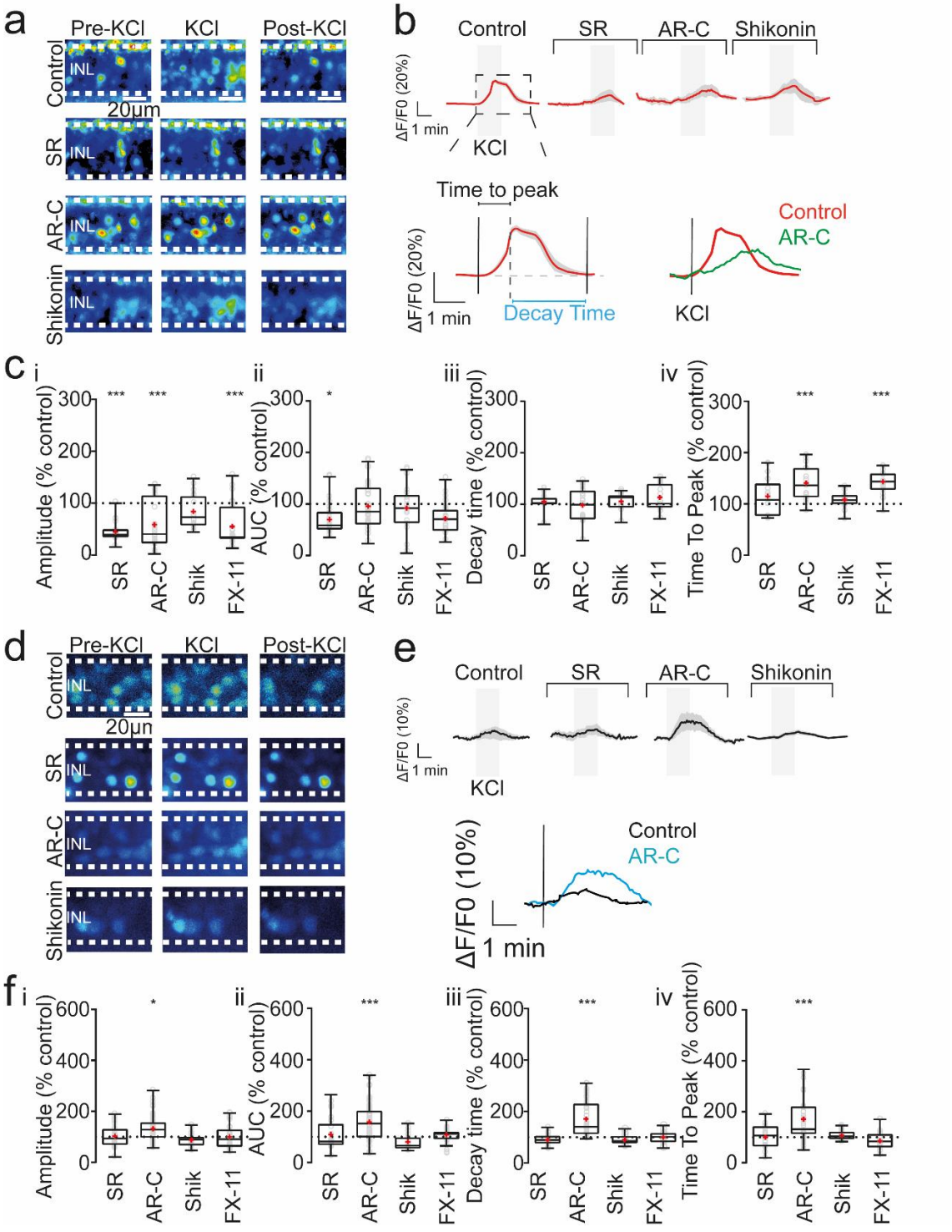

Fig. 2.-Depolarization of the inner neurons is reduced and slowed under inhibition of lactate metabolism. (**a, d)**, Representative images of Fluo4-AM and Corona-gren-loaded cells in the INL, before and at two time points after an application of KCl in the bath perfusion, in control and retinas

incubated with the SR, AR-C and Shik. **(b and e) (top)**, Traces of one single experiment in each condition (red line= mean, grey shadow= standard deviation), indicating the KCl stimulation with the grey boxes. **(b and e) (bottom)**, Overview of the kinetic parameters measured in the imaging responses. The time to peak is how long the response takes to reach the peak from the stimulation starts. While the decay time is how long the response takes to return to the baseline from the peak. In the right we can observe a comparison between control mean vs AR-C mean revealing a small and slower response in the last. **(ci-iv)**, Statistical analysis of the different parameters in the calcium imaging experiments. In the amplitude, the SR ($p= 0.0028$) and AR-C ($p= 0.0004$) shown a decreased in the amplitude, whereas the shik condition had practically the same amplitude than control ($p= 0.9987$). But, when retinal slices are incubated with FX-11, a reduction was observed ($p= 0.0001$). Regarding the AUC, a reduction was observed only in the SR ($p= 0.0148$), while no difference was observed either AR-C ($p= 0.9999$), shik ($p= 0.9675$) or FX-11 condition ($p= 0.2046$). The decay time had no effects also, when we compared the SR ($p= 0.7238$), AR-C ($p= 0.9954$), shik ($p= 0.9991$) or FX-11 condition ($p= 0.7323$) with the control. Interestingly, the time to peak was affected only in the AR-C ($p< 0.0001$) and FX-11 condition ($p <0.0001$), whereas that SR ($p= 0.2514$) and shik condition ($p= 0.5138$) were unaffected. **(fi-iv)**, Statistical analysis in the sodium imaging experiments. These results revealed an increase in the amplitude only in the AR-C condition ($p= 0.0015$), but no differences were observed in the SR ($p= 0.9981$), shik ($p= 0.9999$) or FX-11 ($p= 1.0893$). Similar results were obtained in the AUC, only AR-C condition ($p= 0.0002$), while in the SR ($p= 0.3665$), shik ($p = 0.6889$) and FX-11 ($p= 1.0783$) were unaltered. In the kinetics parameters, the decay time as well as in the other conditions revealed an increment in the AR-C condition ($p= 0.0020$) but no in the SR ($p> 0.9999$), shik ($p= 0.9797$) and FX-11 ($p>0.9999$). Finally, the same results were observed in the time to peak, an increase in the AR-C condition ($p= 0.0008$), and no changes were obtained in the SR ($p> 0.9999$), shik ($p> 0.9999$) and FX-11 ($p> 0.9999$). Box plots display the median ± min and max values and the mean in red. Individual values are displayed as open circles (gray). The control is represented as a dashed line in 100%, then the results are showed as percentage of the control. Asterisks indicate * $p < .05$, ** $p < .01$, *** $p< .001$. INL= Inner nuclear layer; SR= MCT1 blocker; AR-C= MCT2 blocker; Shikonin= PKM2 inhibitor; FX-11= LDH-A inhibitor.

The lactate transport is important to maintain neuronal activity in the inner retina.

Given that the principal function of neurons is propagating electrical signals, it is intuitive to think that their functions depend on the metabolism. Whether inner retinal cells use lactate to meet their physiological activity is one of the questions which remain unclear.

In order to address this issue, we performed calcium imaging experiments because it allows us a global assessment of retinal function. For this, retinal slices from p30 mice were incubated for 15 min (SR, AR-C or shik, Fig. 2a and b), and the change of the relative fluorescence intensities of putative BCs and ACs bodies in the INL after 12 mM K^+ stimulation was measured (Fig. 2b).

We measured the amplitude and the area under the curve (AUC) of the responses (Fig. 2b). Under the blocking of MCT1 (n= 3 retinas, ROIs= 24) and MCT1/MCT2 (n= 3 retinas, ROIs= 30) the amplitude was 44.5% ± 19.0 and 58.5% ± 45.0 of the control (Fig. 2b and 2c), respectively, indicating a reduction of the response compared with the control condition. Interestingly, the acute inhibition of PKM2 with shik (n= 3, ROIs= 20) had no noticeable effect on the amplitude of the calcium responses (Fig. 2b and c, 84.1 % ± 32.4), suggesting that the effect of this drug in the retina is under prolonged treatment (*e.g.,* retinal explants). After that, we changed the target to test the effect of lactate production in the retina, and we inhibited the enzyme Lactate dehydrogenase A (LDH-A) with the selective drug FX-11 (15 µM). This enzyme is responsible directly to convert pyruvate to lactate, and as well as PKM2, is overexpressed in tumor tissue, and is a fundamental regulator of aerobic glycolysis (Le et al., 2009; Miao et al., 2013). Then an inhibition of LDH-A should decrease the aerobic glycolysis rate. Under this condition (n= 3, ROIs= 23), the amplitude was reduced compared to the control (Fig. 2c; 55.1% ± 39.9). In contrast, the AUC did not change in all the conditions either SR (Fig. 2c, 69.9% ± 30.2), AR-C (Fig. 2c, 95.6% ± 43.1), shik (Fig. 2c, 92.2% ± 43.6), and FX-11 (Fig. 2c, 71.9% ± 30.4), suggesting that some kinetics parameters might be affected.

To test the hypothesis that the kinetics are changing, and that is the reason why the AUC is not affected, we analyzed the time to peak and the decay time of the responses. Strikingly, the kinetics parameters were altered in a manner contrary to what we expected. We observed an increase in the time to peak when we inhibited MCT1/MCT2 (Fig. 2b, c, 140.9% ± 31.7) and FX-11 (Fig. 2c, 143.2 ± 23.8), while MCT1 inhibition (114.9% ± 34.5) and PKM2 (108.0% ± 15.8) had not effect. But the decay time was unaffected in any condition (Fig. 4c): SR (105.0% ± 13.8), AR-C (98.2%

± 30.8), shik (105.6% ± 15.6), and FX-11 (113.4% ± 25.5). Altogether, these results indicate that the activity of the INL cells is susceptible to an inhibition of the lactate metabolism, causing a reduction in the amplitude, and a slower response.

The unaffected in the decay time is surprising because by disrupting the energy consumption, the restore of the ion gradients after a depolarization should be affected (Karus et al., 2015a). Nevertheless, because of calcium is important for cells in many functions, they have different intracellular regulator, which can potentially quickly buffer the intracellular calcium concentrations (Brini et al., 2013). For this reason, the next step was to evaluate the ion pump function more directly. We used the sodium probe CoronaGreen (Fig. 2d, e), which might reflect more accurately the relative importance of lactate in the Na^+ pumping. When we measured the amplitude (Fig. 2f) neither the blocking of MCT1 (n= 3, ROIs= 33, 102.1% ± 40.9), PKM2 (n= 3, ROIs= 20, 87.6% ± 26.1), nor LDH-A (n= 3, ROIs= 29, 100.0% ± 45.7) was affected. Similar results were observed in the AUC (Fig. 4f): SR (108.9% ± 64.2), shik (80.7 ± 30.9), and FX-11 (108.3% ± 23.1). Nonetheless, when we blocked MCT1/MCT2 with AR-C the amplitude (131.8% ± 51.5), and the AUC (157.1 ± 70.9) increased significantly (Fig. 2f).

Comparable results were obtained regarding the kinetics parameters: when we blocked MCT1 (100.3% ± 41.7), PKM2 (107.2% ± 19.4), and LDH-A (85.9% ± 31.7) we did not observe changes in the time to peak. Likewise in the decay time: MCT1 (90.9% ± 21.5), PKM2 (89.7% ± 18.9), and LDH-A (99.9% ± 26.3). But when we blocked the MCT2 the time to peak (171.0% ± 85.4), and the decay time (171.0% ± 70.2) increased (Fig. 2f).

Taken together, these results indicate that only when we inhibited MCT2 was depolarization in the INL affected, especially the kinetic responses, suggesting an alteration in ion pumping to restore sodium homeostasis (Karus et al., 2015a; Gerkau et al., 2017). If this idea is correct, then we should observe a change in the basal levels of these ions that may produce the alterations seen above (Fig. 2). To raise this question, we measure basal fluorescence, and calculate the slope of

the baseline to analyze whether there is calcium or sodium accumulation under blocking/inhibition of these different transporters/enzymes related to aerobic glycolysis.

As for relative calcium levels, it is striking that in 3 different conditions (*i.e.,* SR, Shik, and FX-11), the baseline decreased significantly: The blocking of MCT1 reduced by 74.8% ± 43.9, whereas inhibition of PKM2 and LDH-A produced a reduction of 77.1% ± 85.6 and 147.1% ± 78.0, respectively (Fig. S4a, c, d, e). In contrast, incubation with AR-C resulted in a slight increase in relative intracellular calcium levels (34.9% ± 79.2; Fig. S4b, e).

Conversely, for relative sodium levels, the effect was more specific and was only affected by the blocking of MCT2 and to a lesser extent by LDH-A inhibition (Fig. S5). The results are surprising because the proposed hypothesis was that sodium levels would increase under inhibition of lactate metabolism. However, we observed a significant drop in baseline relative sodium of 282.2% ± 155.1 under AR-C incubation, and 31.9% ± 55.7 for the FX-11 condition (Fig. S5b, d, e).

In summary, these results demonstrate that inhibition of lactate metabolism can disrupt many features of neuronal depolarization in the inner retinal cells.

Lactate can be used as an alternative fuel for RBCs

Although this is a general way of assessing neuronal activity, previous experiments indicate that lactate metabolism appears to be essential for maintaining retinal cell activity. We next set out to test the importance of extracellular lactate at the cellular level by studying different currents in retinal cells performing whole-cell patch-clamp recordings. In mammals, the concentration of lactate in the retina fluctuates between 5-50 mM depending on the species (Kolko et al., 2016). Here we measured the lactate released in retinal explants after 4 days in culture and we obtained a concentration of 16.7 mM ± 5.7 lactate in the culture medium, in line with previously reported values (Kolko et al., 2016). Then, *ex vivo* retinas from p30 mice were incubated for 15 min in 4 different conditions: 20 mM glucose (control), 20 mM lactate + 10 mM mannitol (no glucose,

mannitol was used for osmolarity), 40 mM lactate (no glucose) and 20 mM mannitol (no glucose), and we analyzed the outward current (I_{out}), calcium current (I_{Ca}) and membrane potential (V_{memb}) under photopic conditions.

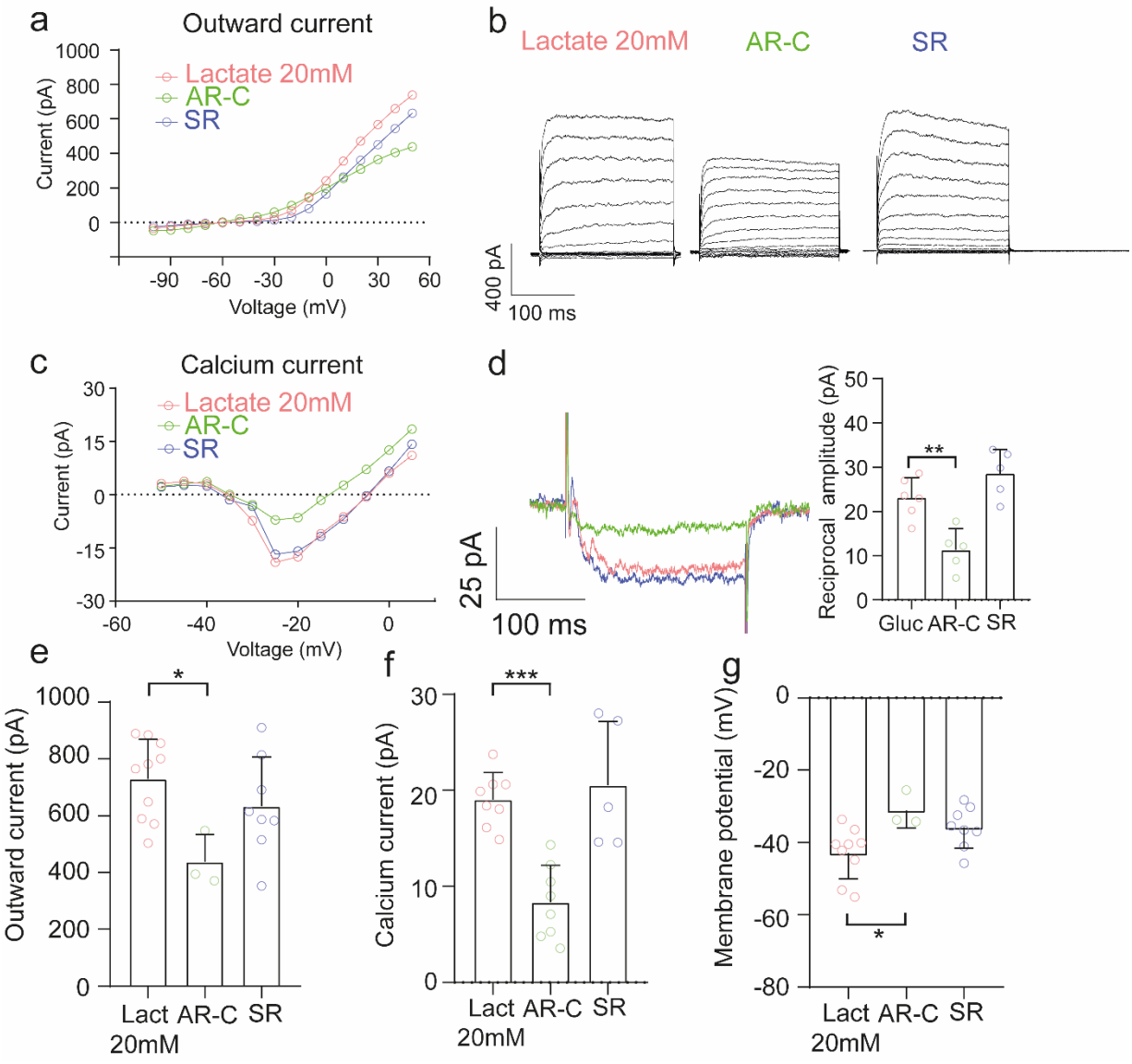

Fig. 3.-Inhibition of lactate transport through MCT2 provokes alterations in RBCs currents. **(a, c)**, Comparison of voltage-current relationship of the outward current and calcium current in the different conditions. **(b, d),** Representative recorded responses to depolarizing voltage steps. The reciprocal feedback was altered only in the AR-C condition (p= 0.0042) but was unaffected in the SR condition (p= 0.1957) compared with the control condition. **(e, f)**, in presence of 20mM

lactate, only when MCT2 is inhibited we observed a decreased in the outward current (p= 0.0224), and calcium current (p= 0.0003), but no differences was noted when MCT1 was blocked either in the outward current (p= 0.3925) or calcium current (p= 0.8146). **(g)**, Similar results were obtained when we measured the membrane potential, but now it reflects as a depolarization in the AR-C condition (p= 0.0321), while in the SR condition is maintained (p= 0.0822). The data were analyzed by ordinary one-way ANOVA, with a subsequent Tukey's multiple comparison post hoc test. Each dot reflects a single recorded cell. Graphs display the mean ± SD; asterisks indicate * p < .05, **p < .01, ***p< .001. SR= MCT1 blocker; AR-C= MCT1 and MCT2 blocker

---

These electrophysiological experiments showed that in retinas incubated with 20 mM lactate, or 40 mM lactate, the RBCs did not change the amplitudes of their I_{Ca}, I_{out} and V_{memb} compared with retinas incubated with glucose (Fig. S1 and Table 1). Whereas retinal cells incubated with 20 mM mannitol (metabolite that is not metabolized), showed a decrease in their I_{Ca}, I_{out}, and an increase in their V_{memb} (Fig. S1 and Table 1). A specific feature of the calcium current in RBCs is the presence of a transient reciprocal feedback coming from A17 (Chávez et al., 2006). This feedback was only affected in the presence of 40 mM lactate and abolished in the mannitol condition (Fig. S1 and Table 1). On the other hand, the 20mM condition maintained the amplitude of this reciprocal. These results indicate that 20mM lactate is able to substitute the role of glucose, suggesting that RBCs can use this metabolite as an alternative substrate to meet their physiological activity. Moreover, an ultra-saturated lactate environment and, a glucose deprivation condition affects the A17 feedback.

Table 1. Summary of the principal electrophysiological characteristics of RBCs under different metabolic conditions. Values are given as mean ± SD, and total number of cells (n).

	I_{out} (pA)	I_{Ca} (pA)	Reciprocal feedback (pA)	V_{memb} (mV)
Glucose	775.9 ± 73.2 (12)	20.8 ± 3.7 (7)	26.5 ± 10.4 (4)	-41.2 ± 5.4 (10)
Lactate 20mM	729.2 ± 140.3 (9)	19.0 ± 2.8 (8)	23.1 ± 4.5 (6)	-41.1 ± 7.6 (9)
Lactate 40mM	841.7 ± 96.7 (8)	17.2 ± 2.1 (6)	3.6 ± 1.7 (4)	-40.8 ± 6.5 (7)
Mannitol	364.6 ± 86.7 (9)	8.2 ± 4.3 (4)	- (4)	-31.5 ± 6.5 (7)
Gluc + SR	667.8 ± 147.9 (8)	18.9 ± 5.5 (3)	28.3 ± 9.9 (3)	-36.1 ± 7.4 (8)
Gluc + AR-C	677.5 ± 84.3 (8)	21.8 ± 6.7 (3)	28.5 ± 2.1 (3)	-37.6 ± 5.3 (9)
Lact 20mM + SR	633.8 ± 173.3 (8)	20.6 ± 6.7 (5)	28.5± 5.4 (5)	-35.8 ± 5.7 (8)
Lact 20mM + AR-C	438.0 ± 95.9 (5)	8.4 ± 3.8 (8)	11.3 ± 4.8 (5)	-31.2 ± 4.9 (5)

Next, we tested the idea about the MCT2 expression in RBCs. To that end, retinal slices were incubated with different MCT inhibitors in the 20 mM lactate condition since this concentration will trigger an influx of this metabolite (see below). When we measured the different currents, we observed that undergo alterations only when MCT1 and MCT2 (Fig. 3 and Table 1) are inhibited at the same time, and not when MCT1 is inhibited only (Fig. 3 and Table 1). These results are in line with the immunostaining results, and the imaging experiments and reveal that MCT2 is expressed in RBCs and that it is important to maintain neuronal activity.

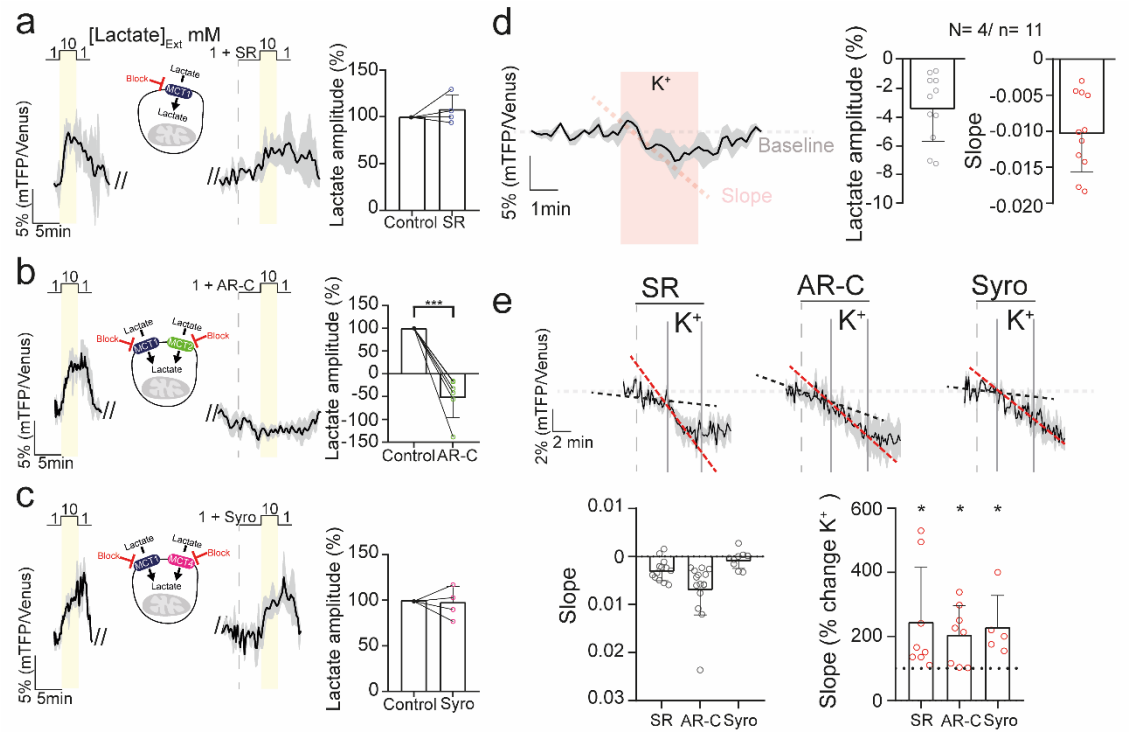

Fig. 4.- A decrease in intracellular lactate levels was observed after bath application of a MCT2 blocker. **(a-c, left)** Lactate influx evoked after a stimulation with 10 mM lactate. (a-c, middle) Lactate influx responses after an incubation with different drugs which target monocarboxylate transporters (MCTs). **(a-c, right)** Statistical analysis of the response amplitude. An evident response disrupted was noted only when MCT2 is blocked (p= 0.0005), but under MCT1 (p= 0.3768) and MCT4 (p= 0.8192) inhibition the amplitude was unaltered. **(d)** Effect of transient depolarization on intracellular lactate. **(e, top)** Effects on lactate dynamics after inhibition of different MCTs and retinal depolarization. Black dashed lines indicate drug-induced change in slope, red dashed lines indicate effect of drug + KCl. **(e, bottom)** Statistical analysis of the slope of the responses in basal condition (only drug, left) and under depolarization (drug + K^+, right). The data reveal that inhibition of MCT2 leads to a reduction in intracellular lactate levels, resulting in lactate consumption. This consumption is exacerbated after a depolarization: SR (p= 0.0456), AR-C (p= 0.0393) and Syro (p= 0.0416). Data were analyzed either with a Paired Student´s t-test or Wilcoxon matched-pairs test. The black trace represents the average of one experiment, while the light grey shadow represents the standard deviation. Graphs display the mean ± SD. * Indicates p < .05. SR= MCT1 blocker; AR-C= MCT1 and MCT2 blocker; Syro= MCT1 and MCT4 blocker. The number of experiments is represented as: N= number of explants; n= number of cells recorded.

Finally, we wondered if lactate can be used over the glucose as metabolite to meet their physiological currents in RBCs. In this regard, we used the 20 mM glucose condition, and we blocked different MCTs. As expected, neither AR-C or SR condition altered nor decreased (Fig. S2 and Table 1) the amplitude of the I_{out}, I_{Ca}, V_{memb}, and the reciprocal feedback, suggesting that RBCs can use lactate as an alternative fuel, but glucose is still preferred upon lactate.

These results indicate that neurons in the inner retina can use extracellular lactate, consuming it through MCT2, and that it is important for maintaining neuronal activity.

Intracellular lactate dynamics in the inner retinal cells

The previous results propose the idea of lactate consumption of the inner retinal cells. Nonetheless, to date, there is a lack of information about the intracellular lactate flux in the retina. For the purpose of investigating the lactate dynamics in the INL cells we expressed the FRET nanosensor h-Syn-Laconic (neurons) and GFAP-Laconic (MCs) in retinal explant cultures, as previously described (San Martín et al., 2013; Calbiague et al., 2022).

Before, we expressed successfully this nanonsensor in retinal MCs in retinal explant cultures (Calbiague et al., 2022). So now we evaluated whether nanosensor expression was functional in inner retinal neurons. For this, we measured the ratio between the emissions obtained from monomeric teal fluorescent protein (mTFP)/Venus in the soma of putative BCs and ACs in the INL (Fig. S3). Then, we saturated the lactate nanosensor with 10 mM of lactate (Fig. S3), and to deplete intracellular levels of these metabolites, we used 10mM pyruvate to take advantage of a property of MCTs called trans-acceleration (Poole and Halestrap, 1993). The delta ratio between the depletion and the saturation for Laconic was 20.3 ± 4.1% (Fig. S3), which is line to the responses in the retina and other cells and tissues (San Martín et al., 2013; Ruminot et al., 2019; Calbiague et al., 2022)**.** Together, these results shown that FRET nanosensor can be functionally expressed in retinal explant cultures to study metabolic dynamics on a single-cell level in neurons.

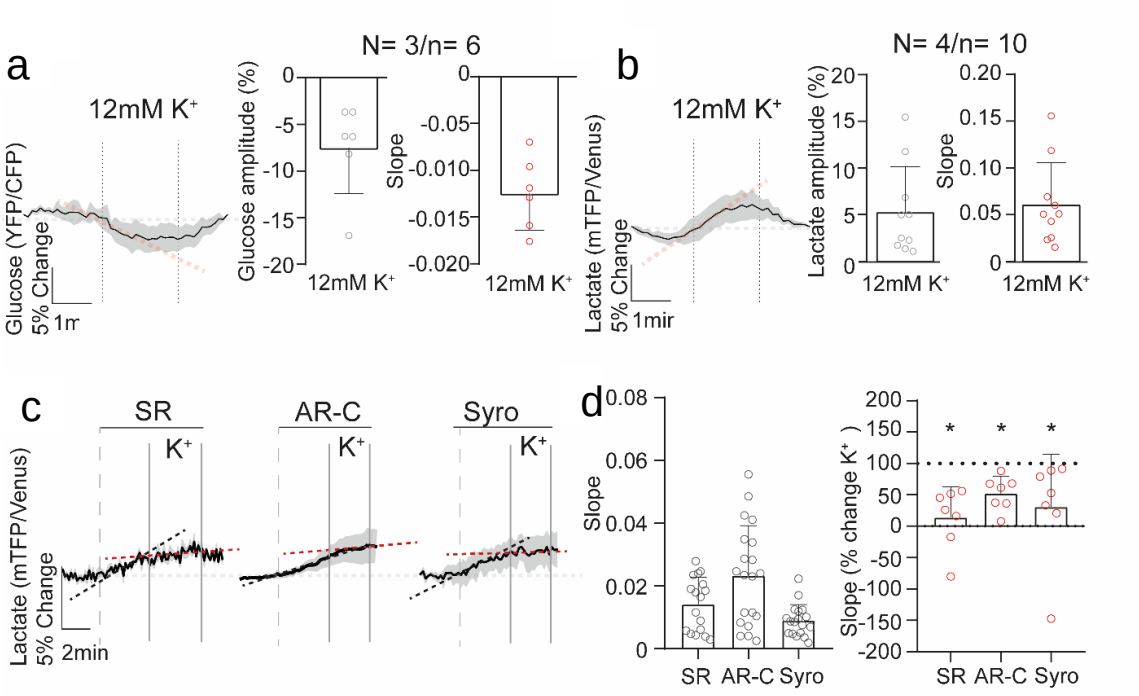

Fig 5.- Lactate dynamics of MCs under different conditions. (a and b) Effect of transient depolarization on intracellular glucose (left) and lactate (right). **(c)** Effects on lactate dynamics after inhibition of different MCTs and retinal depolarization. Black dashed lines indicate drug-induced change in slope, red dashed lines indicate effect of drug + KCl. **(c)** Statistical analysis of the slope of the responses in basal condition (only drug) and under depolarization (drug + K+). A clear accumulation of intracellular lactate was observed after bath application of different MCTs blockers. But this increment ceased significantly after a depolarization in all the conditions: SR (p= 0.0156), AR-C (p= 0.0156), and Syro (p= 0.0156). Data were analyzed either with a Paired Student´s t-test or Wilcoxon matched-pairs test. Graphs display the mean ± SD. * Indicates p < .05. SR= MCT1 blocker; AR-C= MCT1 and MCT2 blocker; Syro= MCT1 and MCT4 blocker. The black trace represents the average of one experiment, while the light grey shadow represents the standard deviation. The number of experiments is represented as: N= number of explants; n= number of cells recorded.

After confirming the functional expression of the lactate sensor, we aimed to elucidate the expression of MCT2 in the INL using the Laconic sensor. Since these transporters work as bidirectional, we applied a 10mM lactate stimulation to trigger a lactate influx into cells. The amplitude of this response was 7.9 ± 3.4%. (Fig. 4). Under the inhibition of MCT1 (9.9 ± 3.6%),

or MCT1 and MCT4 (9.0 ± 3.1%) this amplitude is unaffected (Fig. 4). Nevertheless, when MCT1 and MCT2 are inhibited, the influx amplitude was abolished (Fig. 4), revealing the role of MCT2 in the lactate flux in inner retinal neurons. These results confirm the expression of MCT2 in BCs and ACs.

We then investigated how lactate dynamics change under different conditions in retinal neurons. To that end, we compared the response under basal conditions and moderate depolarization. We perfused the retinal slices with a 12 mM KCl solution, which triggered a transient decrease in intracellular lactate as evidenced by a -4.6 ± 2.0% fluorescence drop (Fig. 4) in inner neurons suggesting a lactate consumption. It is important to note that a percentage of the cells recorded (35.3%) did not respond to this stimulation (Fig. S6).

To compare the lactate dynamics in different inner retinal cells, we did the same experiment but in MCs, to separate between neuronal and non-neuronal component. In these cells, the depolarization produces an increase in lactate levels with a fluorescence peak of 4.9 ± 4.1% (Fig. 5). We also express a glucose nanosensor (Δ6), to analyze glucose levels in MCs. Interestingly, the depolarization triggered a transient decrease of MCs intracellular glucose as evidenced by a -7.5 ± 4.9% fluorescence drop measured with the Δ6 nanosensor (Fig. 12A), suggesting higher glucose consumption triggered by K^+ in MCs. This result is in line with data obtained from astrocytes in the brain (Bittner et al., 2011).

These results reveal a potential different metabolism between inner neurons and MCs, where neurons may consume lactate, while MCs may produce it. To test this hypothesis, we performed a protocol widely used called transport-stop protocol (Bittner, 2010; San Martín et al., 2013; Baeza-Lehnert et al., 2019). This protocol is based on the blocking of MCTs which led to study the intracellular lactate synthesis and consumption. After the blocking of MCTs, the intracellular lactate levels only decreased in the AR-C condition in neurons (Fig. 4e), revealing that inner neurons consume lactate through MCT2 in culture basal condition. Conversely, after blocking of MCTs, the intracellular lactate levels increased in all conditions in MCs (Fig. 5c, d left). It is

interesting, because this results in together suggest that the ANLS hypothesis might operate under this experimental basal condition (Pellerin and Magistretti, 1994).

Remarkably, when the retina was depolarized, the lactate decreased significantly in neurons under all the conditions, even under the blocking of MCT1 (145.5% ± 169.5) and MCT1/MCT4 (129.9% ± 98.2). The reduction under SR and Syro is understandable since whether inner neurons cells does not express those transporters, they should have the same responses as under the depolarization without any drugs (Fig. 4d). Whilst the increase after the blocking of MCT2 (105.7% ± 90.9), reveals that a depolarization triggers an augment in the lactate consumption, then evidently support the notion that inner retinal neurons take up extracellular lactate to meet its physiological activity.

In contrast, in MCs, when the retina was depolarized, the lactate increase ceased, leading to a new and high intracellular lactate baseline. Also, these results suggest that under this condition, lactate consumption became possible (Fig. 5c, d right), and that some MCs can also be lactate consumers (Lindsay et al., 2014; Kanow et al., 2017). These results reveal a flexible and dynamic regulation of glucose and lactate consumption in the inner retina, depending on the activity status of the retina.

Discussion

Although is known that the photoreceptor are the cells which have the highest energy expenditure in the retina (Okawa et al., 2008; Ingram et al., 2020), it is important to understand the metabolism in less energy-consuming cells, cause the metabolism of the entire retina it is crucial to fully comprehend the evolution of the eye design (Baden et al., 2019). Our work here adds important information regarded to the retinal lactate shuttle, combining different technique for the purpose of demonstrate the consumption of extracellular lactate by INL cells (Fig. 6).

The MCT2 expression in the inner retina is not surprising because this transporter is known as the neuronal MCT. Several authors have proposed in their models the neuronal consumption of

lactate through this specific isoform over other (Pierre et al., 2002; Pérez-Escuredo et al., 2016; Magistretti and Allaman, 2018) and are in line with previous immunohistochemical studies in the retina (Gerhart et al., 1999; Chidlow et al., 2004). However, a functional demonstration of this expression and its role in the physiological functions of the inner retina was still needed. Especially in vascular retinas, where the inner cells can obtain metabolites from a wider range of sources compared to photoreceptors (Yu and Cringle, 2001). This is probably the reason why we observed a low impact on the dead cell rate in the TUNEL assay in INL when we blocked MCT2 (only 1.67%), and SR and shik treatments did not show significant alterations. Previous work demonstrates the ability of neuroretina to be metabolically plastic to meet its energy expenditure (Chen et al., 2022). Although this study was focused on the outer retina, some important enzymes involve in different metabolic pathways were expressed in the INL, then we cannot rule out the same capacity for the inner retina.

Furthermore, here we found that under prolonged treatment RBCs showed alterations in all conditions. This is interesting because it indicates a relevant dependence of RBCs on extracellular lactate. However, it is contradictory to the TUNEL results, as the number of RBCs decreased by almost 5%, compared to 1.6% in the TUNEL assay. One possible reason is a change in RBC's identity. Previously, some investigations have shown that a reduction in RBC number is accompanied by a morphological change, so it may be indicative of reactive remodeling preceding the cell death process (Jung et al., 2015; Yang et al., 2019), moreover in the process RBCs can have alterations in important genes that regulate PKCα expression (Jung et al., 2015).

Many studies have suggested dysregulation of calcium and sodium homeostasis under metabolic disturbances (Llorente-Folch et al., 2015; Gerkau et al., 2017), and one possible explanation is the role of ATP production in the maintenance of ionic gradients after depolarizations (Country, 2017)**.** Since transport of ions across biological membranes against concentration gradients is ATP-dependent, a disruption in the metabolism will affect the restoration of ions gradients (Karus et al., 2015a). Indeed, a delayed return to baseline is what we observed in the sodium signaling,

strengthening the previous idea. Thus, this sluggish return can produce an accumulation of these ions in the cytoplasm leading to a reduction (and slower) in the influx of different ions: in this study, specifically in calcium signaling (see ref (Gerkau et al., 2017)) and is the possible justification for depolarization under AR-C and mannitol conditions in RBCs, and in a long-term view probably the reason for the cell death process.

Regarding the substantial increment in sodium responses, the decrease in sodium baseline can explain these results. However, it does not fit entirely with our idea. This result might be explained by the role of these ions in mitochondrial function. Many studies have showed that an increase in cytoplasmic calcium concentrations, directly produce a rise in mitochondrial calcium levels, that regulate numerous enzymes (Denton, 2009; Gellerich et al., 2009; Rossi et al., 2019). Subsequently, to recycle calcium ions, mitochondrial Ca^{2+} efflux is mediated by the electrogenic Na^{+}/ Ca^{2+} exchanger, NCLX. (Cabral-Costa and Kowaltowski, 2020; Delierneux et al., 2020; Assali and Sekler, 2021). The activation of this exchanger might reduce the cytoplasmatic sodium. This reduction can be enhanced after a depolarization produced by high intracellular calcium levels, causing an activation of ion pumps (Attwell and Laughlin, 2001). A previous study proposed a non-canonical modulation of ATP levels mediated by Na^{+}/K^{+} pump, where the Na^{+} flux is capable to control glycolysis and ATP production (Baeza-Lehnert et al., 2019). Therefore, the regulation of calcium and activation of Na^{+} pumping might induce the reduction on sodium in the cytoplasm.

Since our experiment cannot directly demonstrate this idea in its entirety (we still need to rectify the involvement of NCLX), we only propose this mechanism to explain our results, and further experiments will be necessary to test this model. Furthermore, this explanation is only for one condition tested here, whereas many questions remain open in other conditions (*i.e.,* SR, Shik, and FX-11). However, these enzymes are apparently not expressed in inner neurons, so indirect effects are likely to be involved.

Whether the ion gradients are affected, then we should expect alterations in different electrical responses. Specifically, an inhibition of MCTs attenuates b-wave with a delayed of implicit time

but in presence of extracellular lactate a partial recovery was obtained (Bui et al., 2004). These results suggest a possible consumption of extracellular lactate by BCs to maintain electrical responses. Our results support this notion, because an inhibition of MCT2 produces alterations in many parameters in calcium and sodium signaling after a general depolarization, and more specific in outward current, calcium current and membrane potential in RBCs. Additionally, the attenuation induced in the currents and membrane potential by a glucose deprivation (*i.e* mannitol condition) is prevented in presence of extracellular lactate (Fig. 3) (Karus et al., 2015b). However, here we show that glucose is preferred to lactate to maintain its physiological activity (Winkler et al., 2004).

Our results clearly indicate a lactate consumption by inner neurons, and this consumption is exacerbated under a depolarization, indicating that the ANLS hypothesis is completely feasible in our conditions (Poitry-Yamate et al., 1995). Interestingly, this observation is not really extrapolatable to all inner neurons, since as is shown in Fig. S6, not all neurons display a lactate consumption after a depolarization. Although this is likely because of the wide cell type heterogeneity that conform the INL (Shekhar et al., 2016b).

Given that all our experiments were carried out in scotopic conditions, is adequate to think that this metabolic model is subjected to this specific environment. This makes the retina a complex but interesting tissue to study metabolism, because different cells might have different metabolism under different light levels, and the metabolites to meet their metabolic demand can shuttle between, RPE, PRs, and ONL, and now INL.

In summary, the observations reported here allow us to point out that inner retina participate in the retinal lactate shuttle, where MCs release lactate under basal condition, and inner neurons potentially consume a percentage of this extracellular lactate to meet their neuronal activity (Fig. 6).

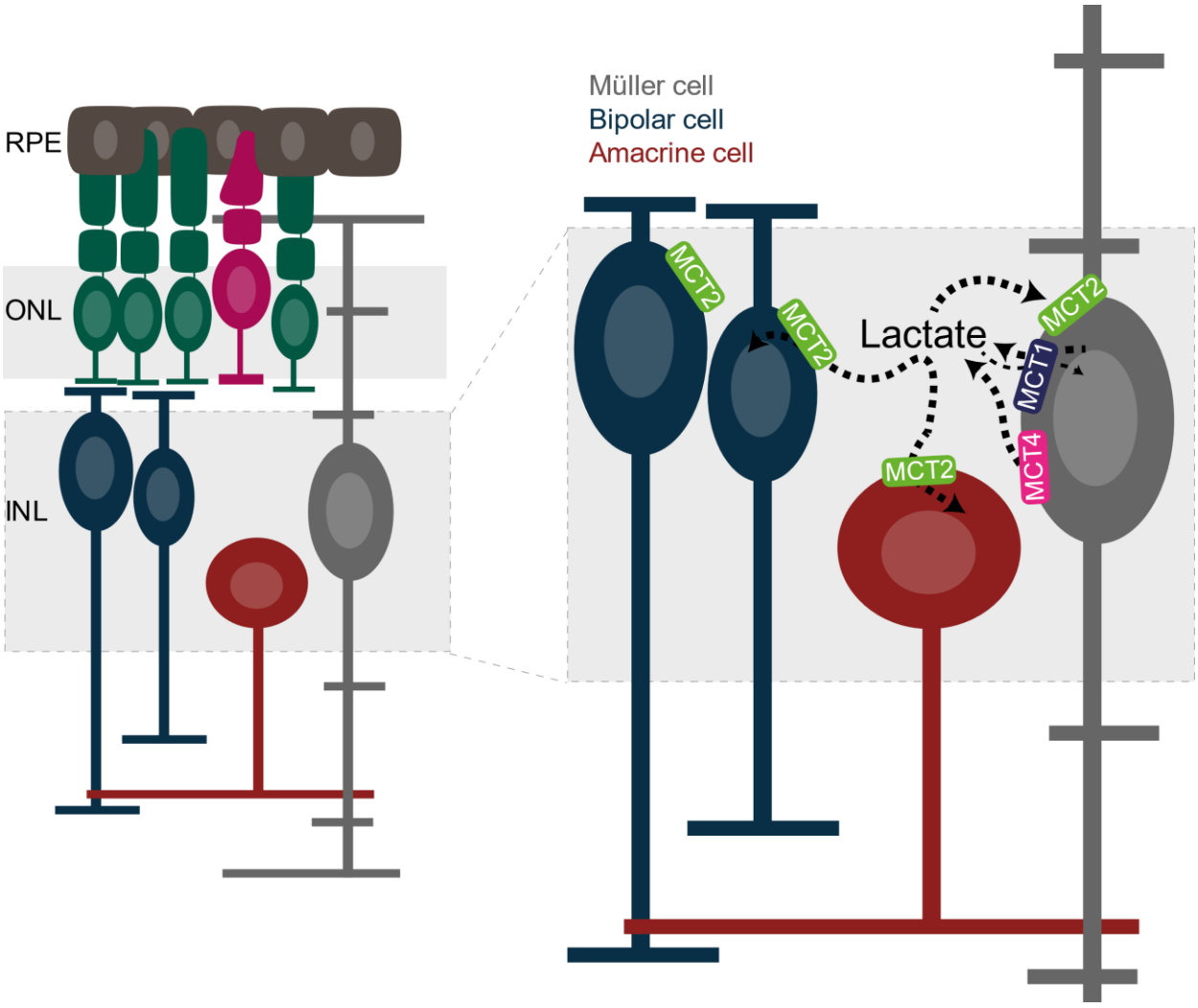

Fig. 6.- Model for the lactate dynamics in the inner retinal cells. General model proposing a consumption of lactate by inner retinal cells. A previous work (Calbiague et al. 2022) demonstrated the functional expression of MCT1, MCT2 and MCT4 in MCs, where MCT2 regulates lactate influx (in a minor role also MCT1), and MCT4 of lactate efflux, contributing to the accumulation of extracellular lactate. In this study me proposed that this extracellular lactate produced by MCs and probably other retinal cell types is consumed by BCs and ACs through MCT2. MCT1= Monocarboxylate transporter 1; MCT2= Monocarboxylate transporter 2; MCT4= Monocarboxylate transporter 4.

Acknowledgments

This study was supported by FONDECYT grant No. 1210790, the National Agency for Research and Development (ANID) scholarship 2018 - 21180443 (V.M.C). Also, we wish to thank Dr. Ivan Ruminot, Dr. Felipe Baeza-Lehnert, and Dr. Felipe Barros from Centros de Estudios Científicos (CEC) in Valdivia (Chile) for sharing its expertise in FRET measurements, and to Felipe Tapia from Universidad de Valparaíso for helping in the data analysis.

Methods

Animals

Wild type C57Bl/6 and C3H mice were housed under standard white cyclic illumination, with water and food *ad libitum*, and were used irrespective of gender. All efforts were made to minimize the number of animals used and their suffering. Protocols compliant with the German law on animal protection and were reviewed and approved by the ‘‘Einrichtung für Tierschutz, Tierärztlichen Dienst und Labortierkunde’’ of the University of Tübingen and were approved by the bioethics committee of the University of Valparaiso, in accordance with the Chilean animal protection law No. 20.380. To isolate the eyes, animals were deeply anesthetized by inhalation using isoflurane and euthanized via decapitation.

Organotypic retinal explant culture

Retinal explants obtained from post-natal (p) day 9 wild-type mice were cultured as previously described (Valdés et al., 2016; Belhadj et al., 2020; Calbiague et al., 2020). Briefly, the retinas were treated for 15 min with 0.12% Proteinase K (Cat. No. P2308, Sigma-Aldrich) at 37°C for isolation of the retina together with its RPE. Then, the eyes were placed for 5 min in DMEM medium with 10% fetal bovine serum (FBS) to deactivate Proteinase K. Finally, the retina was placed with the RPE facing down on cell culture inserts (Millicell, Cat. No. PICM0RG50, Merck Millipore) with DMEM culture medium (Cat. No. 31600034, Thermo Fisher Scientific), containing 10% FBS (Sigma-Aldrich) with 15 mM glucose, which was replaced every two days. The cultures

were incubated at 37°C in 5% CO_2, and 95% humidity for 14 days in a water-jacketed incubator (Thermo Scientific).

Immunostainings

Retinas from p30 mice were fixed in 4% paraformaldehyde for 45 minutes, washed in PBS buffer, cryopreserved with solutions containing 10, 20, and 30% sucrose before embedding in tissue-freezing medium, and stored frozen at -20°C. Transverse sections of 14 µm diameter were obtained with a cryostat (Leica CM-1900) and deposited on poly-L-lysine-coated slides, which were dried at 37°C for 30 min and rehydrated for 10 min in PBS at room temperature (RT). For immunofluorescent labelling, the slides were incubated with blocking solution (10% normal goat serum, 1% bovine serum albumin in 0.3% PBS-Triton X 100) for 1 h at RT. The primary antibodies: Anti-MCT1 (SLC16A1) (Cat. No. AMT-011, Alomone labs, RRID: AB_2756669), Anti-MCT2 (SLC16A7) (Cat. No. AMT-012, Alomone labs, RRID: AB_2340997), Anti-MCT4 (SLC16A4) (Cat. No. AB180699, Abcam), Anti-Glutamine synthetase (Cat. No. AB73593, Abcam, RRID: AB_2247588), Anti-glutamate-aspartate transporter (Cat. No. AGC-021, Alomone labs, RRID: AB_2039885), Anti-PKCα, and Anti-calretinin were diluted 1:100 in blocking solution and incubated at 4°C overnight. The slides were washed 3 times for 10 min each with PBS. Subsequently, the secondary antibody, diluted 1:350 in PBS, was applied to the slides, which were incubated for 1 h at RT. Finally, the slides were washed with PBS and covered in Vectashield with DAPI (Vector).

TUNEL assay

Fixed slides from retinal explant cultures were dried at 37°C for 30 min and washed in phosphate buffered saline (PBS) solution at room temperature (RT), for 15 min. Afterwards, the slides were placed in TRIS buffer with proteinase K at 37°C for 5 min to inactivate nucleases. The slides were then washed with TRIS buffer (10 mM TRIS-HCL, pH 7.4), 3 times for 5 minutes each. Subsequently, the slides were placed in ethanol-acetic acid mixture (70:30) at -20°C for 5 min followed by 3 washes in TRIS buffer and incubation in blocking solution (10% normal goat serum,

1% bovine serum albumin, 1% fish gelatin in 0.1% PBS-Triton X100) for 1h at RT. Lastly, the slides were placed in the terminal dUTP-nick-end labelling (TUNEL) solution (labelling with either fluorescein or tetra-methyl-rhodamine; Roche Diagnostics GmbH, Mannheim, Germany) in 37°C for 1 h and covered in Vectashield with DAPI (Vector, Burlingame, CA, USA) thereafter.

Microscopy and cell counting

Fluorescence microscopy was performed with a Z1 Apotome microscope equipped with a Zeiss Axiocam digital camera (Zeiss, Oberkochen, Germany). Images were captured using Zen software (Zeiss) and the Z-stack function (14-bit depth, 2752*2208 pixels, pixel size = 0.227 µm, 9 Z-planes at 1 µm steps). The raw images were converted into maximum intensity projections using Zen software and saved as TIFF files.

Inner retinal cells stained by the TUNEL assay were counted manually on 3 images per explant, the average cell number in each INL area was estimated based on DAPI staining and used to calculate the percentage of TUNEL positive cells.

Retinal slice preparation for imaging and electrophysiological experiments

For FRET experiments, the explants were separated from the culture inserts and were placed in a chamber with extracellular solution. For imaging and electrophysiology experiments, p30 mice were used. Eyes were enucleated and the retina was kept in extracellular solution during the remainder of the procedure. The eye was cut along the *ora serrata* to separate the anterior and posterior chambers, and the retina was separated carefully from the choroid – sclera. The extracellular solution for maintaining both types of slices contained (in mM): 119 NaCl, 23 NaHCO3, 1.25 NaH2PO4, 2.5 KCl, 2.5 CaCl2, 1.5 MgSO4, 20 glucose and 2 Na^+ pyruvate, aerated with 95% O2 cand 5% CO2, pH 7.4. Finally, in both cases, the tissue was embedded in type VII agarose (Cat. No. 39346-81-1 Sigma Aldrich) dissolved in a solution composed of (in mM): 119 NaCl, 25 HEPES, 1.25 NaH_2PO_4, 2.5 KCl, 2.5 $CaCl_2$, 1.5 $MgSO_4$ at a pH of 7.4. Subsequently, the tissue was cut with a vibratome (Leica VT1000S) to 200 µm thickness. The slices were transferred to the microscope recording chamber, sustained by a U-shaped platinum

wire and superfused with oxygenated extracellular solution at room temperature (20°C) under photopic conditions.

For FRET imaging, experiments were performed in extracellular solution containing (in mM): 119 NaCl, 23 NaHCO3, 1.25 NaH2PO4, 2.5 KCl, 2.5 CaCl2, 1.5 MgSO4, 5 glucose and 1 lactate and, aerated with 95% O2 and 5% CO2, pH 7.4. The lactate and glucose concentrations were chosen to do not saturate the FRET sensors.

Calcium and sodium imaging

For imaging experiments, 200 µm retinal slices were obtained as previously described, and were then incubated for a period of 1 h in a dark room in 2 ml of extracellular solution containing 5 µM fluo-4 AM (Thermo Fisher Scientific) or 7 µM Corona Green AM (Thermo Fisher Scientific), 0.04% Pluronic Acid. After were imaged as previously (Calbiague et al., 2020). Relative fluorescence intensities (ΔF/F0) of the regions of interest (ROIs) were obtained by dividing all images through the initial (pre-pulse) image of the series. In this study, all ROIs were chosen from the somata of putative inner retinal neurons, located in the INL. To decrease the effect of photobleaching, periods of light stimulation last for 1 s and are followed by 10 s of darkness for the duration of the experiment.

For experiments, the retinal slices were incubated for 15 min with either SR-13800, AR-C155858, Shikonin, or FX-11 and then stimulated with 12 mM KCl through perfusion.

Electrophysiology

Retinal slices from p30 *ex vivo* retinas were visualized with an upright microscope (Nikon Eclipse FN1) equipped with a 40x water-immersion objective, infrared differential interference contrast and a digital camera (TCH 1.4 LICE, Tucsen Photonics). Images were captured with ISCapture software and processed by Adobe Photoshop CS (Adobe Systems Incorporated). Patch clamp recordings were made from RBCs, whose tentative identity was corroborated by comparing the axon terminal stratification within IPL after dialysis of Lucifer yellow through the patch pipette.

Standard intracellular solution contained (in mM): 125 K^+ gluconate, 10 KCl, 10 HEPES, 2 EGTA, 2 Na_2ATP, 2 NaGTP and 1% Lucifer yellow. Recording electrodes were fabricated using borosilicate glass capillaries (1.5 mm OD, 0.84 mm ID; WPI) and pulled to resistances between 10 – 15 MΩ on a Flaming/Brown electrode puller (Sutter P-97). Experiments were only performed if the patch seal resistance was above 1 GΩ and series resistance below 30 MΩ. Signals were amplified with an EPC7- plus patch clamp amplifier (HEKA Elektronik), digitized and sampled at 10 kHz with an A/D board (Digidata 1550, Molecular Devices). Recordings were acquired using the software PClamp 10.4 (Molecular Devices).

For experiments, the retinal slices were incubated for 15 min with either SR-13800 or AR-C155858 and then different protocols were applied. Between the experiments, cells were held at a resting membrane voltage of −60 mV. To measure outward currents, 10 mV voltage steps (200 ms duration) from −100 mV to 40 mV were applied to obtain the voltage-dependent current patterns.

To measure voltage-activated Ca^{2+} currents, cells were patched with an internal solution containing (in mM): 90 Cs-methanesulfonate, 20 TEA-Cl, 10 HEPES, 10 EGTA, 10 Na_2-phosphocreatine, 2 MgATP, and 0.2 NaGTP with pH adjusted to 7.4 with CsOH. To obtain the currents, cells were held at a resting membrane voltage of −60 mV and 5 mV voltage steps (100 ms duration) from −70 mV to +20 mV, were applied.

Finally, to study the membrane potential, the current was clamped at 0 pA, and the average of 1 minute of recording was used to define the membrane potential.

FRET measurements

At p11 and p12 the explants were transduced by overnight incubation with $5x10^6$ plaque-forming units (PFU) of Ad Laconic, AAV-Laconic or Δ6, and imaged after two weeks in cultures. Adenoviral serotype vectors encoding FRET nanosensor Ad FLII12Pglu-700Δ6 (Takanaga et al., 2008)) and Ad Laconic (San Martín et al., 2013) were a gift from Dr. Ivan Ruminot from the Centro de Estudios Científicos (CECs) in Valdivia, Chile. The AAV-GFAP-Laconic was constructed by the viral vector

facility of ETH Zurich (Laconic: Addgene #44238; hGFAP promoter fragment: DOI: 10.1002/glia.20622).

Since the lactate and glucose sensors used here have similar excitation/emission spectra (Laconic: 460/492 nm for mTFP and 515/526 for Venus; Δ6: 440/480 nm for CFP and 513/530 nm for YFP), retinal slices were excited at 430 nm and visualized at 480 nm and 530 nm peak wavelength, as previously reported (San Martín et al., 2013; Barros et al., 2014). All experiments were performed at room temperature (22–25°C) with an upright fluorescence microscope (Olympus BX51) equipped with a 40x water-immersion objective, an Optosplit II emission image splitter (Cairn, UK), and a Sensicam QE digital camera (Cooke Corp.). Data acquisition was performed by a custom software written in Python 4.0.1.

At the end of the experiments, data were exported for off-line analysis of fluorescence intensities from each channel. To obtain the FRET ratio for Laconic (mTFP/Venus) and Δ6 (YFP/CFP), fluorescence intensity values from each ROI and background were measured in ImageJ, version 1.52p (NIH, RRID: SCR_003070). In this study, all ROIs were chosen from the somas of MCs and putative inner retinal neurons. The FRET data are displayed as the relative FRET ratio, in percentage of change over time of single experiments.

To calculate the delta ratio between the depletion and the saturation for both sensors, the minimum response (depletion) was obtained during the application of 10 mM pyruvate, and the maximum response (saturation) during 10 mM lactate stimulation, their difference yielding the delta ratio. To evaluate the effect of different MCT blockers on lactate influx, the positive amplitude peak was measured before and after drug application. The decay time of these responses was calculated as the time required to return to the baseline from the response peak. In both cases, the lactate response and the decay time were first normalized per cell based on the control response and then averaged throughout the experiments. Finally, the slopes of the responses were calculated by fitting a linear regression and obtaining the slope via the lineal function: $y = mx + b$, where ***m*** is

the slope. Statistical analysis was performed using GraphPad Prism software (RRID:SCR_002798).

Pharmacology

Since there is only a limited number of commercial MCT inhibitors available, based on prior reports (Murray et al., 2005; Ovens et al., 2010; Vélez et al., 2021) we used three potent and specific inhibitors to isolate MCT isoforms: SR-13800 for MCT1 (SR; Cat. No. 5431, Tocris), AR-C155858 (AR-C; Cat. No. 4960, Tocris) for MCT1 and MCT2, and Syrosingopine (Syro; Cat. No. SML1908, Sigma Aldrich) to inhibit MCT1 and MCT4. To study intracellular enzymes, involve in the lactate production, we used Shikonin (Shik; Cat. No. S7576, Sigma Aldrich) for inhibiting the isoform pyruvate kinase (PK) M2, and FX-11 for inhibiting the isoform lactate dehydrogenase A (LDH-A) (Cat. No. HY-16214, Medchem express).

Data analysis

All data were first analyzed for normality using the Shapiro–Wilk test. If the test determined that the data did not conform to a normal distribution, significant differences were established with the Wilcoxon Matched-Pairs Signed Ranks Test, and Kruskal-Wallis test followed by a Dunn´s multiple comparison test. Whether the Shapiro-Wilk test determined that the data conformed to a normal distribution, significant differences were stablished with the Paired t test, and Ordinary One-Way ANOVA multiple comparison test, followed by Tukey's multiple comparisons test.

The α value was set to 0.05. Unless otherwise stated, data values are given as mean ± SD. Significance levels as indicated by asterisks were: * $p < 0.05$; ** $p < 0.01$, *** $p < 0.001$.

References

Ames, A., Li, Y.-Y., Heher, E. C., and Kimble, C. R. (1992). Energy metabolism of rabbit retina as related to function: high cost of Na+ transport. J. Neurosci. 12, 840–853. doi:10.1523/JNEUROSCI.12-03-00840.1992.

Assali, E. A., and Sekler, I. (2021). Sprinkling salt on mitochondria: The metabolic and pathophysiological roles of mitochondrial Na+ signaling mediated by NCLX. Cell Calcium 97, 102416. doi:10.1016/j.ceca.2021.102416.

Attwell, D., and Laughlin, S. B. (2001). An energy budget for signaling in the grey matter of the brain. J. Cereb. Blood Flow Metab. 21, 1133–1145. doi:10.1097/00004647-200110000-00001.

Baden, T., Euler, T., and Berens, P. (2019). Understanding the retinal basis of vision across species. Nat. Rev. Neurosci. 21, 5–20. doi:10.1038/s41583-019-0242-1.

Baeza-Lehnert, F., Saab, A. S., Gutiérrez, R., Larenas, V., Díaz, E., Horn, M., et al. (2019). Non-Canonical Control of Neuronal Energy Status by the Na + Pump. Cell Metab. 29, 668-680.e4. doi:10.1016/j.cmet.2018.11.005.

Bittner, C. X. (2010). High resolution measurement of the glycolytic rate. Front. Neuroenergetics 2, 1–11. doi:10.3389/fnene.2010.00026.

Bittner, C. X., Valdebenito, R., Ruminot, I., Loaiza, A., Larenas, V., Sotelo-Hitschfeld, T., et al. (2011). Fast and reversible stimulation of astrocytic glycolysis by K+ and a delayed and persistent effect of glutamate. J. Neurosci. 31, 4709–4713. doi:10.1523/JNEUROSCI.5311-10.2011.

Brini, M., Calì, T., Ottolini, D., and Carafoli, E. (2013). “Intracellular calcium homeostasis and signaling,” in In Metallomics and the Cell, 119–168. doi:10.1007/978-94-007-5561-1_5.

Bui, B. V, Kalloniatis, M., and Vingrys, A. J. (2004). Retinal Function Loss after Monocarboxylate Transport Inhibition. Invest. Ophthalmol. Vis. Sci. 45, 584–593. doi:10.1167/iovs.03-0695.

Cabral-Costa, J. V., and Kowaltowski, A. J. (2020). Neurological disorders and mitochondria. Mol. Aspects Med. 71, 100826. doi:10.1016/j.mam.2019.10.003.

Calbiague, V., Chen, Y., Cádiz, B., and Paquet-durand, F. (2022). Imaging of lactate metabolism in retinal Müller cells with a FRET nanosensor. bioRxiv, 1–16. doi:10.1101/2022.10.05.510984.

Calbiague, V. M., Vielma, A. H., Cadiz, B., Paquet-Durand, F., and Schmachtenberg, O. (2020). Physiological assessment of high glucose neurotoxicity in mouse and rat retinal explants. J. Comp. Neurol. 528, 989–1002. doi:10.1002/cne.24805.

Chávez, A. E., Singer, J. H., and Diamond, J. S. (2006). Fast neurotransmitter release triggered by Ca influx through AMPA-type glutamate receptors. Nature 443, 705–708. doi:10.1038/nature05123.

Chen, J., Xie, J., Jiang, Z., Wang, B., Wang, Y., and Hu, X. (2011). Shikonin and its analogs inhibit cancer cell glycolysis by targeting tumor pyruvate kinase-M2. Oncogene 30, 4297–4306. doi:10.1038/onc.2011.137.

Chen, Y., Zizmare, L., Calbiague, V., Yu, S., and Herberg, F. W. (2022). Retinal energy metabolism : Photoreceptors switch between Cori , Cahill , and mini-Krebs cycles to uncouple glycolysis from mitochondrial respiration. bioRxiv.

Chidlow, G., Wood, J. P. M., Graham, M., Osborne, N. N., Wood, J. P. M., and Graham, M. (2004). Expression of monocarboxylate transporters in rat ocular tissues. Am. J. Physiol. Physiol. 288, 416–428. doi:10.1152/ajpcell.00037.2004.

Christofk, H. R., Vander Heiden, M. G., Harris, M. H., Ramanathan, A., Gerszten, R. E., Wei, R., et al. (2008). The M2 splice isoform of pyruvate kinase is important for cancer metabolism and tumour growth. Nature 452, 230–233. doi:10.1038/nature06734.

Contreras-Baeza, Y., Sandoval, P. Y., Alarcón, R., Galaz, A., Cortés-Molina, F., Alegriá, K., et al. (2019). Monocarboxylate transporter 4 (MCT4) is a high affinity transporter capable of

exporting lactate in high-lactate microenvironments. J. Biol. Chem. 294, 20135–20147. doi:10.1074/jbc.RA119.009093.

Coppini, R., Ferrantini, C., Mazzoni, L., Sartiani, L., Olivotto, I., Poggesi, C., et al. (2013). Regulation of intracellular Na + in health and disease: pathophysiological mechanisms and implications for treatment . Glob. Cardiol. Sci. Pract. 2013, 30. doi:10.5339/gcsp.2013.30.

Country, M. W. (2017). Retinal metabolism : A comparative look at energetics in the retina. Brain Res. 1672, 50–57. doi:10.1016/j.brainres.2017.07.025.

Delierneux, C., Kouba, S., Shanmughapriya, S., Potier-Cartereau, M., Trebak, M., and Hempel, N. (2020). Mitochondrial Calcium Regulation of Redox Signaling in Cancer. Cells 9, 1–24. doi:10.3390/cells9020432.

Denton, R. M. (2009). Regulation of mitochondrial dehydrogenases by calcium ions. Biochim. Biophys. Acta - Bioenerg. 1787, 1309–1316. doi:10.1016/j.bbabio.2009.01.005.

Euler, T., Haverkamp, S., Schubert, T., and Baden, T. (2014). Retinal bipolar cells: Elementary building blocks of vision. Nat. Rev. Neurosci. 15, 507–519. doi:10.1038/nrn3783.

Euler, T., and Wässle, H. (1995). Immunocytochemical identification of cone bipolar cells in the rat retina. J. Comp. Neurol. 361, 461–478. doi:10.1002/cne.903610310.

Gellerich, F. N., Gizatullina, Z., Arandarcikaite, O., Jerzembek, D., Vielhaber, S., Seppet, E., et al. (2009). Extramitochondrial Ca2+ in the nanomolar range regulates glutamate-dependent oxidative phosphorylation on demand. PLoS One 4, 4–8. doi:10.1371/journal.pone.0008181.

Gerhart, D. Z., Leino, R. L., and Drewes, L. R. (1999). Distribution of monocarboxylate transporters MCT1 and MCT2 in rat retina. Neuroscience 92, 367–375.

Gerkau, N. J., Rakers, C., Petzold, G. C., and Rose, C. R. (2017). Differential effects of energy deprivation on intracellular sodium homeostasis in neurons and astrocytes. J. Neurosci. Res. 95, 2275–2285. doi:10.1002/jnr.23995.

Halestrap, A. P. (2013). Monocarboxylic Acid Transport. Compr. Physiol. 3, 1611–1643. doi:10.1002/cphy.c130008.

Hurley, J. B., Lindsay, K. J., and Du, J. (2015). Mini-Review Glucose , Lactate , and Shuttling of Metabolites in Vertebrate Retinas. 1092, 1079–1092. doi:10.1002/jnr.23583.

Ingram, N. T., Fain, G. L., and Sampath, A. P. (2020). Elevated energy requirement of cone photoreceptors. Proc. Natl. Acad. Sci. U. S. A. 117, 19599–19603. doi:10.1073/pnas.2001776117.

Jung, C. C., Atan, D., Ng, D., Ploder, L., Ross, S. E., Klein, M., et al. (2015). Transcription factor PRDM8 is required for rod bipolar and type 2 OFF-cone bipolar cell survival and amacrine subtype identity. Proc. Natl. Acad. Sci. U. S. A. 112, E3010–E3019. doi:10.1073/pnas.1505870112.

Kanow, M. A., Giarmarco, M. M., Jankowski, C. S. R., Tsantilas, K., Engel, A. L., Du, J., et al. (2017). Biochemical adaptations of the retina and retinal pigment epithelium support a metabolic ecosystem in the vertebrate eye. Elife 6, 1–25. doi:10.7554/eLife.28899.

Karus, C., Mondragão, M. A., Ziemens, D., and Rose, C. R. (2015a). Astrocytes restrict discharge duration and neuronal sodium loads during recurrent network activity. Glia 63, 936–957. doi:10.1002/glia.22793.

Karus, C., Ziemens, D., and Rose, C. R. (2015b). Lactate rescues neuronal sodium homeostasis during impaired energy metabolism. Channels (Austin). 9, 200–208. doi:10.1080/19336950.2015.1050163.

Kolko, M., Vosborg, F., Henriksen, U. L., Hasan-Olive, M. M., Diget, E. H., Vohra, R., et al. (2016). Lactate Transport and Receptor Actions in Retina: Potential Roles in Retinal Function and Disease. Neurochem. Res. 41, 1229–1236. doi:10.1007/s11064-015-1792-x.

Le, A., Cooper, C. R., Gouw, A. M., Dinavahi, R., Maitra, A., Deck, L. M., et al. (2009). Inhibition of lactate dehydrogenase A induces oxidative stress and inhibits tumor progression. Proc. Natl. Acad. Sci. 107, 2037–2042. doi:10.1073/pnas.0914433107.

Lindsay, K. J., Du, J., Sloat, S. R., Contreras, L., Linton, J. D., Turner, S. J., et al. (2014). distributions reveal key metabolic links between neurons and glia in retina. Proc. Natl. Acad. Sci. 111, 15579–15584. doi:10.1073/pnas.1412441111.

Llorente-Folch, I., Rueda, C. B., Pardo, B., Szabadkai, G., Duchen, M. R., and Satrustegui, J. (2015). The regulation of neuronal mitochondrial metabolism by calcium. J. Physiol. 593, 3447–3462.

Luo, W., and Semenza, G. L. (2012). Emerging roles of PKM2 in cell metabolism and cancer progression. Trends Endocrinol. Metab. 23, 560–566. doi:10.1016/j.tem.2012.06.010.

Magistretti, P. J., and Allaman, I. (2018). Lactate in the brain: From metabolic end-product to signalling molecule. Nat. Rev. Neurosci. 19, 235–249. doi:10.1038/nrn.2018.19.

Miao, P., Sheng, S., Sun, X., Liu, J., and Huang, G. (2013). Lactate dehydrogenase A in cancer: a promising target for diagnosis and therapy. IUBMB Life 65, 904–910. doi:10.1002/iub.1216.

Murray, C. M., Hutchinson, R., Bantick, J. R., Belfield, G. P., Benjamin, A. D., Brazma, D., et al. (2005). Monocarboxylate Transporter Mctl is a Target for Immunosuppression. Nat. Chem. Biol. 1, 371–376. doi:10.1038/nchembio744.

Okawa, H., Sampath, A. P., Laughlin, S. B., and Fain, G. L. (2008). Report ATP Consumption by Mammalian Rod Photoreceptors in Darkness and in Light. Curr. Biol. 18, 1917–1921. doi:10.1016/j.cub.2008.10.029.

Ovens, M. J., Davies, A. J., Wilson, M. C., Murray, C. M., and Halestrap, A. P. (2010). AR-C155858 is a potent inhibitor of monocarboxylate transporters MCT1 and MCT2 that binds to an

intracellular site involving transmembrane helices 7-10. Biochem. J. 425, 523–530. doi:10.1042/BJ20091515.

Pellerin, L., and Magistretti, P. J. (1994). Glutamate uptake into astrocytes stimulates aerobic glycolysis : A mechanism coupling neuronal activity to glucose utilization. Proc. Natl. Acad. Sci. 91, 10625–10629.

Pérez-Escuredo, J., Van Hée, V. F., Sboarina, M., Falces, J., Payen, V. L., Pellerin, L., et al. (2016). Monocarboxylate transporters in the brain and in cancer. Biochim. Biophys. Acta - Mol. Cell Res. 1863, 2481–2497. doi:10.1016/j.bbamcr.2016.03.013.

Pierre, K., Magistretti, P. J., and Pellerin, L. (2002). MCT2 is a major neuronal monocarboxylate transporter in the adult mouse brain. J. Cereb. Blood Flow Metab. 22, 586–595. doi:10.1097/00004647-200205000-00010.

Poitry-Yamate, C. L., Poitry, S., and Tsacopoulos, M. (1995). Lactate Released by Miiller Glial Cells Is Metabolized Photoreceptors from Mammalian Retina. J. Neurosci. 15, 5179–5191.

Poole, R. C., and Halestrap, A. P. (1993). Transport of lactate and other monocarboxylates across mammalian plasma membranes. Am. J. Physiol. - Cell Physiol. 264, 761–782. doi:10.1152/ajpcell.1993.264.4.c761.

Rossi, A., Pizzo, P., and Filadi, R. (2019). Calcium, mitochondria and cell metabolism: A functional triangle in bioenergetics. Biochim. Biophys. Acta - Mol. Cell Res. 1866, 1068–1078. doi:10.1016/j.bbamcr.2018.10.016.

Ruminot, I., Schmälzle, J., Leyton, B., Barros, L. F., and Deitmer, J. W. (2019). Tight coupling of astrocyte energy metabolism to synaptic activity revealed by genetically encoded FRET nanosensors in hippocampal tissue. J. Cereb. Blood Flow Metab. 39, 513–523. doi:10.1177/0271678X17737012.

San Martín, A., Ceballo, S., Ruminot, I., Lerchundi, R., Frommer, W. B., and Barros, L. F. (2013). A Genetically Encoded FRET Lactate Sensor and Its Use To Detect the Warburg Effect in Single Cancer Cells. PLoS One 8. doi:10.1371/journal.pone.0057712.

Wang, L., Tornquist, P., and Billl, A. (1997). Glucose metabolism in pig outer retina in light and darkness. Acta Physiol. Scand. 160, 75–81.

Warburg, O. (1924). The metabolism of carcinoma cells. J. Cancer Res. 9, 148–163.

Winkler, B. S., Starnes, C. A., Sauer, M. W., Firouzgan, Z., and Chen, S. (2004). Cultured retinal neuronal cells and Müller cells both show net production of lactate. 45, 311–320. doi:10.1016/j.neuint.2003.08.017.

Wong-riley, M. (2010). Energy metabolism of the visual system. Eye Brain 2, 99.

Wong, N., Ojo, D., Yan, J., and Tang, D. (2015). PKM2 contributes to cancer metabolism. Cancer Lett. 356, 184–191. doi:10.1016/j.canlet.2014.01.031.

Yang, Y., Liu, W., Sun, K., Jiang, L., and Zhu, X. (2019). Tmem30a deficiency leads to retinal rod bipolar cell degeneration. J. Neurochem. 148, 400–412. doi:10.1111/jnc.14643.

Zhao, X., Zhu, Y., Hu, J., Jiang, L., Li, L., Jia, S., et al. (2018). Shikonin Inhibits Tumor Growth in Mice by Suppressing Pyruvate Kinase M2-mediated Aerobic Glycolysis. Sci. Rep. 8, 1–8. doi:10.1038/s41598-018-31615-y.

Supplementary figures

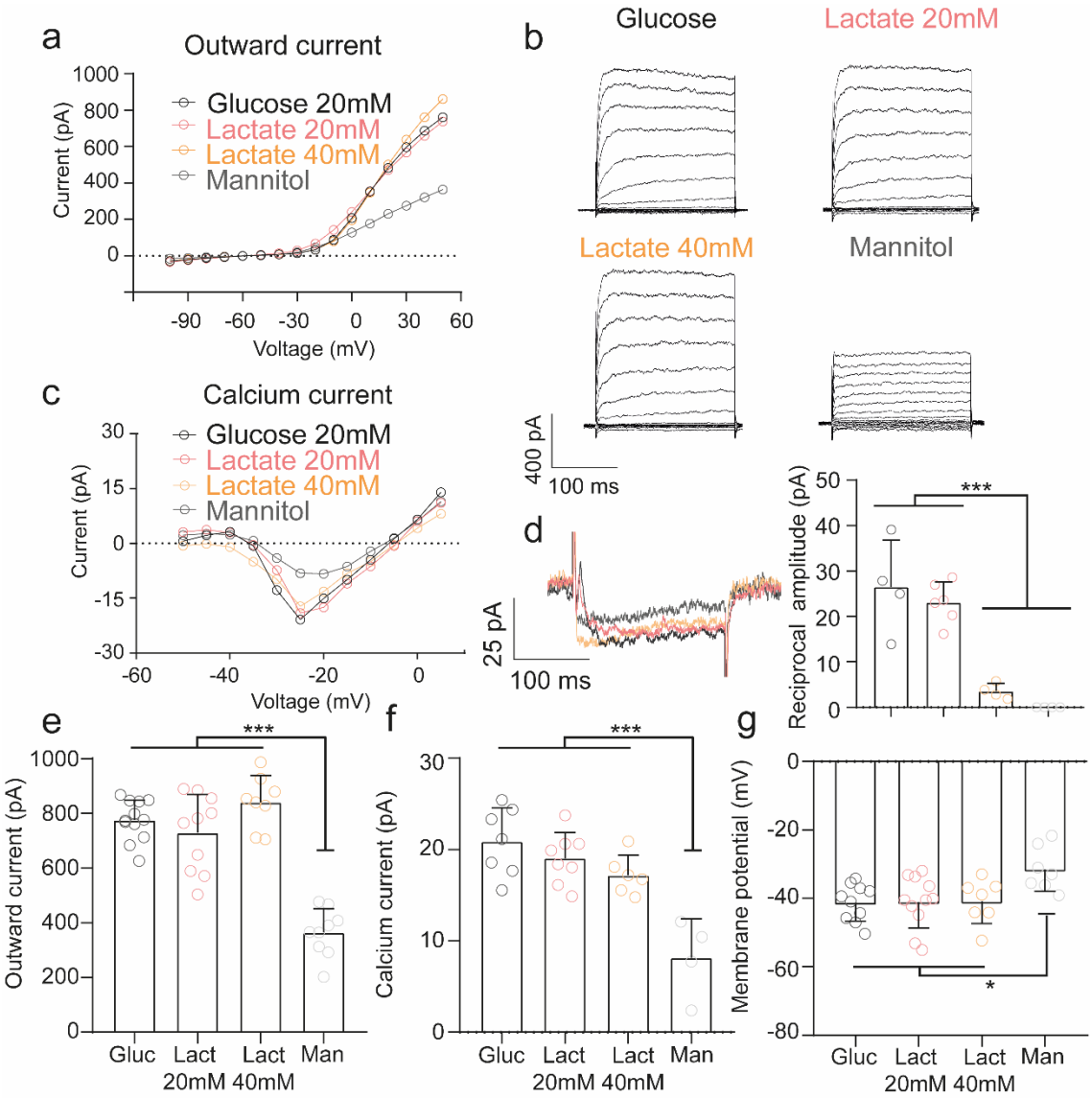

Fig. S1.- RBCs can use lactate in absence of glucose to maintain their currents. (a, c), Comparison of voltage-current relationship of the outward current and calcium current in the different conditions. **(b, d),** Representative recorded responses to depolarizing voltage steps. The reciprocal feedback was altered only in the mannitol condition (p= 0.0002), and lactate 40mM condition (p<0.0001) but was unaffected in the lactate 20mM (p= 0.7856) compared with the control condition. **(e, f)**, In absence of glucose, only in the mannitol condition we observed a decreased in the outward current (p< 0.0001), and calcium current (p< 0.0001), but no differences was noted in the lactate 20mM and 40mM condition either in the outward current (p= 0.7079; p=

0.4973) or calcium current (p= 0.6924; p= 0.2019). **(g)**, Similar results were obtained when we measured the membrane potential, but now it reflects as a depolarization in the mannitol condition (p= 0.0256), while in the lactate 20mM and 40mM condition are maintained (p= 0.9999; p= 0.9993). The data were analysed by ordinary one-way ANOVA, with a subsequent Tukey's multiple comparison post hoc test. Each dot reflects a single recorded cell. Graphs display the mean ± SD; asterisks indicate * p < .05, **p < .01, ***p< .001.

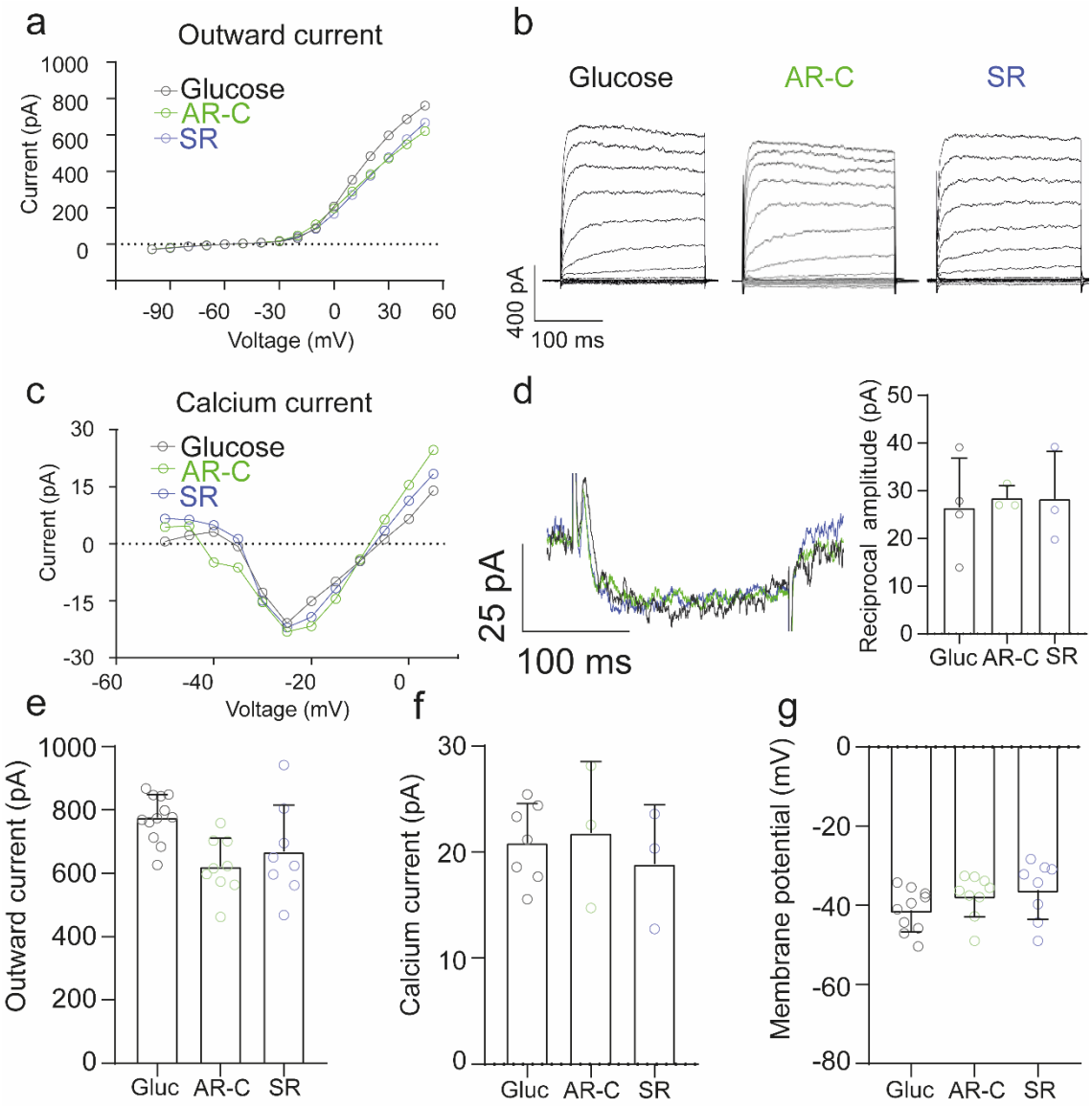

Fig. S2.- The inhibition of lactate transport does not affect the RBCs current in presence of glucose. (a, c), Comparison of voltage-current relationship of the outward current and calcium current in the different conditions. **(b, d),** Representative recorded responses to depolarizing voltage steps. In presence of glucose the reciprocal feedback was not altered in the AR-C (p= 0.9501), and SR condition (p= 0.9592) compared with the control condition. **(e, f)**, Likewise, neither in the AR-C (p= 0.0913) or SR (p= 0.0693) condition the outward current was affected, as well as the calcium current (p= 0.9581, p= 0.8267, respectively). **(g)**, Similar results were obtained when we measured the membrane potential, with no change in the AR-C (p= 0.3938) or SR (p= 0.1921). The data were analysed by ordinary one-way ANOVA, with a subsequent Tukey's multiple

comparison post hoc test. Each dot reflects a single recorded cell. Graphs display the mean ± SD. SR= MCT1 blocker; AR-C= MCT1 and MCT2 blocker

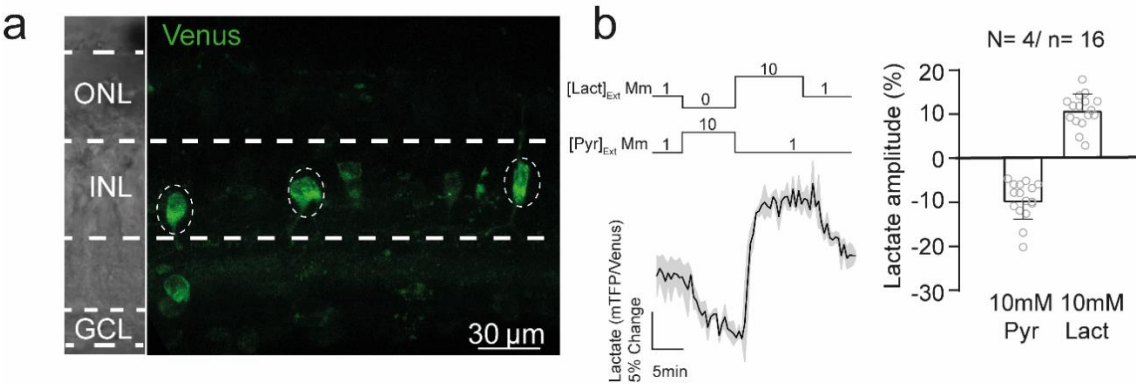

Fig. S3.- The Laconic nanosensor can be functionally expressed in inner retinal neurons. **(a)** Confocal image of Laconic expression in retinal explants after two weeks in culture, dashed circles show the area recorded. **(b)** Dynamic range of the lactate sensor in inner retinal neurons. ONL= outer nuclear layer; INL= inner nuclear layer; GCL= ganglion cell layer. The black trace represents the average of one experiment, while the light grey shadow represents the standard deviation. The number of experiments is represented as: N= number of explants; n= number of cells recorded. Graph displays the mean ± SD.

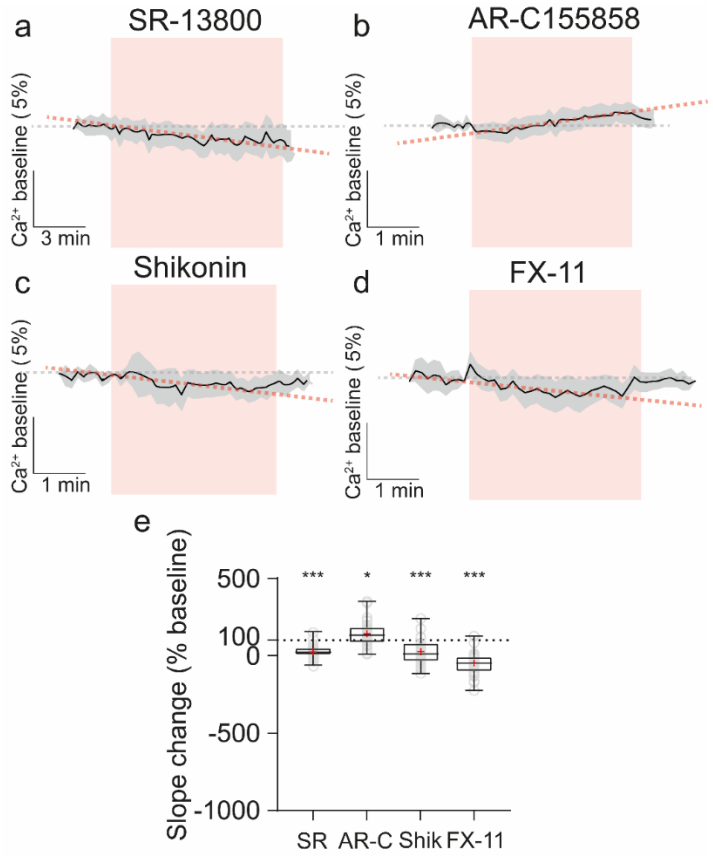

Figure S4.- Alterations in relative basal calcium levels during impaired lactate metabolism. (a-d). Traces of a single experiment in each condition (black line=mean, gray shade=standard deviation), indicating with the red boxes the incubation under different drugs. The gray dashed line shows the slope in the pre-incubation condition, while the red dashed line represents the change in slope during incubation with drugs. **(e)** Statistical analysis of basal calcium levels. Box plots showed alterations in all conditions: Under inhibition of MCT1 (SR; $p<0.0001$), PKM-2 (Shik; $p<0.0001$), and LDH-A (FX-11; $p<0.0001$) we observed a significant reduction of basal levels. However, inhibition of MCT2 (AR-C; $p= 0.0148$) revealed an increase in relative calcium levels. Control is represented as dashed line at 100%. Graphs show median ± minimum and maximum values and mean in red. Individual values are shown as open circles (gray). Asterisks indicate * $p < .05$, ***$p< .001$. SR= MCT1 blocker; AR-C= MCT2 blocker; Shikonin= PKM2 inhibitor; FX-11= LDH-A inhibitor.

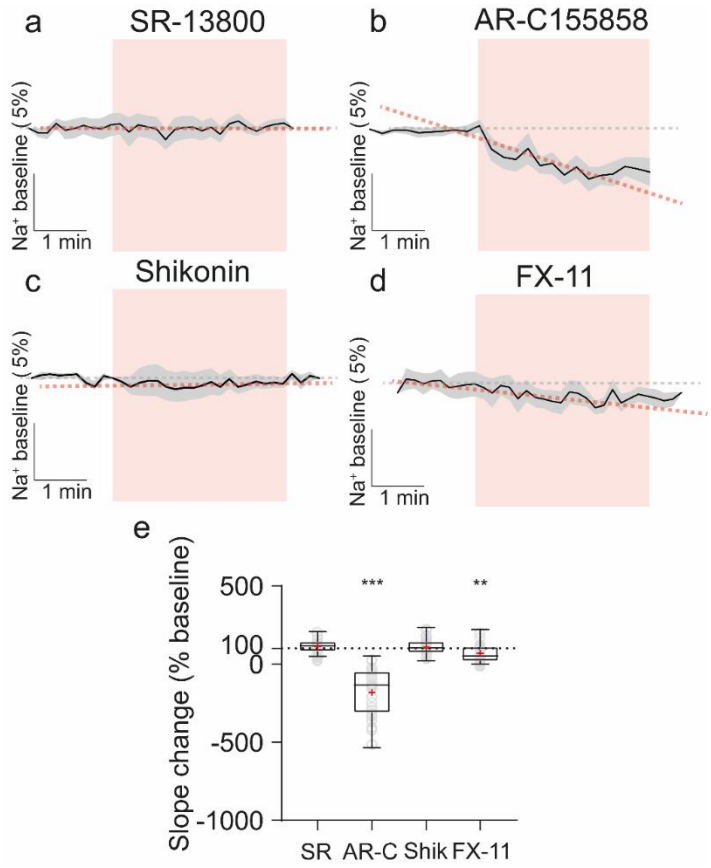

Figure S5.- Disruption in lactate metabolism impaired relative basal sodium levels. (a-d). Traces of a single experiment in each condition (black line=mean, light gray shadow=standard deviation), indicating with the red boxes the incubation under different drugs. The gray dashed line shows the slope in the pre-incubation condition, while the red dashed line represents the change in slope during incubation with drugs. **(e)** Statistical analysis of basal sodium levels. Box plots showed alterations only under two conditions: Under MCT2 blockade (AR-C; P<0.0001) and slightly under LDH-A inhibition (FX-11; P= 0.0014). While under MCT1 blockade (SR; P= 0.0602) and PKM2 inhibition (Shik; P= 0.19) the basal sodium level was not affected. Control is represented as dashed line at 100%. Graphs show median ± minimum and maximum values and mean in red. Individual values are shown as open circles (gray). Asterisks indicate * p < .05, **p< .01. SR= MCT1 blocker; AR-C= MCT2 blocker; Shikonin= PKM2 inhibitor; FX-11= LDH-A inhibitor.

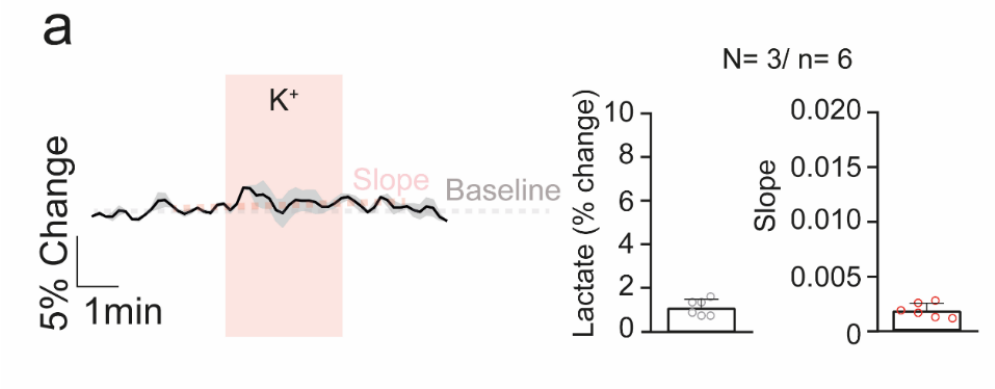

Figure S6.- Depolarization by bath application of KCl has no effect in a group of inner retinal cells. **(a, left)** Representative traces of one experiment showing no responses after a depolarization. The black trace represents the average of one experiment, while the light grey shadow represents the standard deviation. **(a, right)** Quantification of both amplitude and slope during the bath application of potassium does not demonstrate any alteration of these parameters. Graphs display the mean ± SD. The number of experiments is represented as: N= number of explants; n= number of cells recorded.